Pathomechanisms of disease-progression in urothelial and prostate cancer

Inaugural dissertation

to

be awarded the degree of Dr. sc. med.
presented at
the Faculty of Medicine
of the University of Basel

by

David Christian Müller

from Zürich, Switzerland

Basel, 2021

Approved by the Faculty of Medicine

On application of

Prof. Dr. Lukas Bubendorf

Prof. Dr. Dr. Cyrill A. Rentsch

Prof. Dr. Beat Roth

Basel, 09. August 2021

Prof. Dr. Primo Schär
Dekan

Table of content

SUMMARY 6

ZUSAMMENFASSUNG 7

INTRODUCTION 8

Cancer development and its clonal evolution 8
Intratumor heterogeneity 10

Personalized medicine 11
Introduction and definition 11
Current status 11
Liquid biopsy and disease monitoring 12
Immunotherapy 13
Limitations to personalized medicine 14

Urothelial cancer 15
Introduction 15
Clonal evolution and intratumor heterogeneity in urothelial cancer 15
Personalized medicine in urothelial cancer 16
Liquid biopsy 17
Immunotherapy in urothelial cancer 17

Prostate cancer 17
Introduction 17
Clonal evolution and Intratumor heterogeneity in prostate cancer 18
Personalized medicine in prostate cancer 19
Liquid biopsy 19

Hypothesis 20

The applicant's contribution 21

PUBLICATIONS 22

Donor-derived, metastatic urothelial cancer after kidney transplantation associated with a potentially oncogenic BK polyomavirus[167] 22
Abstract 22
Introduction 22
Materials and methods 24
Results and discussion 25
Supplement 29
Patient and methods 29
Results 32
Tables and figures 35

Heterogeneity of DNA ploidy in the context of clonal evolution in prostate cancer 44

Abstract 44
Introduction 44
Material and Methods 45
Results 48
Discussion 52
Supplement 57

Immunocytochemistry for ARID1A as a Potential Biomarker in Urine Cytology of Bladder Cancer[221] 60
Abstract 60
Introduction 60
Materials and methods 62
Results 65
Discussion 66

DISCUSSION 69

REFERENCES 74

CURRICULUM VITAE ..... FEHLER! TEXTMARKE NICHT DEFINIERT.

Meiner Familie

Summary

The concept of (clonal) evolution has been used in cancer research for decades. Recent technological progress made it possible to further elucidate cancer populations on a unprecedented resolution. Using these new technologies, we are able to depict the evolutionary pattern of an individual cancer. Delineation of these patterns is crucial for understanding the pathomechanisms of therapy-resistance and disease-progression, especially in the era of personalized medicine.

In this PhD-studies we use two different approaches. First, we analyse different cancer manifestations within the same patients. This way, we are able to understand the clonal relationship between the different tumorsites.

In case of the first publication, we took samples from different locations and different time points from a single patient. We could show an association of an early cancer onset with a previously unknown viral mutation in a Polyomavirus B.K. strain. A virus which's oncogenic potential is controversially discussed in the literature.

With our second publication we were able to depict the clonal relationship of different tumor locations within the same prostate. An understanding of this relationship might identify clinically relevant clones. This is of special importance in prostate cancer due to its multifocality. While doing this, we additionally validated the use of morphological assessment to determine a cancer cell's ploidy status.

Besides understanding a tumor's escape routes, another pillar of successful personalized therapy is the correct assessment of patients before therapy. The use of quality biomarkers is crucial in this context.

ARID1A mutational status has shown to be of predictive value of therapy response to BCG therapy in patients with non-muscleinvasive bladder cancer. So far, the evaluation of ARID1A status has been done on tissue samples. In our last publication we were able to show that analysing ARID1A in urine using immune-cytology is feasible. Therefore, we established a protocol to acquire this information in a non-invasive way.

Zusammenfassung

Die Idee, Konzepte der Evolutionsbiologie in der Krebsforschung anzuwenden, ist bereits Jahrzehnte alt. Neue technologische Fortschritte ermöglichen es nun, die evolutionäre Geschichte eines einzelnen Tumors in nie dagewesener Genauigkeit darzustellen. Dies ist insbesondere in der heutigen Zeit der personalisierten Medizin wichtig. Das evolutionäre Verhalten eines Tumors unter Therapie bestimmt letztlich das Ansprechen auf diese. Nur mit Hilfe eines genauen Verständnisses davon, wie ein Tumor therapieresistent wird, kann ein nachhaltiger Erfolg in der Therapie von fortgeschrittenen Tumorleiden erreicht werden.

In der hier präsentierten Dissertation verfolgen wir zwei verschieden Ansätze. In den ersten beiden Arbeiten versuchen wir, die Evolution der vorhandenen Tumorpopulation nachzuvollziehen. Dazu analysierten wir Proben von unterschiedlichen Krebsmanifestationen aus den gleichen Patienten. Im Falle der ersten Publikation stammen diese u.a. von unterschiedlichen Organen und von unterschiedlichen Zeitpunkten.

Auf diese Weise konnten wir in der ersten Publikation, völlig unerwartet, die Entwicklung eines Urothelkarzinoms in einem relativ jungen Organ mit einer vorher noch nicht beschriebenen Mutation eines Polyomavirus B.K. in Verbindung bringen. Ein Virus, dessen onkogenes Potential kontrovers diskutiert wird.

In der zweiten Publikation untersuchten wir verschiedene Tumorpopulationen innerhalb einer betroffenen Prostatadrüse. Dies ist beim Prostatakrebs insbesondere deswegen von Bedeutung, da häufig mehrere Herde von Krebszellen in einer Drüse vorliegen können. Ein genaueres Wissen über deren evolutionäres Verhältnis zueinander erlaubt eine bessere Einschätzung der klinischen Relevanz einer einzelnen Tumorpopulation. Zudem konnten wir zeigen, dass mit Hilfe der morphologischen Beurteilung einer Prostatakrebsprobe, zuverlässig Aussagen über die Ploidität einer Zelle getroffen werden können.

Personalisierte Medizin steht in einer grossen Abhängigkeit von guten Biomarkern. Nur mit deren Hilfe ist eine Beurteilung möglich, ob eine gezielte Therapie bei einem Patienten ansprechen kann. Neben der biologischen Wertigkeit eines Biomarkers ist dessen Wert auch von dessen Verfügbarkeit abhängig.

In unserer letzten Arbeit konnten wir zeigen, dass auch die immunzytologische Analyse des ARID1A-Proteins, eines bekannten prädiktiven Markers für das Ansprechen einer BCG-Therapie beim nicht muskelinvasiven Blasenkarzinoms, im Urin und nicht nur im Gewebe zuverlässig den Proteinstatus des entsprechenden Tumors wiederspiegelt. Somit kann diese Information auch ohne eine invasive Biopsie des Tumors gewonnen werden.

Introduction

Cancer development and its clonal evolution

"Cancers evolve by a reiterative process of clonal expansion, genetic diversification, and clonal selection within the adaptive landscape of tissue ecosystems." – M. Greaves[1].

In 1976, Peter C. Nowell first applied the concept of evolutionary biology to cancer cells and their development[2]. During this evolution to a neoplastic state, cancer cells have to successively acquire critical capabilities known as "hallmarks of cancer[3]". These hallmarks represent the tool-box cancer cells use during the process of a Darwinian natural selection[2]. The most prominent enabling characteristic for these acquisitions and a central hallmark itself is "genome instability and mutations". The exact mechanism may differ from tumor to tumor and vary by time. They may range from random single nucleotide mutations, to copy number alterations (CNA) of genes, all the way to abnormalities of entire chromosomes[3] and the genome[4].

Microenvironment constraints and/or the immune system successfully intercept most of the cells initiating the malignant transformation process[5–7]. A cancer cell must evade these defense mechanisms while it randomly acquires mutations. In the clinical context, this time frame is the cancer's latency period. To establish itself as a manifest cancerous tissue, the acquisition of selectively advantageous "driver" mutations is crucial. Simultaneously, selectively neutral mutations, i.e., passenger mutations, are also gained.

The main characteristics of a driver mutation are a mutation rate above the background mutation rate and its contribution to clonal expansion[8–10]. Driver mutations affect oncogenes or tumor suppressor genes (TSG). The anticipation of the biological consequences of different mutations, i.e., their interpretation, may be challenging. While activating hotspot mutations in oncogenes and truncating mutations in TSG are easily interpretable regarding cancerogenic contribution, the impact of CNAs is not as clear since CNAs do not always lead to changes in gene expression[11]. Nevertheless, oncogene amplification has also been identified as a driver mutation, e.g., *ERBB2* amplification in breast cancer[12] and *AR* amplification in prostate cancer[13].

The standard model of cancer genesis is the two-hit hypothesis by Knudson[14]. It applies to the bi-allelic loss of TSGs and, therefore, the promotion of cancer progression. However, a complete deletion, i.e., homozygotic loss, of a TSG is only present in a subset of cancers, and the loss of a single TSG allele has also been identified as a driving mutation since. A single-

allelic TSG loss may even be selected over a bi-allelic TSG loss if the latter causes cell death, i.e., obligate haploinsufficiency. The relevance of a mutation often cannot be evaluated without its genomic context. For example, the haploinsufficiency of *PTEN* is more tumorigenic than the homozygotic loss when the wild-type of *TP53* is present. However, following the loss of *TP53*, it is the other way around, and the homozygotic loss is more beneficial to the tumor cell[15]. Another example is the cooperation of *PTEN* homozygotic loss and the *TMPRSS2-ERG* rearrangement in advanced prostate cancer. This may explain why the complete loss of *PTEN* is associated with advanced tumors[16]. In hereditary cancer syndromes, the mutation of a single TSG may be sufficient for cancer development, whereas, in sporadic cancer, approximately four or more TSG have to be affected[17].

The concept of genomic context and dosage-sensitive effects also applies to oncogenes. Very high expression levels may induce apoptosis or cell senescence, e.g., *RAS*[18] and *MYC*[19], or be beneficial for cancer cells, e.g., *EGFR*[20].

The entirety of the genomic context in an individual cancer can be referred to as a mutational signature[10]. These signatures are influenced by age, environmental, and behavioral factors and may hint at cancer-causing events[21].

The development of cancer is traditionally thought to originate via somatic mutations followed by clonal expansion[22,23], i.e., linear evolution[24]. However, due to genomic instability, clonal expansion in cancer most often is accompanied by the random acquisition of additional driver and passenger mutations. Therefore, more sub-clones appear, and evolution is branched[24].

Within Darwinian evolution, the gain of a fitness advantage leads to the clonal expansion of the according population. If not restrained, this leads to a selective sweep[25]. If it is restrained, either by the expansion of a concurring, simultaneously expanding clone, i.e., clonal interference, or by limited resources, it leads to neutral evolution[24,26]. The state of clonal interference may be typical of early cancer development prior to the rise of a dominant sub-clone and disease progression[27].

Selective sweeps usually originate from preexisting sub-clones, especially under the selective pressure of anti-cancer therapy[28]. The often occurring lack of resources in the state of clonal interference may also select for cell migration and emigration from the primary tumor, i.e., metastasis[29,30]. The metastatic state is the culmination of the evolutionary process of cancers and is responsible for 90% of cancer-related death[31].

The accumulation of mutations in malignant clones may either evolve step-by-step by gradual additions of genetic alterations and subsequent clonal expansions or by a single catastrophic

event during mitosis generating multiple lesions at the same time, i.e., punctuated evolution[24], as is the case in chromothripsis[32,33].

The extent to which a tumor acquires a mutational burden may vary between tumor types[34]. Elucidating a tumor's clonal architecture is optimally done by serial, single-cell, deep-sequencing mutational analyses. These allow a depiction of the mutational sequence according to Darwin's evolutionary speciation tree as truncal mutations (driver) and as branches (passenger) and may best show a tumor's mutational diversity in space and time, i.e., its level of intratumor heterogeneity.

Intratumor heterogeneity

Intratumor heterogeneity (ITH) is mostly generated by imperfect genetic replication. Morphological differences within the same tumor biopsy have been part of pathologists' practice for a long time. In some cancer types, tumor grading relies on the implementation of scores to take this into account. A prime example is the Gleason-score system in prostate cancer, which was first described in the 1960s[35]. However, this assessment does not include nuclear pleomorphism, which is associated with tumor aneuploidy[36].

Aneuploidy, defined as the presence of an abnormal number of chromosomes in a cell, is a common property of cancer cells and is capable of altering the transcription of high numbers of genes (reviewed in[37,38]) and can even outnumber the prevalence of single nucleotide mutations in certain tumor cohorts[39]. Therefore, aneuploidy is an indication as well as a driver of genomic instability. A longitudinal study on Barrett-esophagus showed the cumulative acquisition of aneuploidy over time, prior to the cells' malignant transformation[40]. Aneuploidy is found to positively correlate with the overall somatic mutation rate, including *TP53* mutations and the expression of cell cycle and cell proliferation markers. Interestingly, it inversely correlates with the expression of markers for cytotoxic immune cell infiltrates[41,42].

The widespread availability of high-throughput massive parallel sequencing, i.e., next-generation sequencing (NGS), has changed our insight into genomic ITH dramatically. With every cell division, new mutations are introduced into cancer cell's genomes, making no cancer cell identical within one tumor[43–45]. ITH is a sign of the complexity of cancer as a disease. Still, most of the genome profiling studies underestimate ITH, since they look at a "snapshot" taken from a single, spatially restricted sample taken at a single point in time[46]. The sequencing of multiple regions of the same tumor biopsy revealed the presence of intratumor heterogeneity and branched clonal evolution[45]. Given the single-cell origin of a sub-clone, they usually occupy a distinct area of a tumor and, therefore, cause spatial heterogeneity[47].

This distinct space may be within the primary tumor or, with more relevant clinical implications, at a metastatic site. Here, ITH becomes even broader. Years after the resection of the primary tumor, the analysis of metastatic tissue revealed spatial and temporal differences[48,49]. The exact evolutional model of the genealogy of metastasis remains unclear. It is discussed whether metastases occur late, after a linear progression within the primarius, or early and, therefore, in a parallel progression (reviewed in[50]).

Personalized medicine

Introduction and definition

Using terms of the clonal evolution of cancer, personalized medicine (PM) is the search for individual evolution-drivers and the use of therapies targeted against them.

The terminology to describe this process is not uniform. Other names, like precision medicine, precision oncology, or stratified medicine, may be used alike. The almost synonymous term of targeted therapy emphasizes the pharmacogenomic aspect of PM, using therapeutic agents targeting key signaling pathways involved in cancer[51].

The concept of considering individual patients' characteristics when applying diagnostic and therapeutic procedures is not new. Selecting the most appropriate treatment for a given patient, to maximize efficacy and minimize toxicity, has long been a fundamental part of clinical routine. It means to, steer the application of the right diagnostic procedure or treatment, at the right dose, at the right time, based on the individually predicted response to therapy or risk of disease[52]. However, sweeping achievements in life-science technologies brought changes to our understanding of PM. NGS first revolutionized the field of (pharmaco-) genomics and, subsequently, expression profiling and proteomics. With this, it opened the door to a whole new level of patient assessment.

Current status

Driven by early success, the promise of PM strongly echoed through biomedical research[53], clinical practice[11], as well as pharmaceutical marketing[54], in the past decade. Notable examples are: targeting of the *BCR-ABL* translocation driver mutation in chronic myeloid leukemia and its successful treatment with imatinib[55], trastuzumab for HER2-expressing breast cancers[56], and vemurafenib in *BRAF* (V600E) mutated melanomas[57]. This has led to an

increased level of investment in PM by politics[58]. The number of FDA approved targeted therapies has risen significantly[59].

Besides breast cancer and melanoma, other tumor entities with a high prevalence of targetable driver mutations are lung cancer (adenocarcinoma (~60% of patients)[60] and squamous-cell carcinoma (~70%)[61]), head and neck squamous cell cancer (>50%)[62] and colorectal cancer (~70%)[63]. Affected genes are involved in a wide variety of cellular functions, ranging from signaling cascades, and subsequently cell-cycle regulation, to epigenetic regulation, e.g., members of the SWI/SNF like ARID1A (reviewed in[64]).

In addition, these mutations are not exclusive to a histological cancer type. Therefore, the success of targeted therapies led to the onset of so-called “basket trials”. As part of these, patients are no longer steered to a particular therapy by their histological cancer type, but by the molecular changes they harbor[65,66]. Which subsequently led to the first approval of histological cancer type agnostic drugs[67,68].

One application of PM is screening, defined as looking for, so far, undiagnosed diseases in patients or populations[69]. Biomarker-driven molecular testing can be referred to as molecular screening[11]. Examples are the detection of hereditable cancer syndromes like *BRCA1+2* mutation associated gynecological tumors or WNT mutations in Familial adenomatous polyposis (FAP), reviewed in[70].

Another approach to genomics-driven PM is patient-derived cell-culture. A patient’s cancer tissue is obtained and cultured either as a xenograft[71] or as an organoid[72]. These individual models may be used to predict a drug response[73]. However, these models have not yet been implemented into routine clinical practice.

<u>Liquid biopsy and disease monitoring</u>

Liquid biopsy is the analysis of information at the genomic or protein-level by using biomarkers attained in body fluids. Sources of this information may include circulating tumor cells (CTCs), cell-free DNA (cfDNA), e.g., circulating tumor DNA (ctDNA) in blood, and circulating RNA. The most common form is the detection of ctDNA in metastatic cancer patients (reviewed in[74,75]). Compared to tissue biopsies, the great advantage of liquid biopsy is the easier, i.e., less invasive, availability of genomic information about the cancer[76]. Additionally, the use of ctDNA provides the possibility of a cross-section among all relevant cancer sites in a patient’s body, and, therefore, may help to overcome biopsy-bias, i.e., the possibility of misevaluation by a limited number of tissue samples due to the spatial heterogeneity of a tumor. So far, the use

of ctDNA as a routine in clinical practice is established, notably for the detection of *EGFR* mutations in non-small cell lung cancer[77] and *KRAS* mutation in colorectal cancer[76]. The mutational load of ctDNA has also been shown to be predictive of response to checkpoint-inhibitor based immunotherapy[78,79].

Additional to the detection of prognostic and/or predictive biomarkers for therapy selection, the combination of easy accessibility and cross-sectional character of information makes liquid biopsies highly suitable for repeated analyses under therapy, i.e., monitoring, of therapy response, cancer adaption, and clonal evolution[80]. Therefore, it is promising to overcome biopsy bias (reviewed in[81]).

Despite recent technological advances in the field, the exact mechanisms of ctDNA release has not yet been revealed[82]. It is assumed to be released by apoptosis, necrosis, and/or active secretion. Therefore, the interpretation of changes in the ctDNA, especially of quantitative levels, can only be done in the individual disease and therapy regime context. It may derive from dying cancer cells due to therapy as well as due to necrosis during rapid tumor progression. However, the information provided is reflecting the biological process behind it in real-time, since the ctDNA half-life is between 16 min and a few hours[83,84].

Immunotherapy

One way to exploit the knowledge about cancer genomics is its combination with immuno-oncology. Cancer cells are thought to harbor qualities to evade an immune response. This immuno-evasion is a hallmark of cancer[3]. The idea behind immunotherapy is to enhance the immune recognition of cancer cells by the patient's immune system[85] and subsequently lead to their destruction[86]. One way to achieve this is the use of monoclonal antibodies, designed to interfere with and inhibit an immune checkpoint. Immune checkpoints are used by the immune system to identify innate body cells by checking for specific molecules on the cell-surface, so-called "don't eat me"-signals. If this signal does not correspond to the according molecule on the surface of the immune cell, cell-death is initiated in the non-conform cell. The immune checkpoints inhibitors first approved by the FDA were ipilimumab (CTLA-4-signaling)[87], nivolumab[88], and pembrolizumab[89] (both PD-1-signaling). Despite targeting specific checkpoints, the expression levels pattern of the checkpoint's ligand and receptor in immunohistochemistry have a limited value for predicting therapy response[90]. By contrast, tumor mutational burden (TMB), i.e., the number of mutations per base, was found to be significantly associated with therapy response[91,92].

Additionally, due to its differing mutational signature, a cancer cell creates so-called neo-antigens. New molecules, not yet recognized as alien, are presented to the immune cell. Additionally to being used as a predictive biomarker, cancer genomics can be able to predict the look of individual cancer neo-antigens, and personalized cancer vaccines may be created against these[93]. However, this approach is still in its clinical infancy (reviewed in[94]).

Limitations to personalized medicine

Despite these promising features, the current status of PM has not fully met its expectations. There is still a disparity between development efforts and their efficacy in improving human health[95]. Less than 10% of anti-cancer drugs in phase I clinical trials are approved for marketing[96]. This can be regarded as a sign of the complexity of the entire process of identifying a potential drug target and eventually administering a highly specific and sustainably potent agent.

From a biological point of view, the main obstacle for PM is intratumor heterogeneity. The presence of targetable driver mutations may be exploitable if they are truncal, i.e., present in all tumor sub-clones. If they represent branches, no matter how close to the trunk, targeted therapy induces a selection of subclones that are resistant to the applied therapy[97,98]. For example, in non-small cell lung cancer, *EGFR* targeted therapy may select for resistance-defining *MET* mutation harboring sub-clones[28]. As a consequence, the duration of response is often limited and followed by drug resistance and cancer progression[99].

Drug resistance can be gained by other processes than subclonal selection as well. Cancer cells are highly adaptable in altering and varying different cell signaling pathways, which lead to cell proliferation[100,101] as well as suppressing cell death initiating pathways (reviewed in[102]). - A cancer cell, harboring the targeted mutation, may just downregulate the according pathway and upregulate another[103].

In biomedical research, evidence is typically achieved by quantitative research. Prospective studies with large cohorts are used to generate statistical power to identify significant differences between groups. However, already the definition of PM and a unique pattern of mutations within a patient create a conflict with the paradigm of quantitative research. Against this background, the promise of PM feeds the temptation for clinicians as well as patients to use study eligibility to justify off-label and off-study use of targeted therapy[104], raising the question of how do we empower patients to give truly informed consent.

One way to overcome this is to approve mandatory companion diagnostic with a drug. This means that the administration of targeted therapy would depend on the use of a specific tool for patient assessment, thereby adding to the many already existing challenges that the implementation of a new anti-cancer drug faces[96]. This points directly to the need to develop accurate, unbiased, and reproducible diagnostic tools.

Urothelial cancer

Introduction

Urothelial cancer (UC) can be found in the entire urinary tract. Its most common form is bladder cancer (BC). The most important risk factor for developing UC is tobacco smoking. Approximately 75% of patients with BC present with superficial, i.e., non-muscle invasive BC (NMIBC). The remaining 25% present with advanced muscle invasive BC (MIBC). The gold standard for therapy of patients with NMIBC is surgery, i.e., transurethral resection. Clinically most relevant is high-grade UC. Approximately 40% of patients with high-grade NMIBC show a recurrence without progression, and 33% relapse with progression to MIBC. Of these patients, 40% will die of UC. The high-grade UC 10year rates are 74% for recurrence, 33% for progression, and 12% for cancer-related mortality[105]. The therapy standard for MIBC is radical cystectomy. It may be intended to curate in case of local disease or, in a metastatic setting, to avoid urinary tract complications. The standard systemic therapy for metastatic disease is platinum-based chemotherapy.

Clonal evolution and intratumor heterogeneity in urothelial cancer

UC has been proposed to be used as a model to study clonal evolution because of its tendency to relapse at different locations across the urothelium over time[106,107]. Three different types of hypotheses exist to explain this pattern: field-cancerization, intraepithelial migration, or seeding (reviewed in[108]).

The idea of a field-cancerization, or field-effect, was introduced already in the 1950s[109]. In 1979, Koss introduced the concept of a field-effect within the urothelium and the subsequent need for mapping biopsies[110]. The field-effect proposes the presence of a cancerogenic impact across the entire urothelium. This theory is backed by the identification of environmental factors like cigarette smoke and chemical agents as risk factors for UC. During the process of excretion of cancerogenic substances within the urine, the entire urothelium is exposed to the respective substance.

Prior to the NGS era, studies showed that genomic changes were not only present in UC but also in the adjacent morphologically healthy tissue[111,112]. These findings suggest either the presence of a field-effect (field first, tumor later) or intraepithelial migration of premalignant cells is present (tumor first, field later).

The role of epigenetically altered early forerunner-cells was recently highlighted[113]. These cells might then seed subsequent cells with genomic alterations. Over time, this may result in a branched evolutionary tree with a very short trunk among the same patient's spatial or temporal distinct tumors. This is in line with the hypothesis discussed by Höglund[108], that cancer stem cells are present and shed different cancer sub-clones over time, and maybe supported by the high number of stem cells present in the urothelium[114].

An interesting path of genomic evolution was depicted by Warrick et al.[115]. They show that early UC precursors, in the form of urothelial dysplasia or NMIBC low-grade, acquire the loss of either *p16* or *RB1* and then progress to a conventional, genomically unstable UC.

UC is a heterogeneous disease[116] and has one of the highest genomic mutation rates among cancers[10]. Its heterogeneity is seen in the variety of morphological subtypes as well as in the different molecular subtypes[117]. Even the morphological subtypes are molecularly heterogeneous within themselves[115]. ITH also included spatial heterogeneity of possibly targetable mutations, which has major implications for clinical decision making[118]. Investigating temporal heterogeneity during the progression from NMIBC to MIBC, inconsistent results were found. One study of 29 patients found a strong continuity of clones[119], while a smaller study revealed more heterogeneity over time in 4 patients[120].

Pre- and post-treatment analyses of matched MIBC samples showed the impact of cisplatin-based chemotherapy. Only 28% of the pre-treatment mutated genes were still mutated after therapy[121]. The overall number of present subclones was reduced after chemotherapy, indicating a therapy-induced selective sweep[122]. Additionally, Faltas et al. were able to show that the evolution within the investigated patients was branched and that the first clinically detectable tumor clone was also a branch itself[121].

Personalized medicine in urothelial cancer

In MIBC, the concept of molecular ITH and its implications on outcomes has been studied extensively. The presence of specific mutations and/or mutational signatures may be predictive of survival[117], response to neoadjuvant chemotherapy[123,124], and response to immune checkpoint inhibitors[125,126]. Currently, several options for targeted therapy, besides immune checkpoint inhibitors, are emerging for MIBC (reviewed in[127]). The most implemented of these

is the mTOR pathway targeting agent everolimus[128]. Other examples are agents targeting *VEGFR-2*[129] and pan-*FGFR*[130].

Liquid biopsy

The concept of liquid biopsy has been established in urothelial cancer, especially for bladder cancer. Numerous studies were able to detect ctDNA in the blood of muscle-invasive[131–133] and, more challenging, non-muscle-invasive bladder cancer patients[134]. CtDNA was also successfully used to detect actionable mutations in UC[135]. Additionally, the anatomical location of UC allows analyzing urinary cfDNA. According mutations correlated with mutations found in ctDNA and cancer tissue, and high levels of cfDNA and ctDNA were associated with disease progression[134].

Immunotherapy in urothelial cancer

Immunotherapies have been established in the treatment of UC[136] for decades, starting in 1976 with the first use of BCG in bladder cancer[137]. Today, it is used in patients with intermediate-risk and high-risk non–muscle-invasive bladder cancer (NMIBC)[138] and has developed into the most successful immunotherapy against cancer in human[136], prior to the era of immune checkpoint inhibitors. However, approximately 30% to 40% of patients do not respond[139], and patients with BCG-failure have a worse prognosis compared to patients who undergo radical cystectomy directly[140].

Whereas BCG is used for NMIBC, it is not applicable for MIBC or metastatic UC. Here, the standard treatment is platinum-based cytotoxic chemotherapy, which may be applied in a neoadjuvant or adjuvant setting before or after radical cystectomy[141]. In the US, the FDA has approved five different agents targeting the PD-1 immune checkpoint for first- or second-line treatment of metastatic UC so far. A wide variety of trials investigating the use of immune checkpoint inhibitors in combination or NMIBC are currently ongoing[142] (reviewed in[143]).

Prostate cancer

Introduction

Prostate cancer (PC) is the most diagnosed malignancy in men in the western world. It is a complex disease with multiple forms of clinical presentation. It ranges from clinically indolent, where patients undergo surveillance strategies, i.e., active surveillance or watchful waiting, to aggressive and potentially lethal disease with various local and systemic treatment options[144].

At metastatic state, the most administered therapy is androgen deprivation therapy (ADT). ADT slows down the clinical progression but does not alter the disease mortality.

Clonal evolution and Intratumor heterogeneity in prostate cancer

PC often presents itself as a multifocal disease, i.e., multiple, assumingly independent, areas of cancer growth within the same organ. PC may even arise from multiple, independent clonal expansions [145,146]. The various lesions can also grow together and form a heterogeneous single lesion[147].

Interestingly, using whole-genome sequencing, Gundem et al. showed that metastasis-to metastasis spread of tumor sub-clones was common in PC. This might involve the exchange of a single sub-clone as well as several sub-clones at the same time[148].

In a single case study, Haffner et al. depicted the clonal relationship of different tumor sites within the prostate and metastatic tissue[103]. The lethal subclone was initially present in a Gleason pattern 3 lesion in the prostate, clinically often assumed irrelevant, and evolved over the years into the driver of a lethal disease. Interestingly, there were also other morphologically, more aggressive patterns present in the initial biopsy.

Histological heterogeneity in PC is taken into account using the Gleason score, the strongest single prognostic marker[36]. However, there is still a high spatial heterogeneity, with only approximately 10% of biopsies being concordant within the same patient[149].

Recent longitudinal studies showed heterogeneity of the ploidy status, a sign of genomic instability. Aneuploidy correlated with a high Gleason score[150] and an increased risk of lethal PC[151]. Additionally, there is a more than a fourfold increased rate of structural changes in PC from primary to metastatic tumor tissue[152]. However, possibly due to a lack of methodological standardization, controverting data on the predictive value of aneuploidy in PC has been published[151,153,154]. This might also be due to undersampling with a single biopsy since areas with differing ploidy levels within the same PC sample have been described[146,155].

Extensive NGS studies revealed that PC's genomic mutation frequency is very low compared to other cancers[10,156]. Mutated genes that are more common in metastatic tissue, an indication for their relevance in lethal disease, were *TP53*, *AR*, *PTEN*, *RB1*, *FOXA1*, *APC*, *KMT2C*, *KMT2D*, and *BRCA2*[157]. The percentage of the altered genome is clinically prognostic[156]. The distribution of these mutations is very heterogenous[158,159]. The most common genetic alteration in castration-resistant PC is AR amplification, present in 60% of patients (reviewed in[160]).

The level of morphological and molecular ITH in PC shows that a single-biopsy approach is likely to suffer from a biopsy bias and will undersample the disease's complexity[146].

Personalized medicine in prostate cancer

Current prognostic factors in routine clinical practice are the TNM classification, PSA, and Gleason Score. However, there is still a struggle to differentiate clinically relevant from indolent disease, possibly because these parameters cannot fully assess a tumor molecular heterogeneity[159].

Recent advances in the treatment of advanced PC have been achieved with the implementation of new drugs targeting the androgen receptor (AR). Additionally, the presence of mutations in DNA damage repair genes was predictive of response to PARP-inhibitor olaparib[161].

Liquid biopsy

The work of Antonarakis et al.[100] was the first liquid biopsy work on prostate cancer that echoed throughout the entire uro-oncological research and clinical community. Investigating CTCs, it described the onset of an AR splice variant, i.e., AR-V7, which was of a predictive value for resistance to enzalutamide and abiraterone treatment.

Wild-type *AR* amplification, analyzed by liquid biopsy, is another therapy resistance mechanism for enzalutamide[162] and abiraterone[163] therapies. This is also the case in patients treated with enzalutamide after systemic chemotherapy with docetaxel[164].

In line with the work of Mateo et al.[161] on tissue biopsy material, the group of Wyatt showed that patients with a bi-allelic *BRCA2* loss, detected in ctDNA, benefited from DNA-damage repair targeted therapy[165].

Furthermore, one can also measure the impact of therapy on the quantitative level of ctDNA. The ctDNA fraction in patients' blood declined with the start of ADT, especially pronounced after one week[166]. In the same work in patients with hormone-naïve metastatic PC, ctDNA and sequencing of core-needle biopsy material had complementary effects in detecting relevant mutations, indicating a risk of undersampling using only a single approach. However, if sufficient amounts of ctDNA were available, there was also a high concordance between both types of biopsies.

Hypothesis

The use of today's genomic tools enables us to depict a tumor's clonal evolution as well as to establish appropriate biomarkers to assess its clinical behavior.

"More research should be directed towards understanding and controlling the evolutionary process in tumors before it reaches the late stage usually seen in clinical cancer."

- P.C. Nowell, 1976[2]

The applicant’s contribution

As a first author in all three publications, the applicant contributed to the conception of the work, data collection, data analysis and interpretation, and drafting the articles.

Publications

Donor-derived, metastatic urothelial cancer after kidney transplantation associated with a potentially oncogenic BK polyomavirus[167]

Abstract

BK polyomavirus has been linked to urothelial carcinoma in immunosuppressed patients. Here, we performed comprehensive genomic analysis of a BK polyomavirus-associated, metachronous, multifocal and metastatic micropapillary urothelial cancer in a kidney transplant recipient. Dissecting cancer heterogeneity by sorting technologies prior to array-comparative genomic hybridization followed by short tandem repeat analysis revealed that the metastatic urothelial cancer was of donor origin (4-year-old male). The top 50 cancer-associated genes showed no key driver mutations as assessed by next-generation sequencing. Whole genome sequencing and BK polyomavirus-specific amplification provided evidence for episomal and subgenomic chromosomally integrated BK polyomavirus genomes, which carried the same unique 17-bp deletion signature in the viral non-coding control region (NCCR). Whereas no role in oncogenesis could be attributed to the host gene integration in chromosome 1, the 17-bp deletion in the NCCR increased early viral gene expression, but decreased viral replication capacity. Consequently, urothelial cells were exposed to high levels of the transforming BK polyomavirus early proteins large tumour antigen and small tumour antigen from episomal and integrated gene expression. Surgery combined with discontinuation of immunosuppression resulted in complete remission, but sacrificed the renal transplant. Thus, this report links, for the first time, BK polyomavirus NCCR rearrangements with oncogenic transformation in urothelial cancer in immunosuppressed patients.

Introduction

Several studies have reported an increased incidence of malignancies after solid organ transplantation, and have indicated a role of infections in tumourigenesis[168,169]. In particular, an association between BK polyomavirus (BKPyV) infection and the risk of urothelial cancer (UC) has been discussed[170,171]. The BKPyV genome contains three different functional regions, called the early viral genome region (EVGR), the late viral genome region (LVGR), and the non-coding control region (NCCR). Indeed, EVGR proteins such as large tumour antigen (LTag) and small tumour antigen (sTag) have been linked to oncogenic cell transformation[172].

We describe the case of a kidney transplant recipient developing BKPyV-associated, multifocal and micropapillary UC. At the age of 42 years, he received a kidney transplant from a deceased 4-year-old male donor. Eight years post-transplantation (ptx), LTag-positive UC of the bladder was diagnosed and treated by endoscopic resection. Nine years ptx, local UC recurrence was diagnosed and surgically removed, but 1 year later the patient was diagnosed with a second recurrence presenting as LTag-positive, multifocal micropapillary, muscle-invasive UC of the graft kidney pelvis, which metastasized to the bladder wall and to a pelvic lymph node (Figure 1A; supplementary material, Figure S1A and Table S1). Following surgical removal, immunosuppression was discontinued, and, despite multiple recurrences and progression to metastatic UC disease, the patient remained UC recurrence-free during 4 years of follow-up.

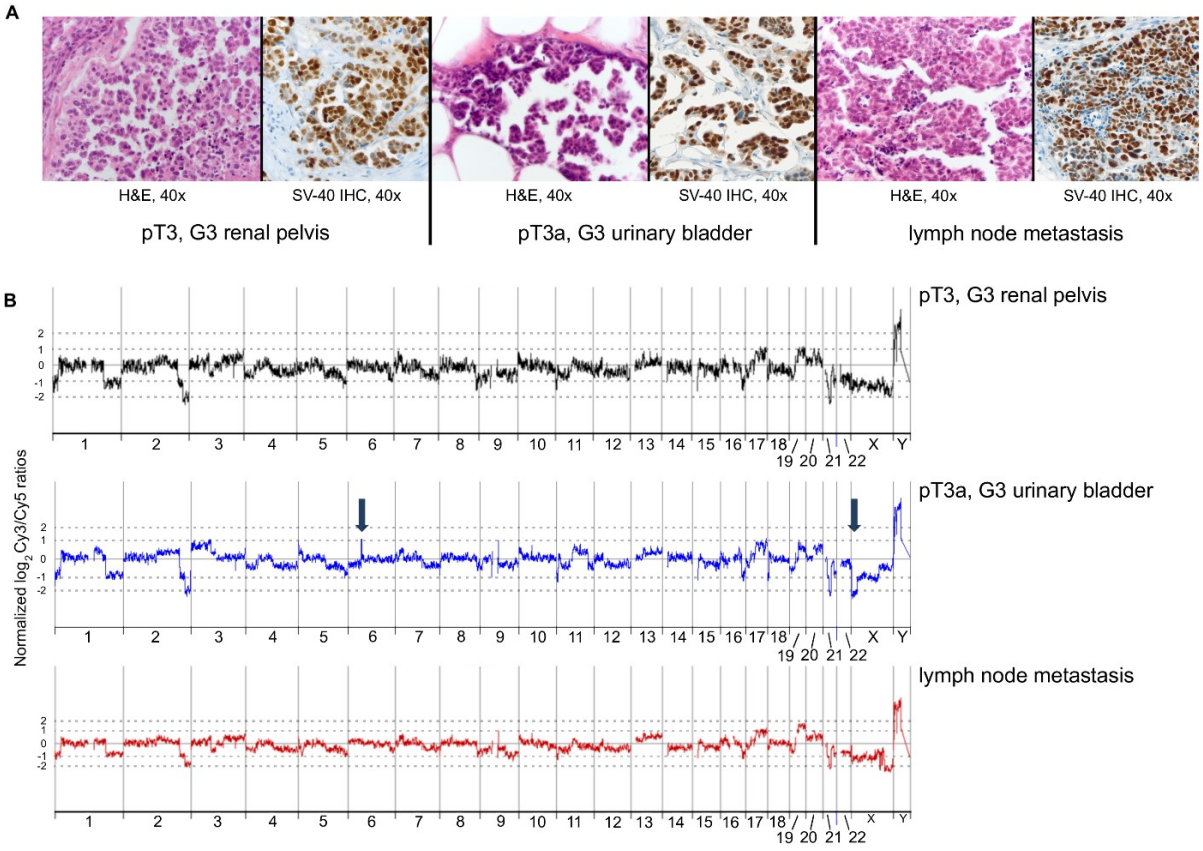

Figure 1. Morphological and genomic characterization of cancer sites 10 years ptx. (**A**) Haematoxylin and eosin (H&E) staining and SV40 LTag immunohistochemistry (IHC) of micropapillary UC of the kidney transplant recipient. The morphological picture indicates a close relationship of the different sites and differs from the previous tumour appearances (not shown). (**B**) ArrayCGH profiles with copy number alterations of aneuploid cancer populations 10 years ptx. Arrows indicate key differences. x-axis: chromosome number. y-axis: normalized log2 Cy3/Cy5 ratios (relative count of DNA probe signals). The samples appear to be highly related, suggesting that the lymph node metastasis was derived directly from the renal pelvis, as the bladder showed a unique deletion in the X chromosome (right arrow). In contrast, there was no evidence of a clonal relationship with the previous tumour appearances (supplementary material, Figure S2).

Materials and methods

This study was performed in accordance with the principles expressed in the Helsinki Declaration (1975; revised 1983), and was approved by the Ethical Committee Nordwest- und Zentralschweiz in Basel, Switzerland (EKNZ 2014-313).

Immunohistochemistry with an anti-simian virus 40 (SV40) LTag antibody (MRQ-4 mouse clone; Ventana Medical Systems, Tucson, AZ, USA) on the Ventana BenchMark XT platform demonstrated LTag expression. Fresh-frozen tissue obtained from the recent surgical specimens 10 years ptx was used for further analyses. Formalin-fixed paraffin-embedded tissues were available from the 8-year and 9-year ptx biopsies.

We applied DNA content-based cell nucleus sorting followed by array-comparative genomic hybridization (arrayCGH) to determine the evolutionary history of the individual cancer tissues[173]. (Array data have been submitted to the Gene Expression Omnibus repository, accession number GSE90778.) Short tandem repeat (STR) analysis was applied to identify the genealogy of the cancer tissue (supplementary material, Supplementary materials and methods). The IonAmpliseq Cancer Hotspot Panel was used for targeted next-generation sequencing (NGS) (supplementary material, Supplementary materials and methods).

Extracted DNA from tumour and unaffected tissue were tested with quantitative real-time polymerase chain reaction (PCR) for BKPyV genome loads[174], and human aspartoacylase quantitative PCR (qPCR) was used for normalization[175]. BKPyV-specific long-range PCR was performed with outward primers partially overlapping the EcoR1 site present in the VP1 gene (Figure 2; supplementary material, Table S4), yielding a full-length genome of 5116 bp and a short derivative of 3270 bp[176]. The complete BKPyV genomes were determined by Sanger sequencing. Additionally, the episomal BKPyV genomes were deep-sequenced with the Illumina MiniSeq (Illumina, Carlsbad, CA, USA) (supplementary material, Supplementary materials and methods). To detect potential chromosomal integration, shallow whole genome sequencing (WGS) was performed with the Illumina NextSeq 500 (supplementary material, Supplementary materials and methods). Primers spanning the integration breakpoints were used for PCR-based confirmation of WGS results (Figure 2; supplementary material, Table S4, and Supplementary materials and methods).

For functional analysis, the NCCR of the BKPyV-UC genome was amplified and inserted into the bidirectional reporter gene plasmid pHRG1[177,178]. The respective NCCR pHRG1 reporter constructs were sequenced and transfected into HEK293 cells, and activity was quantified by flow cytometry for the EVGR and the LVGR[12]. Recombinant full-length BKPyV genomes were generated by inserting the NCCRs derived from different BKPyV strains into the Dunlop genome[177,178]. COS7 cells were transfected with the recombinant BKPyV (rBKPyV)

genomes[174], and supernatants were used to infect human primary proximal renal tubular epithelial cells (hRPTECs) with rBKPyV as described previously. The hRPTEC culture supernatants were harvested at 1, 3, 5, 7 and 9 days post-infection, and rBKPyV loads released into the culture supernatants were compared by the use of qPCR (Figure 3D)[177,178].

Results and discussion

ArrayCGH and STR revealed that the UC originated from the donor kidney pelvis (Figure 1B; supplementary material, Figure S1B). However, no somatic key driver point mutations were detected in the UC genome (supplementary material, Table S2). Instead, the UC in the pelvis was shown to originate from the donor kidney rather than from the urinary bladder of the 52-year-old recipient, who had a much longer history of potential exposure to carcinogenic agents, such as ongoing cigarette smoking, and a lifetime accumulation of oncogenic events.

Immunohistochemistry indicated LTag expression, and WGS identified one integrated episomal BKPyV genome and two episomal BKPyV genomes (Figure 2) in the 10-year ptx cancer specimens: five read pairs aligned to the viral genome and to human chromosome 1. We identified breakpoints in chr1:16055645–16055650_PLEKHM2 and the capsid coding sequences of Vp1 and Vp2/Vp3, accompanied by a 1355-bp deletion between Vp1 and Vp2/Vp3 (Figure 2; Figures S4 and S5). Importantly, no role in oncogenesis could be attributed to the affected host gene. Three independent primer pairs designed to match the upstream and downstream genome breakpoints amplified exclusively a single band of 3.7 kb, which, upon sequencing, yielded solely the integrated BKPyV genome, ruling out the presence of concatemers (Figure 3A; supplementary material, Table S4). To determine the relative amounts of the integrated BKPyV genome and the two episomal forms, two different PCRs were used: one targeting LTag sequences (LTag_qPCR in Figure 2; Table S4) present in all three UC-derived BKPyV genomes (i.e. the episomes of 5116 bp and 3270 bp as well as the 3761-bp integrated genome), and another one targeting Vp1 sequences exclusively present in the episomal forms (Vp1_qPCR in Figure 2; supplementary material, Table S4). The results were normalized to ACY as a housekeeping gene[175], and revealed an LTag target/Vp1 target ratio of 3:2, as expected for three independent LTag genome and two Vp1 targets.

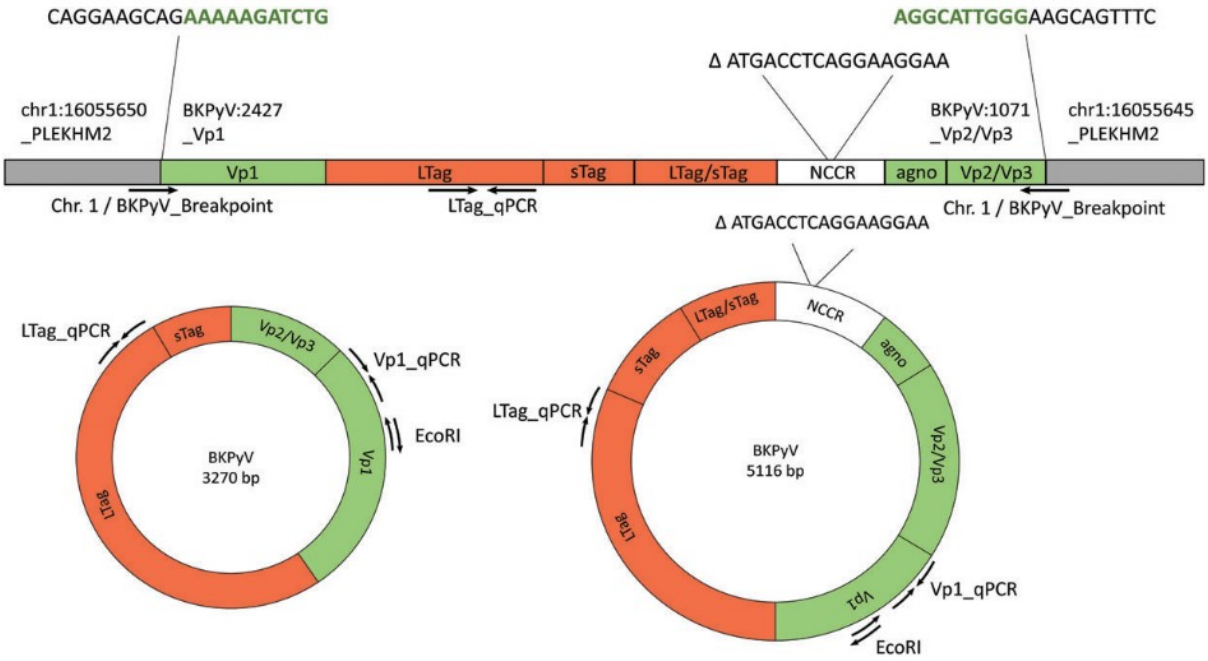

Figure 2. BKPyV genomes in the 10-year ptx UC specimen. The integrated genome and the breakpoints in chromosome 1 were located in the PLEKHM2 gene as identified by WGS. The breakpoint sequences are shown in black for the human chromosome 1 PLEKHM2 gene and green for the BKPyV genome. The locations and directions of primers used for amplification of the episomal BKPyV genome at the EcoRI site or the qPCRs targeting LTag (LTag_qPCR) and Vp1 (Vp1_qPCR) are depicted by arrows. The integrated BKPyV genome is shortened by a 1355-bp deletion between Vp2/Vp3 and Vp1, and by a 17-bp deletion in the NCCR P-block. In addition, an episomal full-length BKPyV genome of 5116 bp and a short genome of 3270 bp were identified. Whereas the larger episomal genome on the right-hand side is the only genome with a complete EVGR and a complete LVGR, the shorter episomal genome has a deletion of 1847 bp removing parts of the common LTag/sTag sequence, the NCCR, agno (agnoprotein-gene), and the Vp2/Vp3.

Importantly, the full-length BKPyV episome and the chromosomally integrated truncated BKPyV genome carried an identical, and so far not reported, 17-bp deletion in the P-block of the UC BKPyV NCCR (Figures 2 and 3B). Functional analyses with a bidirectional reporter vector revealed that this 17-bp deletion NCCR was sufficient to activate EVGR expression, and contributed to LTag expression (Figure 3C). Unlike patient-derived NCCR rearrangements characterized previously[177], however, the UC-derived 17-bp deletion NCCR showed impaired progression into the late viral life cycle and offset efficient lytic replication (Figure 3D). The fact that the intact full-length viral episome carried the same NCCR deletion as the truncated integrated genome argues that this 17-bp deletion occurred first, and was followed by viral genome integration, both of which contribute to LTag expression. It remains challenging to dissect the relative contributions of immunosuppression and ongoing BKPyV replication during this process. It is well known that chronic immunosuppression by itself favours the development of malignancy[168]. However, one would expect exposure to carcinogens and/or hereditary susceptibility to be present before such cells can be unleashed to give rise to established cancer after loss of immune control.

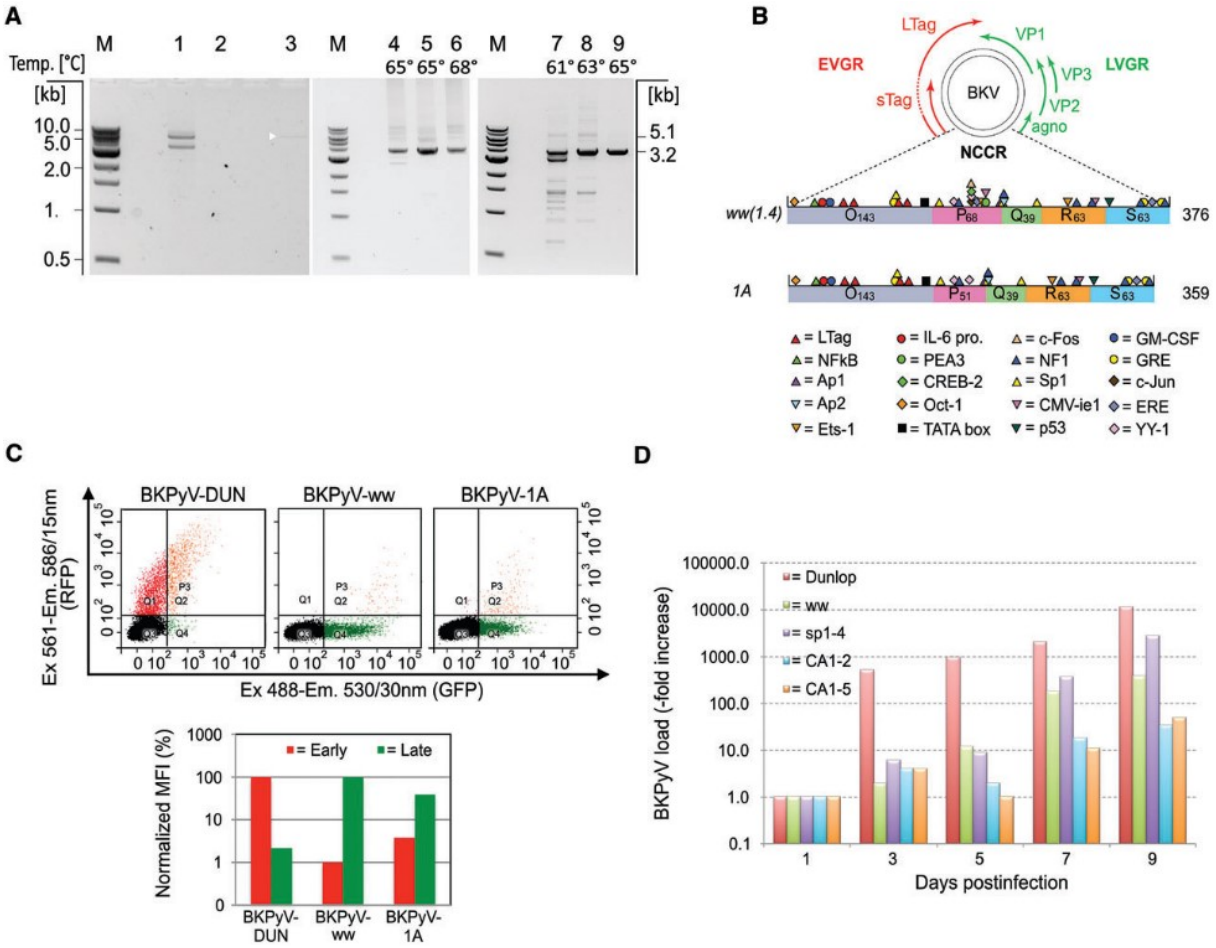

Figure 3. Characterization of the BKPyV genome in the 10-year ptx UC tissue specimen. (A) Gel electrophoresis of PCR products after amplification with outward primers from the EcoR1 site of the VP1 gene (supplementary material, Table S4) yields a full-length BKPyV DNA genome (5116 bp) bearing a small deletion in the NCCR and a smaller subgenomic fragment (3270 bp) lacking the N-terminal Vp2, the NCCR and N-terminal LTag sequences. M, DNA marker in kilobase pairs. Lane 1: 50 ng of UC tissue DNA. Lane 2: negative template control. Lane 3: control BKPyV-positive urine specimen, highlighted by the white triangle. Lanes 4–9: amplification of chromosome 1 integrated BKPyV genome of 3761 bp with breakpoint-specific primers. Lanes 4–6: UC tissue DNA amplified with three different pairs of breakpoint-specific primers (supplementary material, Table S4). Lanes 7–9: UC tissue DNA amplified with pair 1 of the breakpoint-specific primers (supplementary material, Table S4), with an annealing temperature gradient PCR for increasing stringency (61 ◦C, 63 ◦C, and 65 ◦C). (B) Schematic representation of transcription factor binding sites in the BKPyV archetype NCCR (ww1.4) of 375 bp, and the BKPyV-1A NCCR (359 bp) carrying a 17-bp deletion in the P-block P41–P57. Red: EVGR. Green: LVGR. (C) NCCR-driven reporter gene expression of the EVGR (red; dsRed) and the LVGR (green; enhanced green fluorescent protein) in the bidirectional reporter vector pHRG1 following transfection into HEK293 cells. Top panels: flow cytometry. Bottom panels: normalized mean fluorescence intensity (MFI). Positive control: BKPyV-DUN (Dunlop strain). BKPyV-ww: archetype strain. BKPyV-1A: 17-bp deletion NCCR identified in episomal and integrated BKPyV genomes of the UC. (D) Comparison of viral replication in Vero cells after infection of the indicated BKPyV NCCR variants: Dunlop strain, archetype ww(1.4); ww(sp1–4) mutant; and two independent recombinant clones bearing the patient-derived NCCR CA1-2 and CA1-5. Em, emission; Ex, excitation; GFP, green fluorescent protein; RFP, red fluorescent protein.

Apart from surgery, postoperative termination of immunosuppression was sufficient to control metastatic disease. This suggests that aberrant LTag expression resulting from the unique BKPyV NCCR deletion conferred a strong transforming oncogenic drive, which could not be cleared immunologically without discontinuation of immunosuppression[179].

There is growing evidence that reactivation of polyomavirus infection under immunosuppression might play an important role in the development of aggressive UC after renal transplantation[171,180]. A driving role of BKPyV infection is also supported by the low mutational load in cancer-related genes in our case as compared with common UCs, which show some of the highest mutation rates among malignant human tumours[181]. Similarly, low mutational loads have been seen in Merkel cell carcinoma, which is known to be associated with Merkel cell polyomavirus infection[182]. Indeed, all UC manifestations of our patient at 8, 9 and 10 years ptx were LTag-positive, and eventually turned into a metastasizing micropapillary variant at the final, most advanced stage. Thus, the aggressive micropapillary morphology strongly suggests that BKPyV acts as an oncogenic driver, as discussed previously[171,180]. Although high-level urinary BKPyV replication occurs in 20–40% of patients after kidney transplantation, most UCs diagnosed to date have been LTag-negative[183]. The factors that unleash BKPyV oncogenicity in individual patients are presently unknown, but appear to involve constitutive EVGR expression of LTag and sTag[172]. Viral integration into human DNA has been proposed as an important feature of oncogenic polyomaviruses disrupting progression from constitutive EVGR to lytic LVGR expression by removing relevant viral gene sequences[184]. This can occur as a result of breakpoints in the viral DNA followed either by host DNA[185] or by multiple copies of viral DNA[186]. Such integration is supposed to support an imbalance between increased LTag expression and reduced virus-induced cell-lysis resulting in sustained perturbation of pRb and p53, both of which bind to LTag. A rearranged NCCR in the context of BKPyV-associated cancer has been reported[185], in which the Q-block and R-block are deleted from the NCCR of the integrated BKPyV genome. Similar deletions have been detected in kidney transplant patients, e.g. del(5.3), del(3.2), and del(15.10) (supplementary material, Figure S1 of [177]), all of which increased EVGR expression comparably to the 17-bp deletion reported here, but, unlike the 17-bp deletion described here, also conferred increased replicative capacity and cytopathology[177]. Although our analyses provide evidence of both NCCR rearrangement and genomic integration, our functional studies challenge the view that integration of polyomaviruses is a necessary condition for tumourigenesis. The 17-bp deletion in the NCCR P-block in the non-integrated BKPyV genome may lead to the same early versus late gene expression imbalance as an LVGR genomic disruption[185,186]. We have demonstrated that the 17-bp deletion NCCR constitutively activated LTag and sTag EVGR expression, while impairing LVGR expression and the replicative capacity of isogenic derivatives. Thus, viral replication with accumulation of viral particles and subsequent (onco)cytolytic cell death was impaired. Importantly, all stages of the UC in our patient were LTag-positive, suggesting that expression of this virus-encoded transforming function contributed to malignant progression. The now relapse-free time of 4 years after diagnosis of this metastasizing UC also points to the role of regaining anti-tumour immunity

following cessation of immunosuppression, and questions the need for additional aggressive therapeutic interventions in such situations[179].

Taking the above findings together, the occurrence of aggressive LTag-positive UC can be regarded as a rare 'biological accident' in the light of the high prevalence of high-level BKPyV replication in immunosuppressed patients, e.g. after kidney transplantation[185]. However, given the huge number of viral generations in an immunosuppressed host, a rare clinical manifestation can become a relevant complication in the long-term perspective of otherwise successful kidney transplantation. Further studies are needed to explore the relative incidence and clinical importance of such alternative events.

Supplement

Patient and methods
Patient

The recipient suffered from end stage renal disease due to Alport-syndrome. The donor's HLA-status was: blood type: A+; HLA-A: 1, 2; HLA-B: 8, 27; HLA-DR: 13, 7. In comparison, the recipient's status was: blood type A+; HLA-A: 24, 26; HLA-B:44, 50; HLA-DR: 13, 7. The immunosuppressive therapy consisted of tacrolimus, azathioprine, and prednisone for the first 6 months post-transplant (ptx) followed by tacrolimus and azathioprine. 3 months ptx a tissue biopsy was SV40-IHC negative. No further SV40-IHC staining on non-cancerous tissue was performed. 6 months ptx decoy cells were found in the patient's urine (11 /10 High Power Field 400x). Previous urine specimens did not show any decoy cells. In summary, there was no evidence for BKPyV-associated nephropathy (BKPyVAN). Thirteen years after transplantation, the patient is alive but requires continued renal replacement therapy by dialysis. PET/CT scans show no evidence of the urothelial cancer.

Cell nuclei extraction and DNA content-based cell sorting

For the purpose of dissecting the intratumour heterogeneity within one tissue-sample we performed DNA based cell sorting. Formalin-fixed and paraffin-embedded (FFPE) tumour specimens were analyzed morphologically with the Axioskop 2 plus microscope (Zeiss, Oberkochen, Germany). Biopsy samples were fixed in 10% buffered formalin and embedded in paraffin according to standard operating procedures. Cell nuclei extraction was done as previously described[187]. The extracted nuclei were separated by DNA content based on sorting using the Influx (Becton-Dickinson, San Jose, CA) cytometer with ultraviolet excitation. DNA content and cell cycle were analyzed using the software program MultiCycle (Phoenix Flow Systems, San Diego, CA). Sorted nuclei were digested overnight in 180 µl of Incubation Buffer

(Promega Corporation, Madison, WI) and 20 µl of Proteinase K (Promega Corporation, Madison, WI) at 56°C, 650 rpm for genomic DNA extraction.

DNA extraction

Total genomic DNA from sorted populations was extracted with MaxWell 16 FFPE Plus LEV DNA Purification Kit (Promega Corporation, Madison, WI) according to the kit protocol. For NGS purposes, DNA was also directly extracted from the matched FFPE tissues without sorting. Two to three 25 µm sections were placed into 2 ml microtubes. Samples were washed three times with 1 ml Xylene for 5 min to remove the remaining paraffin, following rehydration two times in 1 ml 100 % EtOH, which was then evaporated for 2 min in 26°C. 180 µl of Incubation Buffer (Promega Corporation, Madison, WI) and 20 µl of Proteinase K (Promega Corporation, Madison, WI) were added. Samples were digested overnight at 56°C, 650rpm and DNA was extracted with MaxWell 16 FFPE Plus LEV DNA Purification Kit (Promega Corporation, Madison, WI) according to the kit protocol. Because of impurities of DNA of the 2011 and 2012 samples were purified with Genomic DNA Clean and Concentrator Kit (Zymo Research, Irvine, CA) before using these samples for next-generation-sequencing (NGS).

Array comparative genomic hybridization (aCGH)

In order to investigate copy-number changes within the different tumour populations and to discover the evolutionary history of this individual cancer [6] we performed aCGH. Genomic alterations between samples were evaluated with Agilent SurePrint G3 HMN CGH 4x180 K Oligo Microarray Kit (Agilent Technologies, Santa Clara, CA) according to the manufacturer's protocol. 40-100 ng DNA of each sorted population was subjected to the arrays and normal Female Human Genomic DNA (Promega Corporation, Madison, WI) was used as a reference DNA during aCGH. Reference DNA was digested with DNAse I. References and samples were labelled with Cy-3 dUTP and Cy-5 dUTP respectively, using a BioPrime Array Kit (Invitrogen, Carlsbad, CA). Filtering, hybridization and washing were carried out according to manufacturer's protocol (Agilent Technologies, Santa Clara, CA, USA).

Short tandem repeat analysis (STR)

The investigated samples were the patient's innate kidney as a reference for recipient's DNA and healthy allograft-kidney tissue as a donor's DNA reference. DNA was purified using the Genial® DNA Kit according to the provider's protocol for isolation of total DNA. The DNA was eluted in 30 µl of low TE-buffer. All profiles were genotyped with the PowerPlex® ESI 17 Kit (Promega Corporation, Madison, WI). The kit is based on a five dye technology (blue: 6-FAM™, green: VIC®, yellow: NED™, red: PET®, orange: LIZ®) and contains 16 autosomal STR loci and AMEL (blue: D10S1248, vWA, D16S539, D2S1338; green: AMEL, D8SS1179,

D21S11, D18S51; yellow: D22S1045; D19S433, TH01; FGA; red: D2S441, D3S1358, D1S1656, D12S391, SE33; orange: internal standard). Each run was performed on an Applied Biosystems Genetic Analyzer 3500 (Life Technologies, Carlsbad, CA, USA) with injection voltage 3 kV and injection time 10 seconds. Results were then analyzed with the GeneMapper IDX Software (Version 1.4). The peak threshold was 50 rfu (relative fluorescence units). In order to define the recipient's profile available FFPE tissue from the recipient's innate kidney was used. No non-transplanted donor tissue was available. To define the donor's STR-profile we took healthy FFPE-tissue in adequate distance from the tumour from the allograft. The extracted DNA from the recipient's innate kidney was diluted 1:100 for further analyses.

Targeted Next generation sequencing (NGS)

The IonAmpliseq™ Cancer Hotspot Panel v2 which includes 207 amplicons covering mutations from 50 oncogenes and tumour suppressor genes was used on the IonTorrent platform for targeted sequencing. 10 ng input of extracted genomic DNA was used for library preparation. Chip loading was assisted by the IonChef-System (Life Technologies, Carlsbad, CA, USA). For Sequencing we used the LifeTech Personal Genome Machine (PGM) (Life Technologies, Carlsbad, CA, USA). Sequencing data was analyzed using the IonReporter™ software pipeline (Life Technologies, Carlsbad, CA, USA). Manual review was performed on called mutations in order to reduce the number of false positive calls.

Shallow whole genome sequencing

To further investigate the presence of viral integration into the host genome, we performed WGS. The Illumina NextSeq 500 (Illumina, CA, USA) sequencing platform was used with a 2x150 cycles Mid Output Kit yielding a 10x average read depth. The libraries were prepared using the Illumina Nextera XT DNA Library Prep kit according to protocol. Reads were mapped against the hs37d5 reference genome as well as the BKPyV reference sequence (NCBI acc. no. AB211371). Integration was called if read ends alignment to both reference sequences.

Characterisation of the BKPyV UC

The entire BKPyV genome was sequenced using different primer combinations either directly from the extracted tumour DNA following nested PCR or using the gel-purified long-range PCR products. The sequences were analysed using codon code aligner (Codon Code Corporation, Centerville, MA, USA) and the FASTA files were depicted using ApE[188].

To sequence the BKPyV genome with higher coverage, targeted amplicon sequencing was performed on the Illumina MiniSeq (2x150 cycles using Mid Output Kit) with previously amplified EcoR1 amplicons of 5116bp and 3270bp and libraries prepared with Nextera XT DNA Library Prep kit according to protocol. The data were analysed with the CLC Genomics

Workbench (Qiagen Bioinformatics, Denmark) and the Integrative Genomics Viewer (IGV, Broad Institute, USA). Primers spanning the integration breakpoints were designed based on detection of paired reads from whole genome sequencing aligning to the BKPyV reference sequence and chromosome 1 in the human genome (GRCh37/hg19). Using these primers, the integration of BKPyV into chromosome 1 was confirmed and the integrated parts of the genome sequenced by Sanger sequencing.

Results

Histopathology

The morphological picture of the early tumours from 8 (pTa, high-grade) and 9 years ptx (pT1, high-grade) differs from the one of the three sites obtained 10 years ptx (pT3, G3). In the 8y- and 9y-ptx tissue samples, we saw an ordinary high-grade urothelial carcinoma. The 8y-ptx tumour was papillary while the 9y-ptx tissues also had a solid component. However, the 10y-ptx samples showed a micropapillar morphology, clearly differing from the previous tumour appearance. The histopathological findings of all tumour manifestations are summarized in Table S1.

DNA content based cell sorting of tumour-specimen and aCGH

Fluorescent activated flow sorting of cell nuclei from tumour tissue based on DNA content indicated that all analysed tumour samples were composed of a diploid and an aneuploid tumour cell population. We further investigated the aneuploid populations by arrayCGH. The aneuploid populations from 8y- and 9y-ptx displayed distinct genomic differences with each population harboring several private amplifications and deletions (Figure S2). Consequently, there was no evidence of clonal relationship among these tumours. Furthermore, both aneuploid populations from 8y- and 9y-ptx clearly differed from the three aneuploid 10y cancer samples suggesting that the 8y, 9y and 10y-ptx tumours each represent genomically independent cancer manifestations. Conversely, the aneuploid populations sorted from the pT3 renal pelvis, the pT3 bladder and the metastatic lymph node manifestations at 10y-ptx shared a common profile. The only exceptions were a private amplification at 6p12.3 and a private deletion at Xp22.33 - Xp22.11 in the bladder manifestation of the 10y-ptx tumour (Figure S3 + Figure 1B). Regarding the copy number variations (CNV) of relevant tumour suppressor genes and oncogenes in the 10y ptx samples, we found low-level gains in CTNNB1, ERBB2, GNAS and SRC. ArrayCGH did not show any deletions of tumour suppressor genes. All microarray files have been deposited at the National Center for Biotechnology Information Gene Expression Omnibus (accession number GSE90778).

Short tandem repeat analysis (STR)

DNA-amplification of tumour samples from year 8 and 9 was not successful presumably due to poor DNA quality. However, bulk-tissue cuts of all 10y cancer samples as well as several healthy tissue samples from the donor and the recipient were suitable for STR analysis. We could define a distinct recipient's healthy profile in all 16 STR-systems. Due to contamination with recipient derived blood cells or ingrown stromal cells we expected the donor's healthy specimen to show a mixed profile. As such, main-profile (MP) and a side-profile (SP) were discriminated in the donor's healthy specimen. All detected alleles of the SP were identical with the recipient's profile. All 10y-ptx cancer specimens showed a mixed profile consisting of a donor derived MP and a recipient derived SP. The detailed STR-results are depicted in the Table S3.

In summary, the STR analysis demonstrated that the 10y-ptx cancer manifestations identified in the allograft kidney pelvis (pT3), in the patient's own bladder (pT3a / CIS) and in a single pelvic lymph node metastasis, were all of donor-origin.

Next generation sequencing

Polymerase chain reaction (PCR) based DNA-amplification of tumour samples from 8y- and 9y-ptx was not successful (see above). However, NGS revealed 18 genomic nucleotide variants in all three 10y-ptx cancer samples. According to the University of California, Santa Cruz (UCSC) common single nucleotide polymorphism (SNP) database, 15 of them were reported SNPs. In none of the investigated 50 cancer genes somatic mutations were identified. The remaining three nucleotide variants are not yet classified SNPs or known somatic mutations by publicly available databases. Of these, one did not pass a threshold of 10% allele ratio and therefore has a high odds for being an amplification artefact. The two other nucleotide variants were: KDR / InDel chr4:55962545 and Akt1 / c.138C>A. Further details are shown in Table S2.

Characterisation of the BKPyV UC

The BKPyV viral load in the 10y-ptx UC tissue samples was determined by real-time PCR as 1 BKPyV copy per diploid human cell using the human acetylase gene as normalisation reference [7, 10] . No BKPyV DNA could be detected in healthy tissue from the same time point. To characterise the BKPyV UC genome, two primers targeting the conserved EcoR1 site in the BKPyV VP1 capsid gene were used in an outward orientation. As shown in Figure 2A, two fragments corresponding to a full-length BKPyV genome of 5,116 bp and a shorter fragment of 3,270 bp were generated, whereas no products were obtained from unaffected tissue DNA. Sequencing of the larger fragment revealed a complete BKPyV genome bearing

a total of 49 single nucleotide differences from the BKPyV archetype sequence in LTag, sTag, VP1 and VP2 (data not shown), with the exception of a 17 bp deletion in the P-block of the NCCR (Figure 2B). The shorter fragment represented a truncated BKPyV genome due to a 1.9 kb deletion from the small T-antigen coding region at bp position 4668 to the VP2 coding region at position 1398 bp, which removed the N-terminal coding region of LTag and sTag, and the NCCR, and thereby could not account for the LTag-positive staining. Also removed were the entire agnoprotein and N-terminal parts of the VP2, while the remaining part shared all 36 single nucleotide differences present the complete BKPyV UC genome. These results were confirmed by direct nested PCR and sequencing from the UC tissue. Given the unique BKPyV UC del-NCCR and the well documented role of NCCR rearrangements for constitutive up-regulation of the BKPyV EVGR expression at the expense of LVGR expression [10], a functional analysis was performed by inserting the BKPyV UC-NCCR into the previously described bi-directional reporter construct carrying the red fluorescent protein (dsRed) and the green fluorescent protein (EGFP) as markers for EVGR and LVGR expression, respectively (Figure 2C). Following transfection of human embryonic kidney (HEK) 293 cells and single-cell analysis by flow cytometry, the UC 1A-NCCR conferred a moderate activation of EVGR expression (red) of 2 – 3 fold as compared to the archetype BKPyV ww-NCCR carrying the full-length sequence. To investigate effects of the UC-NCCR deletion on viral replication, recombinant BKPyV genomes were generated that only differed in the respective NCCR and then compared for replicative capacity following infection of hRPTEC cells (Figure 2D). The results demonstrate that the replicative capacity of the BKPyV UC-NCCR strain was significantly impaired compared to the archetype ww-NCCR. In contrast, the laboratory adapted Dunlop-NCCR or a recently identified point mutant sp1-4-NCCR showed a much higher replication rate (Figure 2D). Taken together, the molecular characteristics of the BKPyV-UC strain suggest that this variant significantly activates EVGR expression and contributes to LTag expression, but that this unique 17bp deletion impairs progression into the late viral life cycle and thereby offsets efficient lytic replication.

Tables and figures

Sample	TNM	Morphology	SV-40 Status
Bladder 8y	pTa, high-grade	non-invasive papillary UC	positive
Bladder 9y	pT1, high-grade	mainly solid UC	positive
Allograft-kidney 10y	pT3, high-grade, L1, V1, Pn0	partly necrotic, mainly micropapillary UC	positive
Bladder 10y	pT3a, pN1 (1/5), G3, L1, V0, Pn1	mainly micropapillary UC	positive
Lymphnode metastasis 10y	not available	micropapillary UC	positive

Table S1. Summary of histopathological results

		mutant allele ratio			No. of reads		
gene	**mutation**	**kidney**	**bladder**	**lymphnode**	**kidney**	**bladder**	**lymphnode**
ERBB4	chr2:212812097T>C	0.056	0	0.0065	339	498	153
PIK3CA	c.3100G>C	0.0895	0.0014	0	1999	2799	929
PIK3CA	chr3:178917005A>G	0.02	0.0844	0.0677	750	1007	310
PDGFRA	c.1701A>G	1	1	1	1195	1957	513
PDGFRA	c.2472C>T	0.4905	0.443	0.3766	>2000	>2000	1240
KIT	c.1621A>C	0.034	0.0745	0.146	1999	>2000	1315
KDR	InDel chr4:55962545	0.4566	0.7807	0.605	1520	>2000	524
KDR	c.1416A>T	0.5508	0.6131	0.5972	1910	1998	648
KDR	chr4:55980239C>T	1	1	0.9887	659	990	266
APC	c.4479G>A	0.0725	0.1939	0.2377	1985	1991	1296
CSF1R	chr5:149433596TG>GA	1	1	1	376	1193	625
EGFR	c.2361G>A	0.5303	0.4796	0.5311	594	1203	563
RET	c.2307G>T	0.4992	0.5298	0.4303	1238	1997	1636
RET	c.2712C>G	0.5207	0.3983	0.372	822	1996	1148
HRAS	c.81T>C	0.9325	0.8744	0.8401	696	1999	1676
FLT3	chr13:28610183A>G	1	1	0.9906	1998	1997	1909
AKT1	c.138C>A	0.4949	0.3569	0.466	681	1998	1219
TP53	c.215C>G	0.941	0.9715	0.9435	763	>2000	885
DERL3	chr22:24176287G>A	0.4773	0.6243	0.4764	484	1171	741

Table S2. NGS-results of 10y ptx UC sites

Marker	Recipient Control	Donor Control	Bladder 10y	LN 10y	Kidney 10y
D3S1358	17	**15,16,**(17)	**15**,(**16**,17)	**15**,(**16**,17)	**15,(16,**17)
D19S433	13/15.2	**14,**(13,15.2)	**14**,(13,15.2)	**14**	**14,**(15.2)
D2S1338	22/23	**20,24**	**20**,(22,23)	**20**	**20,**(22,**24)**
D22S1045	11	11**,15,16**	11**,15,16**	n.r.	11**,15,16**
D16S539	12	**11,13**(12)	**11**,12	**11,13,**(12)	**11,13**(12)
D18S51	13/17	**14,17,**(13)	**14,17**,(13)	**14,17**,(13)	**14,17,**(13)
D1S1656	15/16	**16,16.3**	**16.3**,(15,**16**)	**16.3**,(**16**)	**16.3**,(15)
D10S1248	13/14	**16**	**16**,(13,14)	**16**,(13)	**16**,(13,14)
D2S441	11/12	**14**	11,**14**,(12)	(12)	**14**, (11)
TH01	7/9	**6,7**	**7,**(9)	**7**	**7**,(**6**,9)
vWA	18/19	**14,16**,(18,19)	**14,16**, (18,19)	**14,16**,	**14,16**,(18,19)
D21S11	30/31.2	**28,30.2,**(30)	**30.2**,(30,31.2)	**30.2**	**30.2,**(**28,**30, 31.2)
D12S391	17/19	**16,19**,(17)	**16,19**,(17)	**16,19**,17	**16,19**,(17)
D8S1179	12/13	**10,13**,(12)	**10,13**,(12)	**10,13**,(12)	**10,13**,(12)
FGA	21/24	**22**,(21,24)	21,**22**,(24)	**22**,(21)	**22**,(21,24)
SE33	15/30.2	**18,19,**(15)	**18,19**, (15,30.2)	**18,19**	**18,19,**(15,30.2)
Amelogenin	XY	XY	XY	XY	XY

Table S3. Tabular summary of STR results

Primer/Probe Name	Sequence
EcoRI_F	5'-CAA GAA TTC CCC TCC CCA ATT TAA ATG-3'
EcoRI_R	5'-GGG GAA TTC TTG CTG TGC TGT AAC-3'
Chr1 / BKPyV Breakpoint 1_F	5'-CGC AGG AAG CAG AAA AAG ATC-3'
Chr1 / BKPyV Breakpoint 1_R	5'-GAA ACT GCT TCC CAA TGC CTA G-3'
Chr1 / BKPyV Breakpoint 2_F	5'-GGA AGC AGA AAA AGA TCT GTA AAA AAT CC-3'
Chr1 / BKPyV Breakpoint 2_R	5'-GTG TCC AGC AGA AAC TGC TTC CCA ATG-3'
Chr1 / BKPyV Breakpoint 3_F	5'-CAC CAA CCG CAG GAA GCA GAA AAA G-3'
Chr1 / BKPyV Breakpoint 3_R	5'-GCA GAA ACT GCT TCC CAA TGC-3'
BK Vp1 qPCR_F	5'-CCT AGA TGC TAT AAC AGA GGT AG-3'
BK Vp1 qPCR_R	5'-TTC TGG GCT ATC ACT GCT AAA GTT-3'
BK Vp1 qPCR_Probe	6-FAM-A TCC AGA TGA AAA CCT TAG GGG CTT TAG TC-BHQ1
BK LTag_F_DEG2	5'-AGC AGG CAA CDG TTC TAT TAC TAA AT-3'
BK LTag_R_DEG	5'-GAT GCA ACA GCA GAT TCA CAA CA-3'
BK LTag_Probe_DEG	6-FAM-AAG ACC CTA AAG ACT TTC CAT CTG ATC TAC ACC AGT TT-TAMRA
ACY qPCR_F	5'-CCC TGC TAC GTT TAT CTG ATT GAG-3'
ACY qPCR_R	5'-CCC ACA GGA TAC TTG GCT ATG G-3'
ACY qPCR_Probe	6-FAM- CCT TCC AAA TAT GCG ACC ACT CG-TAMRA

Table S4. Primer and probe sequences

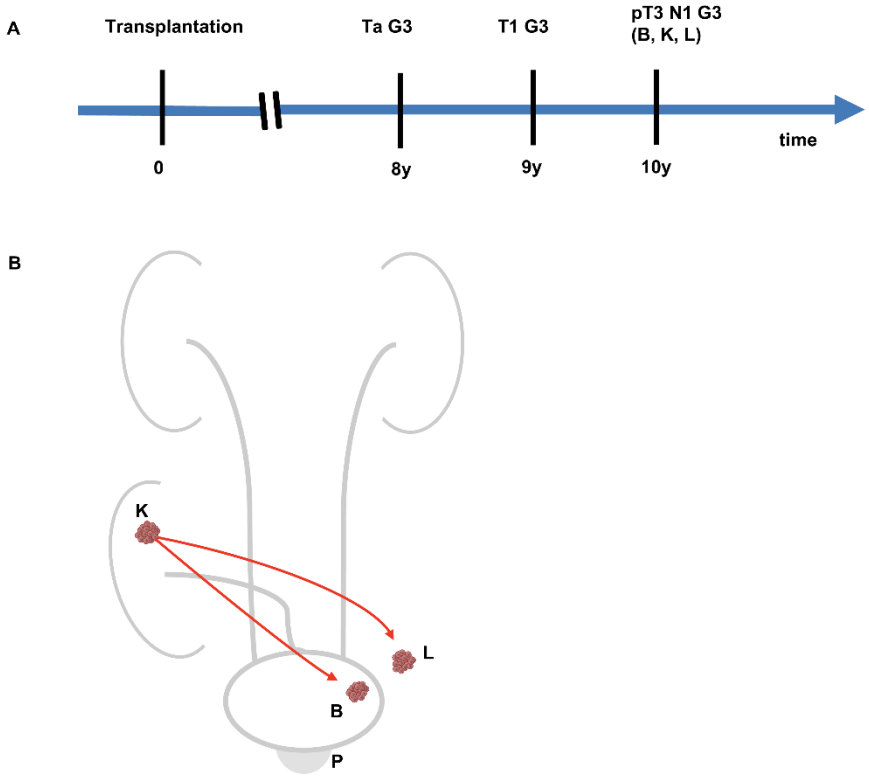

Figure S1. Overview over disease progression and cancer distribution 10y ptx. **A.** Timeline (years ptx) of clinical manifestations of UC in the kidney transplant recipient. **B.** Schematic illustration of cancer localisations and the assumed metastatic spread from the donor kidney UC. Cell-bulk indicates UC localisations. Arrows indicate assumed metastatic spread. (B: Bladder, left bladder side / apex. L: Lymph node, left Arteria iliaca externa. K: Kidney, pyelon of allograft. P: Prostate, adenocarcinoma, Gleason 6 (3+3), max. diameter 7 mm).

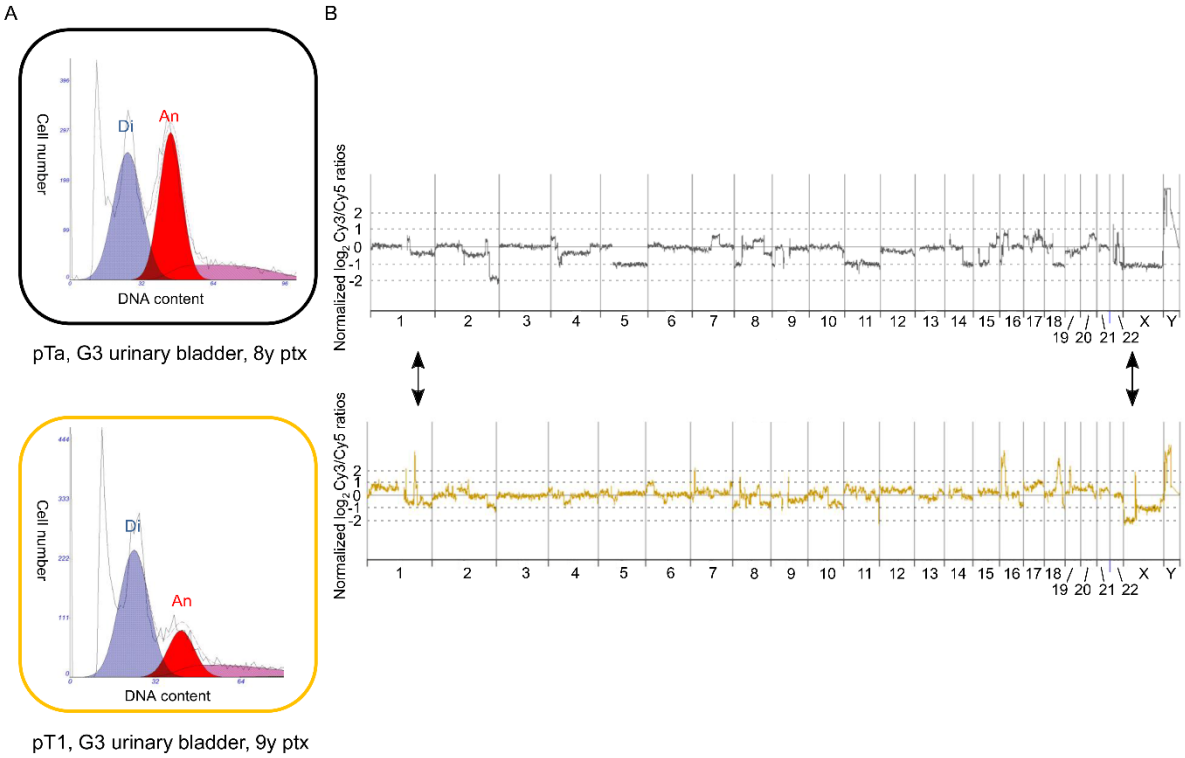

Figure S2. Sorting and arrayCGH profiles of cancer sites 8y and 9y ptx. **A**. Sorting profiles. Di: Diploid population; An: Aneuploid population; X-axis: DAPI-fluorescence units x1000 – linear scale; y-axis: cell nuclei count in total numbers; blue colour: G1/G2-phase diploid population; red colour: G1/G2-phase aneuploid population; violet colour: cells in s-phase. **B**. ArrayCGH profiles with copy number alterations of aneuploid cancer populations 8y and 9y ptx. The two samples appear unrelated; arrows indicate examples of relevant differences. X-axis: chromosome number; Y-axis: Normalized log2 Cy3/Cy5 ratios (relative count of DNA-probe signals).

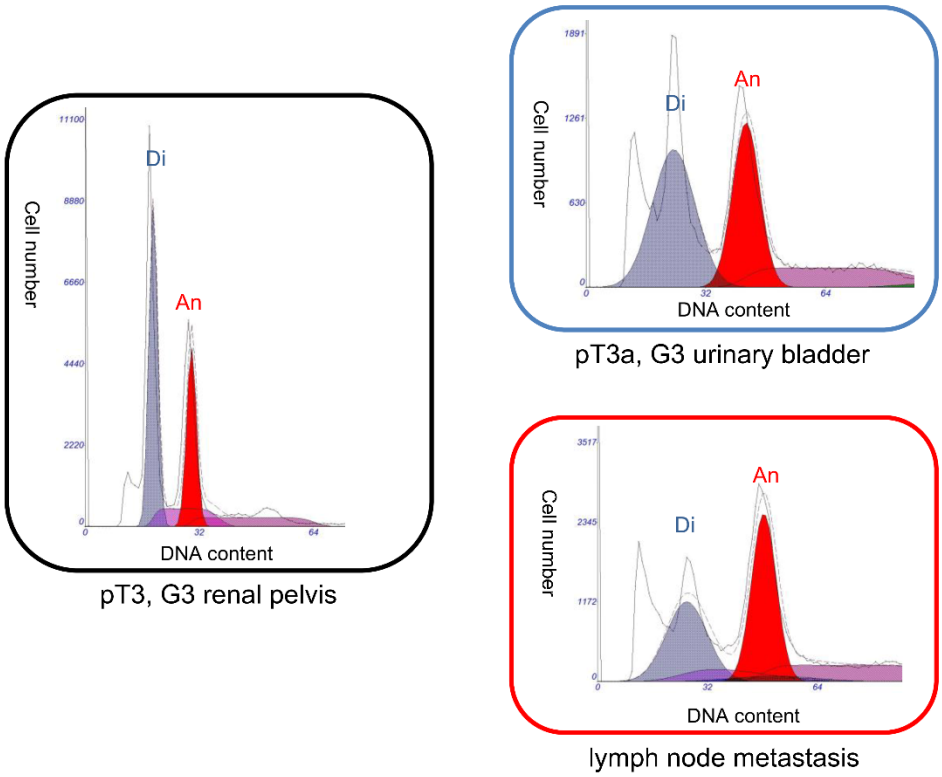

Figure S3. Sorting profiles of UC sites 10y ptx. Di: Diploid population; An: Aneuploid population; x-axis: DAPI-fluorescence units x1000 – linear scale; y-axis: cell nuclei count in total numbers; blue colour: G1/G2-phase diploid population; red colour: G1/G2-phase aneuploid population; violet colour: cells in S-phase.

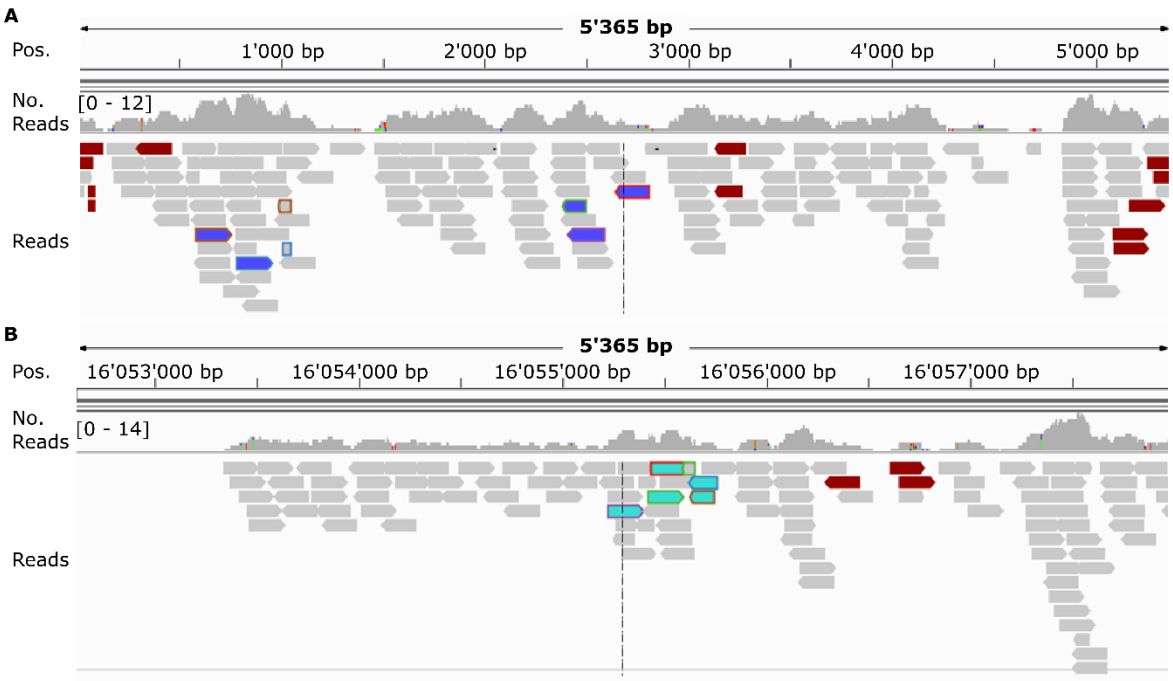

Figure S4. Detection of BKPyV integration site in chromosome 1 using WGS. The image was generated using the integrated genomics viewer (IGV, Broad Institute, MIT). A. Reads from WGS aligned to BKPyV ww strain (GenBank acc. no. AB211371). B. Reads from WGS aligned to the human reference genome hg19 (Chromosome 1 shown). Arrow on top indicates the range of bp in the image section of the genome. Numbers below arrow show the bp position at the reference genome. Numbers in brackets indicate the range of read depth. Fine columns show read depth at single base level. Arrow shaped boxes at the bottom indicate individual reads. Mate pairs are marked in the same colour, at integration of the viral genome into chromosome 1 of the human genome.

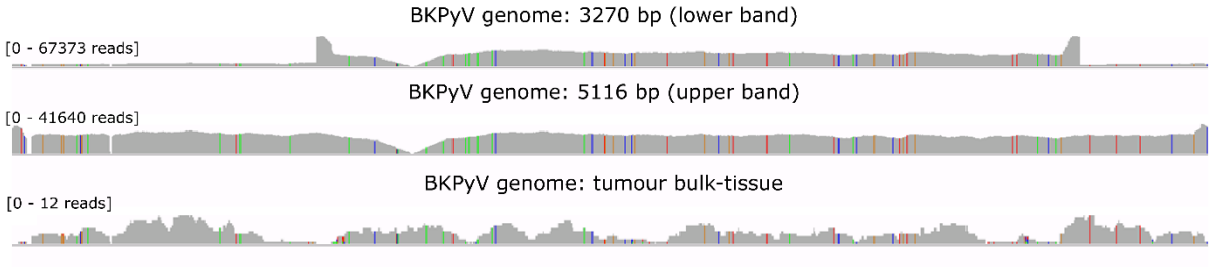

Figure S5. Coverage of targeted amplicon sequencing of BKPyV aligned to BKPyV ww strain (GenBank acc. no. AB211371) as compared to shallow WGS of the same region of the virus. Upper panel, shorter episomal BKPyV genome of 3270bp; middle panel, larger episomal BKPyV genome of 5116bp; lower panel, whole genome sequencing. Numbers in brackets indicate the range of read numbers. Fine columns show read depth at single base level. Colours (other than grey) of columns indicate single nucleotide variants compared to the reference genome.

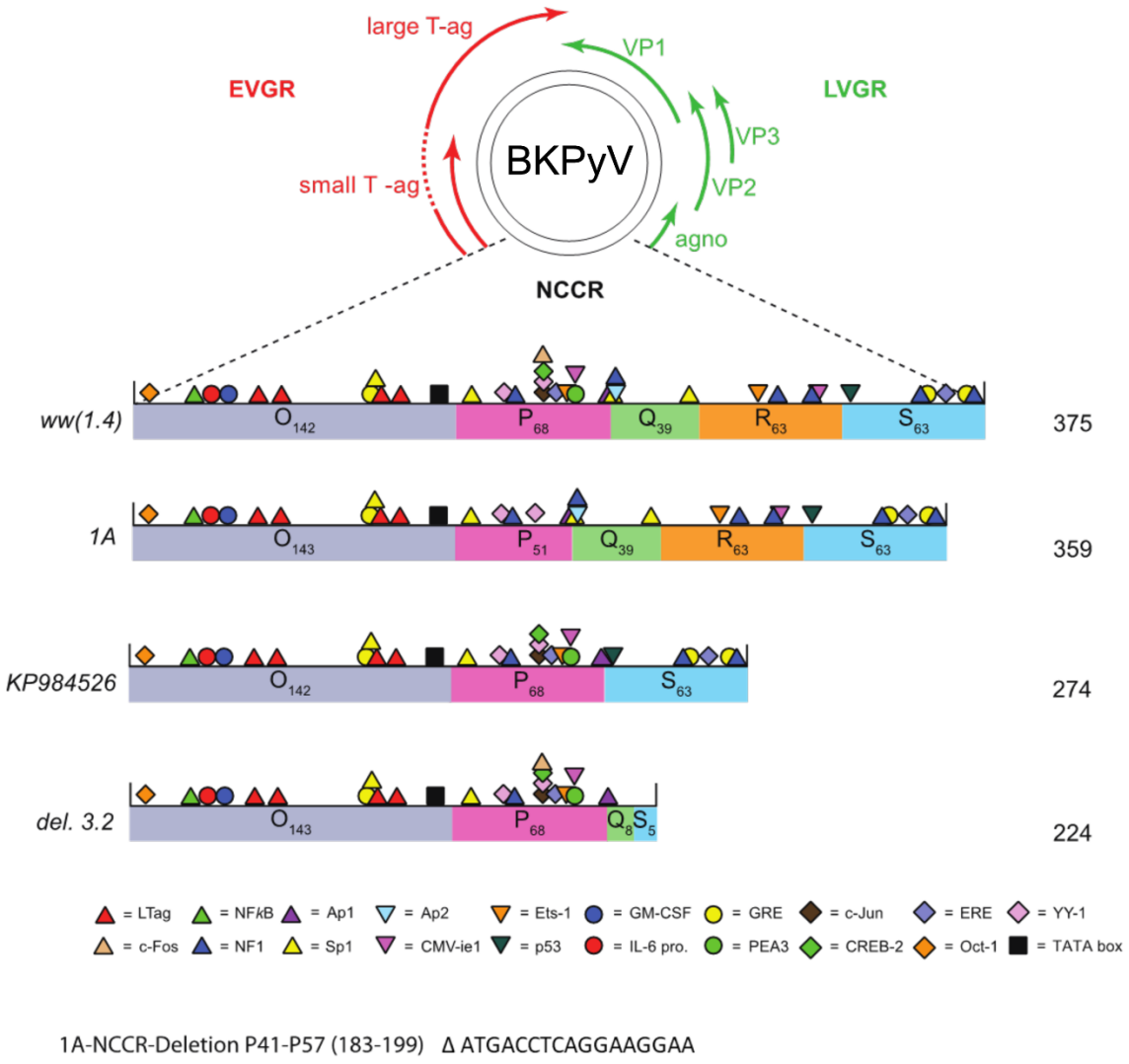

Figure S6. Comparison of BKPyV-NCCR transcription factor binding sites. From top to bottom: (ww1.4) denotes BKPyV archetype NCCR (; 1A 17bp-deletion NCCR P41-P57 (183-199) of the UC reported here; KP984526 NCCR deletion described in [18]; del(3.2) NCCR reported in [10, 11] indicating that deletions of Q and R blocks are not specific for cancer, but promote increased EVGR expression. EVGR, early viral gene region; LVGR, late viral gene region; NCCR, non-coding control region.

Heterogeneity of DNA ploidy in the context of clonal evolution in prostate cancer

Abstract

Background. Prostate cancer is known to be morphologically and molecularly heterogeneous. Genomic heterogeneity might be mirrored by different DNA ploidy status. Aneuploidy is a hallmark of genomic instability and is associated with tumor aggressiveness. However, little attention has been paid to the biological significance of the diploid tumor cell population that sometimes coexist with aneuploid populations. Here, we investigated the relevance of DNA ploidy in tumor heterogeneity and clonal evolution.

Methods. Six radical prostatectomy specimens with intratumoral heterogeneity based on nuclear features on H&E were selected for the study. DNA content of each subpopulation was determined by DNA image cytometry and silver in situ hybridization (SISH). Genomic evolution was inferred from array comparative genomic hybridization (aCGH). Additionally, immunohistochemistry was used to examine the stemness-associated marker ALDH1A1.

Results. Nuclear morphology reliably predicted DNA ploidy status as defined by DNA image cytometry and SISH (n=6/6). In one out of the two samples with conclusive results, aCGH analysis revealed a clonal relationship of the diploid and the aneuploid subpopulations. Furthermore, ALDH1A1 was enriched in two diploid populations.

Conclusions. In this proof-of-concept study, we demonstrated the feasibility to predict the DNA ploidy status of distinct populations within one tumor by morphology on H&E. Furthermore, we found a clonal relationship between the diploid and the aneuploid subpopulation, indicating that the aneuploid population derived from the diploid one. Finally, our analyses pointed to an enrichment of the stemness-associated marker ALDH1A1 in diploid populations, which warrants further investigation in future studies.

Introduction

Prostate cancer (PC) is morphologically and molecularly heterogeneous. One way to measure tumor heterogeneity is at the level of DNA ploidy. Aneuploidy is defined as an abnormal DNA content of somatic cell nuclei due to unbalanced gain or loss of individual chromosomes or large parts of chromosomes[189,190]. This is distinct from polyploidy, which is defined as extra copies of the entire genome, such as tetraploidy (4N). Whereas polyploidy can be found in some types of benign cells as part of a physiological process, aneuploidy is a hallmark of

genomic instability and is associated with disease and tumorigenesis[191]. Consequently, aneuploidy is a common feature of human cancer. Furthermore, it is associated with tumor progression and tumor aggressiveness[192]. This is also supported by increased proliferative activity in aneuploid tumor cell populations[193].

Several studies have analyzed the role of ploidy in PC with respect to tumor progression and clinical outcome[153,194–196]. They have shown a correlation between aneuploidy and other prognostic factors and poor prognosis[197–201]. However, in a multivariate analysis comparing different parameters such as grade, ploidy, surgical resection margins, and capsular penetration, ploidy remained an independent prognostic factor only for a subset of well and moderately differentiated PC[197]. More recently, Stopsack et al. demonstrated that aneuploidy was a negative predictor of outcome even among patients with high-risk PC with Gleason scores 8-10[151]. Moreover, they suggested that aneuploidy might serve as a marker to identify patients at higher risk of progression to lethal disease after curative surgical treatment and might be associated with response to adjuvant therapy with docetaxel.

It has been recognized that diploid and aneuploid tumor cells commonly coexist in PC[199,202,203]. There is marked variation in the reported frequency of such intratumoral heterogeneity of the ploidy status in PC, ranging from 4.2% to 58%. This variation can be partly explained by technical issues, such as different sizes of the specimens analyzed in the studies[203]. However, the biological significance of intratumoral heterogeneity of the ploidy status and the question of whether the diploid and aneuploid subpopulations within a tumor are related to each other or whether they represent independent clones still remains to be clarified.

Here, we aimed to predict the ploidy status of distinct populations within one tumor area by hematoxylin and eosin (H&E) morphology and to explore the clonal relationship between concomitant diploid and aneuploid tumor cell populations.

Material and Methods

Study population/Tissue samples

Radical prostatectomy specimens from six patients with prostate adenocarcinoma were chosen for this study and retrieved from the archives of the Institute of Medical Genetics and Pathology Basel (2012-2014) (Table S5). We specifically selected cases with clear morphological discrimination between a diploid- and an aneuploid-looking cell subpopulation within a tumor, based on the nuclear features on H&E stained whole mount sections. Additionally, these distinct populations needed to be in a close topographical relationship or

within the same tumor area in order to avoid analysis of clonally unrelated tumors within the same prostate (Figure 4). The tumor cell content of either population was at least 200 cells. We defined morphological criteria for the distinction between diploid- and aneuploid-like cells as follows: "diploid-like" tumor cells: monomorphic nuclei (small, round, regular membranes), nucleoli: small and inconspicuous, chromatin: fine and evenly distributed, low nuclear/cytoplasmic ratio; "aneuploid-like" tumor cells: anisonucleosis, pleomorphic cell population, nuclei: large (≥2x the diameter of a benign glandular prostate cell), irregularly shaped, irregular nuclear membranes, nucleoli: large, red, several in number, chromatin: coarse, irregular, high nuclear/cytoplasmic ratio (Table 1).

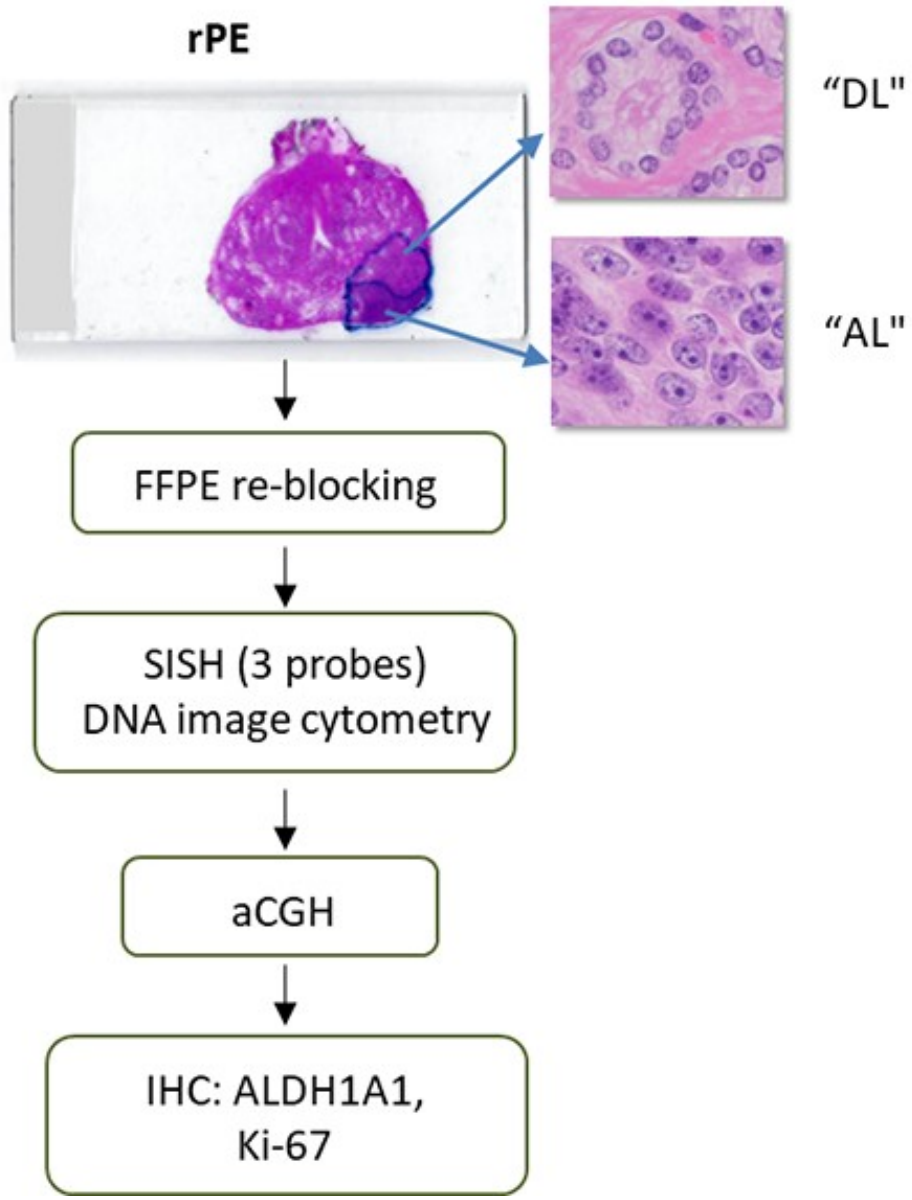

Figure 4. Study design. rPE, radical prostatectomy; DL, diploid-like; AL, aneuploid-like; FFPE, formalin-fixed paraffin-embedded; SISH, silver in situ hybridization; aCGH, array comparative genomic hybridization; NGS, next-generation sequencing; IHC, immunohistochemistry.

	"Diploid-like" tumor cells	"Aneuploid-like" tumor cells
Nuclei	Monomorphic, small, round, regular membranes	Anisonucleosis, pleomorphic, large*, irregularly shaped, irregular membranes
Chromatin	Fine, evenly distributed	Coarse, irregular
Nucleoli	Small, inconspicuous	Large, red, several in number
N/C Ratio	Low	High

Table 1. Morphological criteria for "diploid-like" and "aneuploid-like"; * ≥2x the diameter of a benign glandular prostate cell

Enrichment for tumor cells

To enrich for tumor cells in the two morphologically identified distinct tumor regions, we cut out the respective areas of the original formalin-fixed paraffin-embedded (FFPE) blocks and re-embedded them in separate FFPE blocks. Each of the six selected cases had an FFPE block containing the diploid looking and the aneuploid-looking tumor cell population, respectively.

Silver in situ hybridization

Tissue sections of 4µm were cut from FFPE blocks. Silver in situ hybridization (SISH) with centromere probes for chromosomes (CEP) 7, 17, and 18 was performed according to the manufacturer's protocols using the Ventana ultraView SISH Detection Kit on the BenchMark XT automated slide stainer (Ventana Medical System Inc., Tuscon, AZ). Fifty tumor cells were scored for each probe, and the mean value was determined. Diploid status was defined as mean values between 1.5 and 2 signals per CEP and tetraploid/aneuploid status as mean values of >2 signals per CEP.

DNA image cytometry

DNA image cytometry (DNA ICM) was performed at the Institute of Pathology, Cantonal Hospital St. Gallen. Between 262 and 453 cells were selected from each slide for manual DNA measurement by static DNA ICM using an AutoCyte QUIC DNA workstation (TriPath Imaging Inc., Burlington, North Carolina, USA) on H&E prestained and Feulgen-restained slides. Benign fibroblasts served as reference cells for a diploid DNA content (2c). DNA ploidy classes were defined as (i) diploid with a main peak in the 2c region, (ii) tetraploid with a main peak in the 4c region, and (iii) aneuploid with a main peak around 4c region and a varying number of cells outside. Here, the tetraploid and the aneuploid status will be summarized as non-diploid status as opposed to diploid status.

Immunohistochemistry

Tissue sections of 4µm were cut from FFPE blocks. Standard indirect immunoperoxidase procedures were used for the detection of Ki67 (clone MIB1, prediluted, DAKO, Glostrum, Denmark) and ALDH1A1 (clone ab51028, Abcam, Cambridge, UK) at 1:200 dilution as previously reported[204]. The analyses were performed on the BenchMark XT automated immunostainer using the OptiView detection system (Ventana Medical System Inc.). GraphPad Prism software (version 8) was used for statistical analyses.

Array comparative genomic hybridization

DNA extraction from tumor-enriched re-embedded FFPE blocks was performed with the Maxwell 16 Tissue DNA Purification Kit (Promega Corporation, Madison, Wisconsin). We used an input of 100 ng tumor DNA per sample and performed aCGH, as previously described[173].

Results

Correlation between nuclear morphology and DNA ploidy

To verify the ploidy status of the morphologically distinct tumor populations defined as diploid-like and aneuploid-like on H&E, the DNA content of each subpopulation was estimated by SISH and DNA ICM (Figure 5). SISH was available in all six cases except for CEP 18 in case 2. In all six cases, analysis of nuclear morphology was able to predict DNA ploidy defined by SISH results. DNA ICM was not available for one patient (case 3). For the others, DNA ICM was consistent with morphology and SISH in the majority of cases defined as diploid-like (n=4/5), except in case 4a that revealed a tetraploid population instead of a morphologically predicted diploid population. It is possible that the deeper tissue section sent for DNA ICM no longer contained the diploid-like tumor population. For morphologically aneuploid-like tumor areas, DNA ICM revealed tetraploid/aneuploid populations in the majority of cases (n=4/5), except in case 6b that revealed a diploid population. Likewise, it is possible that the deeper tissue section sent for DNA ICM did not contain the aneuploid-like tumor population. The results are summarized in Table 2.

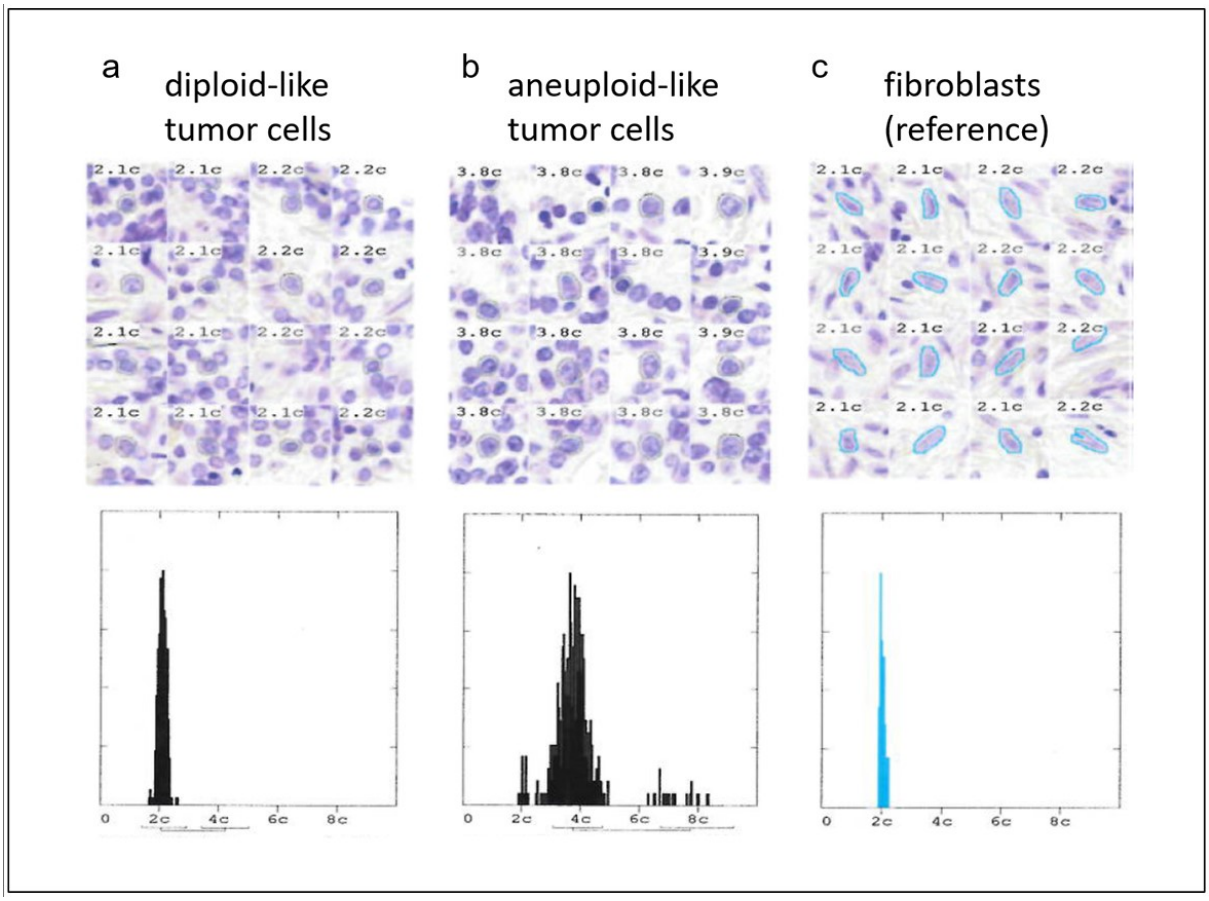

Figure 5. DNA image cytometry from case 1. a Diploid-looking tumor population with a main peak in the 2c region. b Aneuploid-looking tumor population with a main peak in the 4c (tetraploid) region. c Fibroblasts as reference cells for a diploid DNA content (2c).

Case	H&E	DNA ICM	SISH (mean for CEP 7, 17, 18)	ALDH1A1	Ki67 LI (%)
1a	DL	Diploid (2.08c)	<2 (1.9; 1.7; 1.9)	Positive	5
1b	AL	Tetraploid (3.76c)	>2 (3.7; 3.4; 4.0)	Negative	20
2a	DL	Diploid (2.07c)	<2 (1.9; 1.8; N.A.)	Negative	5
2b	AL	Tetraploid (3.92c)	>2 (2.7; 3.6; N.A.)	Negative	15
3a	DL	N.A.	<2 (1.8; 1.8; 1.9)	Positive	5
3b	AL	N.A.	>2 (2.9; 2.9; 3.0)	Negative	10
4a	DL	Tetraploid (3.86c)	<2 (1.7; 1.8; 1.8)	Negative	5-10
4b	AL	Aneuploid (3.44c)	>2 (3.3; 3.0; 3.3)	Negative	15
5a	DL	Diploid (2.02c)	<2 (1.7; 1.5; 1.6)	Negative	5
5b	AL	Tetraploid (3.89c)	>2 (2.9; 2.1; 2.9)	Negative	15-20
6a	DL	Diploid (2.04c)	<2 (1.9; 1.8; 1.8)	Negative	<5
6b	AL	Diploid (2.08c)	>2 (2.9; 4.4; 2.9)	Negative	15

Table 2. Summary of the results. H&E, hematoxylin and eosin; DNA ICM, DNA image cytometry; SISH, silver in situ hybridization; CEP, centromere probes; Ki67 LI, Ki67 labeling index, DL, diploid-like; AL, aneuploid-like; N.A., not available

Clonal relationship between the diploid and the aneuploid tumor population

To investigate clonal relationship, we performed aCGH and compared the chromosomal aberrations found in the diploid- and aneuploid-like tumor populations, respectively. In case 3, we identified several shared deletions (on chromosomes 1q, 4q, 6q, 8p, 13q, and 16q) and one amplification (on chromosome 8q) across the genome in both the diploid and the aneuploid population, suggesting a clonal relationship. The aneuploid population additionally showed an amplification on chromosome 16p (Figure 6).

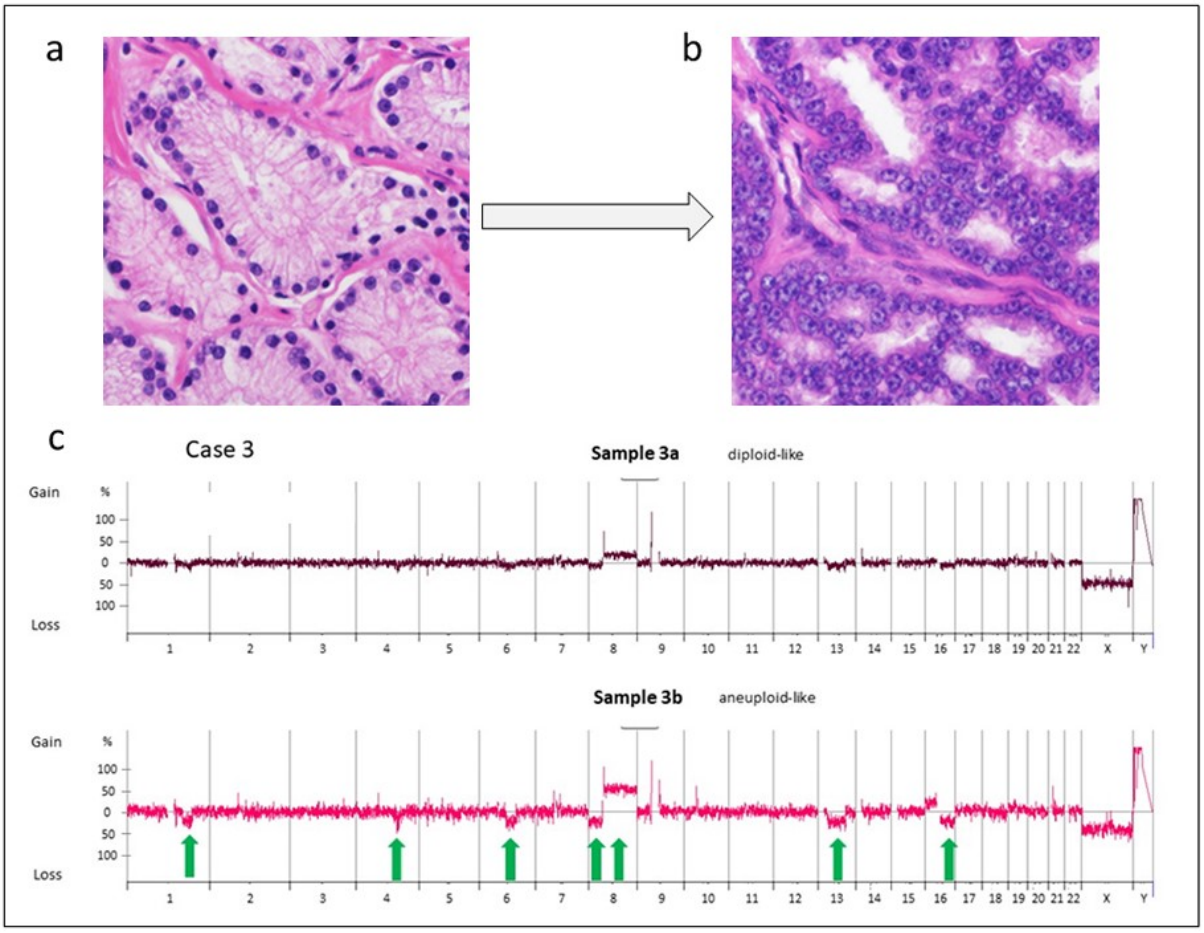

Figure 6. Case 3. a, b Morphology of the diploid-like (a) and aneuploid-like (b) tumor populations (H&E, magnification 400x). c aCGH-profiles indicating several shared chromosomal aberrations in the diploid and aneuploid tumor populations. Numbers indicate chromosomes. Y-axis indicates copy number changes. Arrows indicate relevant (shared) copy number changes.

In cases 1, 4, 5, and 6, aCGH did not reveal any unequivocal copy number variations (CNVs) in the diploid populations, which can partly be explained by a low resolution due to a low tumor cell content. In contrast, the associated aneuploid tumor populations showed several CNVs (Figure S7-S10). In the absence of shared chromosomal aberrations, however, we can neither prove nor rule out a clonal relationship between the diploid and the aneuploid populations. In case 2, the diploid population showed a deletion on chromosome 8p without any other CNVs. The aneuploid tumor population showed deletions on several chromosomes, but did not share the one on chromosome 8p (Figure S11).

Expression of a stemness-associated marker in the diploid tumor population

To test if the diploid tumor populations were enriched for stem cell markers, we performed immunohistochemistry for ALDH1A1. ALDH1A1 expression was exclusively observed in the diploid population of 2/6 cases in 80% and 90% of the tumor cells, respectively. In contrast, all

six aneuploid populations were ALDH1A1 negative. The fraction of Ki67-positive tumor cells (i.e., Ki67 labeling index (LI)) was determined to compare the proliferation index between the diploid and aneuploid populations. In all six cases, Ki67 LI was lower in the diploid population (range: <5-10%; median 5%) than in the aneuploid population (range: 10 - 20%; median 15%; p 0.0313).

Discussion

The transition from a diploid state to an aneuploid state over time has been studied in precancerous lesions such as cervical intraepithelial lesions of the uterine cervix[205] and Barrett dysplasia in the esophagus[206]. Likewise, it is generally accepted that in invasive carcinoma, aneuploidy results from chromosomal changes acquired during the progression of initially diploid tumors[207]. Therefore, it is not uncommon to find diploid and aneuploid subpopulations within the same tumor. Heterogeneity of DNA ploidy in PC has been a topic of interest in studies dating from over 20 years ago[155,199,208]. At that time, the focus was on evaluating the potential prognostic value of ploidy. For example, in 1991, Greene et al. compared the DNA ploidy status in individual cancer foci within prostatectomy specimens in patients with early-stage PC[155]. They found that 60% of all cancer foci were diploid, 40% were non-diploid, and that ploidy status correlated with tumor volume and Gleason grade. Here, we demonstrate the coexistence of diploid and aneuploid subpopulations within one continuous tumor area. Moreover, we show that the ploidy status defined by DNA ICM and SISH can be predicted by morphology on H&E, based on the degree of nuclear atypia (Figure 7). The value of nuclear grading in PC has been previously extensively studied. Helpap and colleagues defined morphological criteria for a nuclear grading based on features of nuclei, chromatin, and nucleoli[209,210] and proposed to combine it with the established Gleason grading to improve grading accuracy[211,212]. However, while the Gleason pattern is generally used to grade PC, nuclear features, or rather the degree of nuclear atypia, has not become part of the routine diagnostic assessment[36].

More recently, Andor et al. correlated genetic and morphological heterogeneity across different tumor types[213]. They found that higher morphological heterogeneity, defined by higher variability in nuclear size and hyperchromasia, was associated with higher genetic heterogeneity. In addition, the presence of more than two clones was associated with worse prognosis. This implicates that morphological heterogeneity could be used as a surrogate marker of genomic instability and prognosis. In light of this existing evidence, our data illustrate the importance of nuclear morphology as a surrogate marker of DNA ploidy with potential prognostic value.

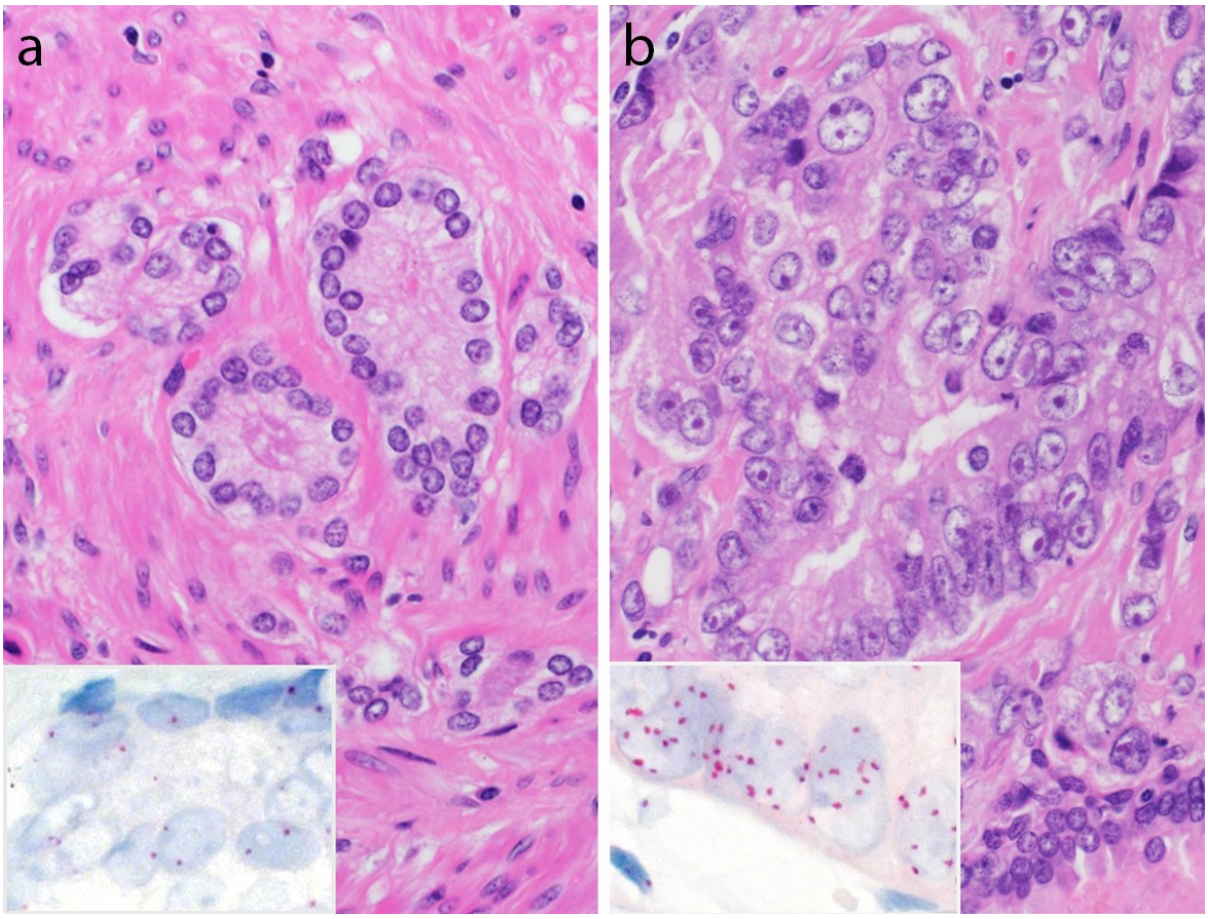

Figure 7. Case 1. a, b Morphology of the diploid-like (a) and aneuploid-like (b) tumor populations (H&E, magnification 200x). Inset: Tumor cells with a normal copy number (a) and increased copy number (b) of CEP17 signals (SISH, magnification 400x).

Exploring the clonal relationship between diploid and aneuploid populations by aCGH in our study was challenged by the low number of CNVs in diploid populations of early prostate cancers. Whole exome sequencing (WES) would be a more sensitive approach to study clonal relationship as it would allow for detection of both somatic mutations and CNVs. Yet the feasibility of this approach in the context of our study was limited by the small specimen size of the respective diploid-like tumor populations and the method of fixation (i.e., formalin), which is not well suited for WES. Nevertheless, aCGH allowed insights into the clonal relationship of distinct tumor populations by outlining the CNV pattern of a subset of samples. As opposed to previous studies investigating intraprostatic tumor heterogeneity in separate tumor areas within the prostate[155,202], we selected PC samples that were in close topographical relationship to each other. This selection increased the probability that the matched samples with diploid-like and aneuploid-like components were clonally related. Following the assumption that the aneuploid population is derived from the diploid one, we expected to find shared chromosomal aberrations within the two populations as well as additional aberrations in the aneuploid population that were acquired over time. Indeed, all six diploid populations showed a virtually

flat copy number profile, whereas numerous aberrations were present in the aneuploid populations. Convincing evidence that the diploid and aneuploid populations are clonally related was found in case 3, where aCGH analysis revealed a subset of shared chromosomal aberrations in both populations. Since the aneuploid population harbored additional chromosomal aberrations, it is plausible to assume that the aneuploid population had evolved from the diploid population. In the other five patients, aCGH did not allow for reliable conclusions either due to lack of CNVs or insufficient content of appropriate-quality tumor DNA of the diploid populations. Interestingly, in patient 2, the presence of a deletion on chromosome 8p in the diploid but not in the aneuploid population could indicate two clonally independent populations or a further acquisition of genomic aberrations of the diploid population after branching of the populations.

PC is known to be a morphologically and molecularly heterogeneous disease. The genomic basis of heterogeneity has been investigated in previous studies, especially with regard to the origin of multifocal disease. Whereas some authors advocate the theory of a "field effect" suggesting that individual foci of multifocal PC are clonally related[214,215], others favor the hypothesis of independent tumor origins[216–218]. These apparently contradictory results may be at least partly explained by the different methods used to assess relationships.

In the present study, we determined the clonal relationship between the diploid and aneuploid population within the same tumor area, which, to the best of our knowledge, has not been addressed before.

We have previously investigated longitudinal clonal evolution over an 8-year period on a multiple biopsy series from a single patient with PC[173]. Similar to the present study, distinct diploid and aneuploid tumor populations were identified in each sample prior to aCGH analysis. Both, a diploid and an aneuploid population were identified at the various time points showing several shared and unique genomic aberrations. Interestingly, a series of identical aberrations was present in the diploid populations across all samples, suggesting that this diploid fraction represented the original clonal population and served as a backbone of clonal evolution. A similar study examined clonal evolution over time in a single patient with metastatic PC[103]. Interestingly, the clonal population found in the metastases originated from a small area of well-differentiated (Gleason pattern 3) carcinoma identified in the radical prostatectomy specimen and not from the predominant, poorly differentiated cancer component (i.e., Gleason pattern 4). This conclusion was based on the detection of shared mutations in the PTEN, TP53, and SPOP genes in the focal Gleason pattern 3 primary tumor and distant metastases, respectively. Of note, the predominant Gleason pattern 4 component in the primary tumor lacked the PTEN and TP53 mutations, suggesting an independent clonal or subclonal origin.

Although there was no information about the ploidy status, well-differentiated PC (i.e., Gleason pattern 3) is likely to be diploid.

In the present study, we have only analyzed the tissue at one timepoint. Nevertheless, based on these observations, we assume that the aneuploid population is likely derived from the diploid one as a result of clonal evolution in most cases. It appears less likely that an aneuploid/tetraploid population adjacent to a diploid population has emerged de novo and is independent from the diploid population. Interestingly, most of the non-diploid populations had a near-tetraploid or tetraploid stemline, suggesting that the diploid population had undergone whole-genome doubling (WGD) during evolution. WGD has recently been recognized as an important and recurrent event during the progression of solid tumors that seems to increase the fitness of tumor cells by relieving the impact of deleterious alterations such as heterozygous deletions[4].

Bearing in mind that PC is genetically heterogeneous, i.e., composed of genetically distinct clonal/subclonal populations, it would be of great interest to identify the original clone or precursor cancer cell in the primary tumor. Previous data indicate that a clone found in the diploid tumor cell population may preferentially drive tumor progression and metastasis[103,173]. Based on this observation, we hypothesized that the diploid population could be enriched for tumor-initiating cells or cancer stem cells (CSC). While the phenotype of prostate CSC is often debated, the aldehyde dehydrogenase isoform ALDH1A1 represents a promising marker, which has been associated with stemness properties and has prognostic and predictive value in PC[204,219,220]. Interestingly, in 2/6 cases, we found a diffuse expression of ALDH1A1 restricted to the diploid population, which was not observed in the concomitant aneuploid population (Figure 8). Thus, although our analyses are limited by a low number of samples, this finding may suggest an enrichment of specific CSC in diploid populations. Given the known contribution of CSC to PC initiation and progression, these findings highlight the need for more comprehensive analyses assessing additional CSC markers in larger cohorts of patients.

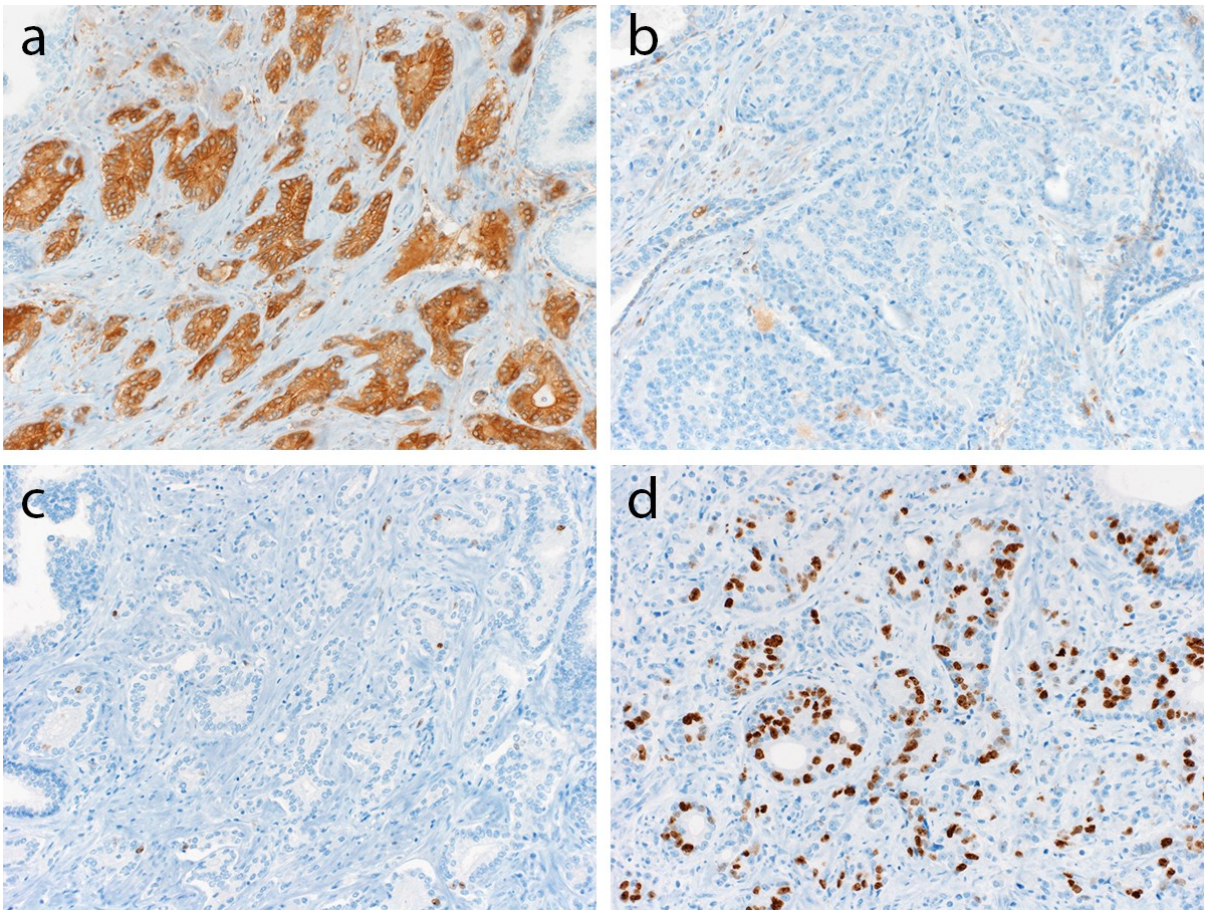

Figure 8. Case 1. a, b Diffuse positivity for ALDH1A1 in the diploid (a) and negativity in the aneuploid (b) tumor population. c, d Low proliferation index (Ki67 LI) in the diploid (c) and high Ki67 LI in the aneuploid (d) tumor population (a-d magnification 200x).

In summary, in this proof-of-concept study we showed that it is possible to predict the DNA ploidy status of distinct populations within one tumor by the degree of morphological nuclear atypia in routine H&E sections. Furthermore, we found a clonal relationship between the diploid and the tetraploid/aneuploid populations that might arise from a WGD event. Finally, our analyses point to an enrichment of the stemness-associated marker ALDH1A1 in specific diploid populations, which warrants further investigation in future studies.

Supplement

Patient No.	Age (years)	TNM-classification	PSA [ng/ml]	Gleason/ISUP Grade
1	48	pT3b, pN0 (0/9), cM0, R1	7.5	9 (4+5)/ISUP 5
2	69	pT2c, cN0, cM0, R1	16.6	7 (3+4), ISUP 2
3	66	pT2c, pN0 (0/15), cM0, R0	6.1	7 (4+3), ISUP 3
4	71	pT3b, pN0 (0/8), cM0, R0	6	9 (4+5), ISUP 5
5	74	pT3b, pN0 (0/8), cM0, R1	2.3	7 (4+3), ISUP 3
6	66	pT2c, pN0 (0/12), cM0, R0	4.7	7 (3+4), ISUP 2

Table S5. Patients' clinical data at the time of surgery. PSA, prostate-specific antigen; ISUP, International Society of Urological Pathology.

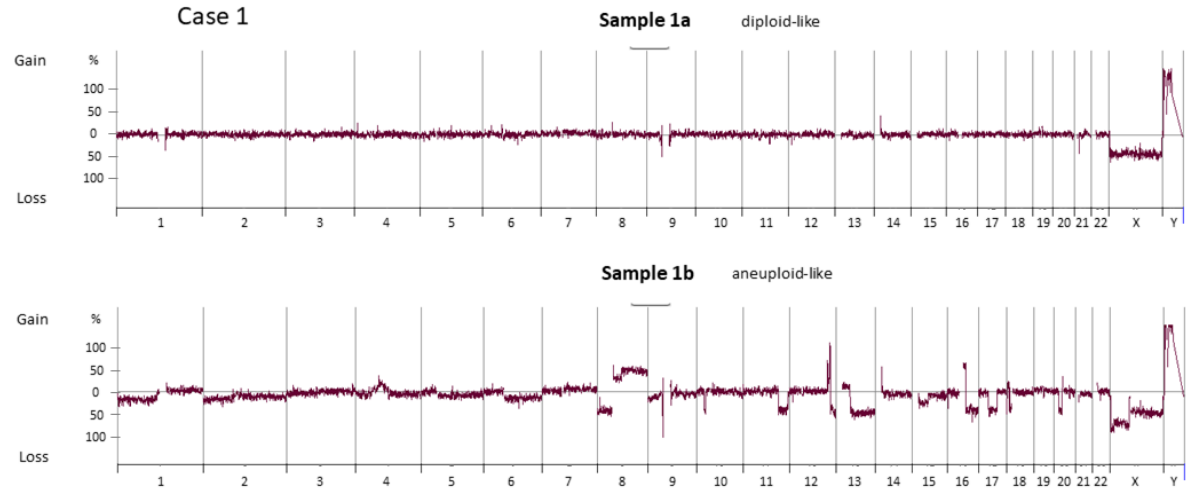

Figure S7. Case 1. aCGH-profiles showing several copy number changes present only in the aneuploid tumor population.

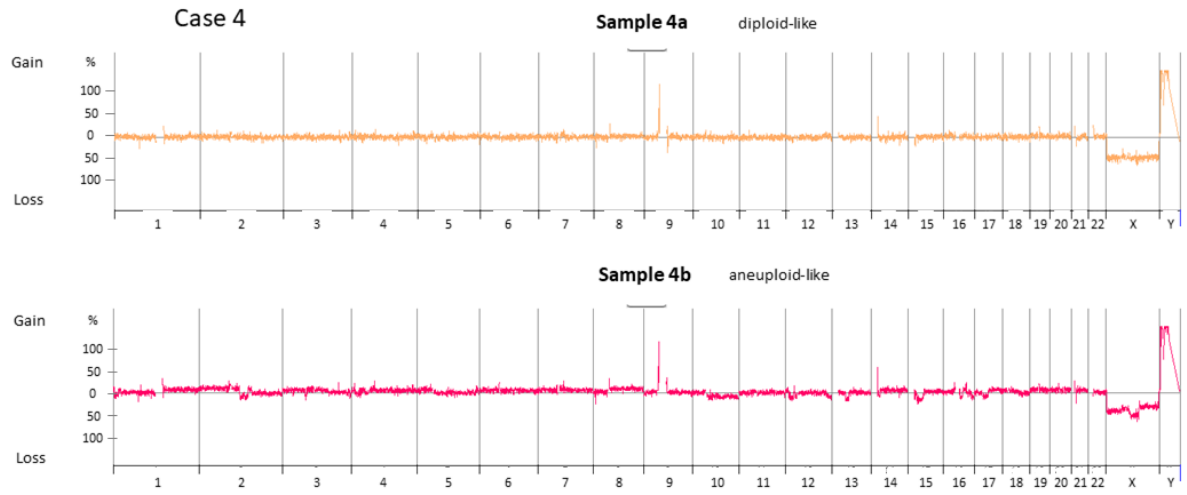

Figure S8. Case 4. aCGH-profiles showing several copy number changes present only in the aneuploid tumor population.

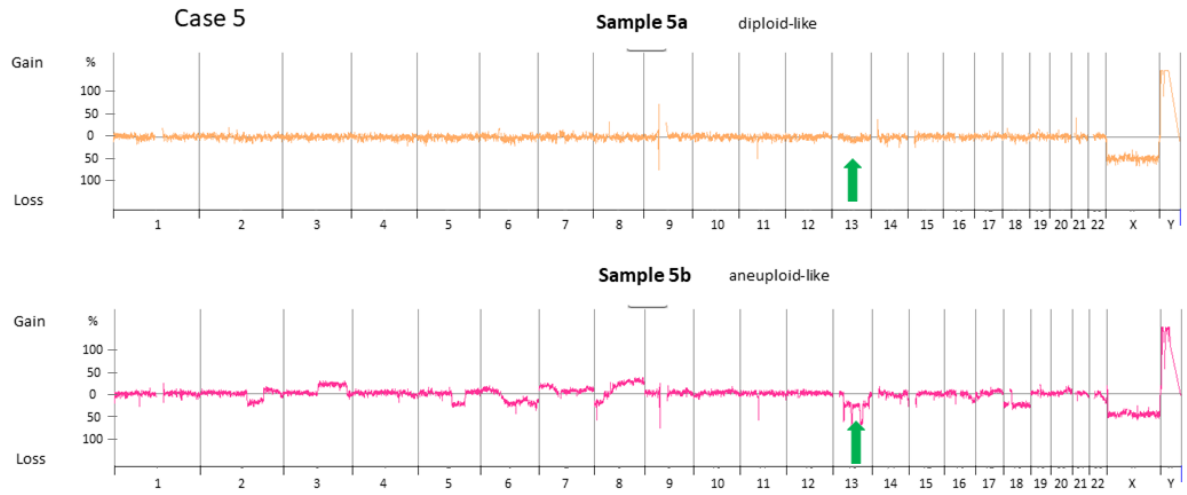

Figure S9. Case 5. aCGH-profiles indicating presumable deletion on chromosome 13q in the diploid tumor population and additional copy number changes, including the deletion on 13q in the aneuploid tumor population.

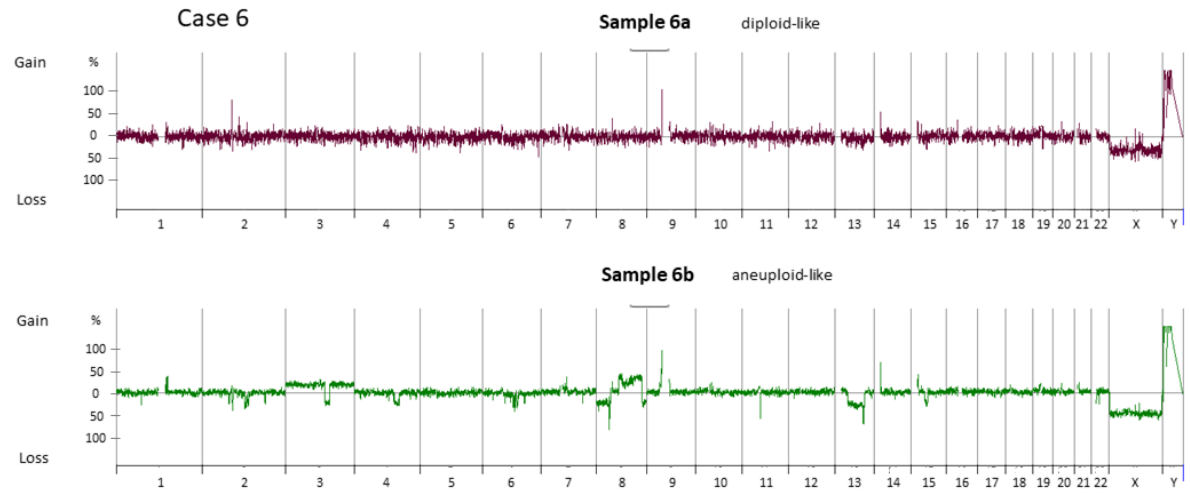

Figure S10. Case 6. The quality of the aCGH of the diploid population was poor and did not allow for a reliable interpretation. The aneuploid population shows several copy number

changes.

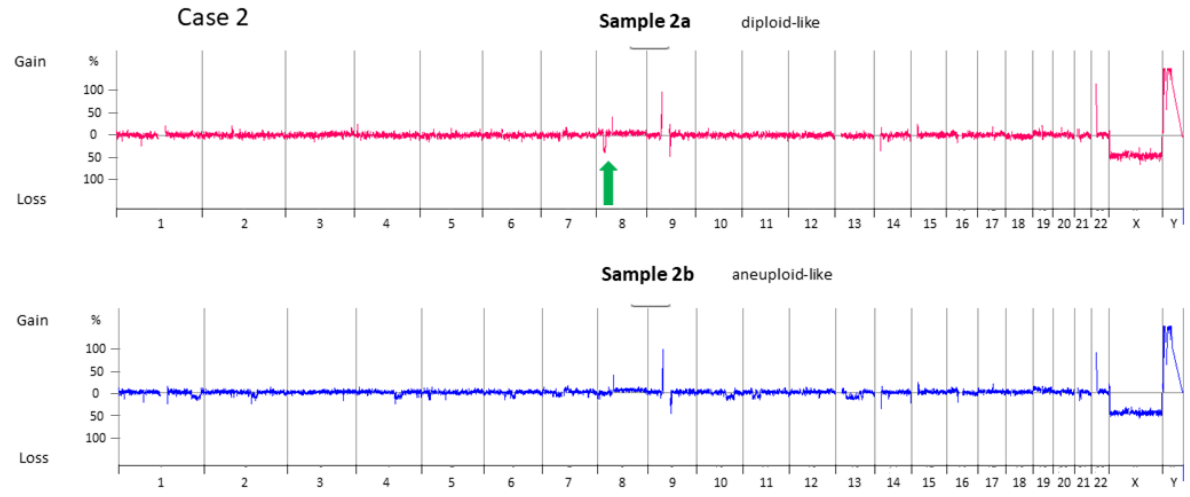

Figure S11. Case 2. aCGH-profile shows a deletion on chromosome 8p present only in the diploid but not in the aneuploid tumor population.

Immunocytochemistry for ARID1A as a Potential Biomarker in Urine Cytology of Bladder Cancer[221]

Abstract

Background: Mutations of AT-rich interactive domain 1 (*ARID1A*) have been associated with a worse outcome after intravesical treatment with Bacille Calmette-Guérin in patients with non–muscle-invasive bladder cancer (NMIBC). Loss of ARID1A protein expression in urine cytology may serve as an indication of an *ARID1A* mutation. Therefore, the authors examined the expression of ARID1A in urine cytology and histological specimens of bladder cancer for correlation with *ARID1A* mutational status.

Methods: The authors constructed a tissue microarray containing samples from 164 tissue samples from 150 patients with NMIBC and 100 tissue samples from 81 patients with muscle-invasive bladder cancer. A second cohort consisted of archived cytological specimens and matched tissue sections from 62 patients with high-grade NMIBC. The authors established immunohistochemistry and immunocytochemistry (ICC) protocols, respectively, for the analysis of ARID1A protein expression in histological and cytological specimens. Confirmatory next-generation sequencing (NGS) was performed on tumor specimens using a targeted NGS panel containing all exonic regions of *ARID1A*.

Results: The prevalence of ARID1A loss of expression on the tissue microarray was 3.6% in NMIBC (6 of 164 tissue samples) and 10% in muscle-invasive bladder cancer (10 of 100 tissue samples) (P = .059). Loss of ARID1A expression in cytology was concordantly immunohistochemistry negative in 6 of 8 matched tissue specimens. NGS confirmed an *ARID1A* mutation on all 6 histology samples with loss of ARID1A expression. When NGS demonstrated an absence of *ARID1A* mutation, histology was concordantly positive (16 of 16 cases).

Conclusions: The authors have suggested ARID1A ICC as a promising surrogate marker for ARID1A mutational status in patients with urothelial carcinoma. Pitfalls in ICC scoring include benign umbrella cells that often are negative for ARID1A. Further prospective studies are needed to determine the clinical relevance of ARID1A ICC in urinary cytology.

Introduction

With the recently proposed and now widely adopted Paris System for Reporting Urinary Cytology, the strength of cytology to diagnose high-grade urothelial carcinoma (HGUC) has

been emphasized and the cytological criteria have been standardized[222,223]. At the same time, there is an emerging role for potential biomarkers to guide personalized intravesical or systemic treatment of urothelial carcinoma (UC). In particular, mutational inactivation of AT-rich interactive domain 1 (*ARID1A*) recently has been proposed as being associated with response to intravesical treatment with Bacille Calmette-Guérin (BCG) and systemic treatment with PD-1/PD-L1 immune checkpoint inhibitors[224,225]. *ARID1A* is a tumor suppressor gene that is located on chromosome 1p36, encoding for a subunit of the SWI/SNF chromatin remodeling complex[226,227]. Inactivation of *ARID1A* has been described in many cancers and in up to 20% of UCs[228]. However, to the best of our knowledge, the relationship between ARID1A alteration, tumor aggressiveness, and prognosis in patients with bladder cancer remains unclear[224,229,230]. ARID1A is an epigenetic-related tumor suppressor and its main targets are regulatory elements for gene expression, known as enhancers, which are predominantly involved in developmental and differentiation programs[231]. Important targets of ARID1A are *MYC* and *E2F* responsive promoters, which regulate the cell cycle and DNA damage checkpoint[232]. It is interesting to note that through abolishing the interaction of ARID1A with MSH2, a protein implicated in mismatch repair, loss of ARID1A may lead to an increased sensitivity to immune checkpoint blockade[225].

ARID1A is a potential biomarker in bladder cancer, as evidenced by a recent study. Patients with tumors harboring an *ARID1A* gene mutation were found to have a decreased response to BCG therapy[224]. However, it is unclear whether the differential response was due to a reduced sensitivity to BCG therapy or whether it was indirectly indicative of more aggressive tumor behavior irrespective of BCG. For decades, intravesical BCG therapy has been a mainstay for the treatment of patients with intermediate-risk and high-risk non–muscle-invasive bladder cancer (NMIBC)[136]. Unfortunately, approximately 30% to 40% of patients do not respond[139]. Because patients with high-risk NMIBC who are undergoing radical cystectomy after BCG failure have a worse prognosis compared with the same category of patients undergoing an immediate radical cystectomy, the ability to predict a response to BCG would be a valuable tool when selecting the most appropriate therapeutic strategy[140].

Compared with solid tissue biopsies, urine specimens have several advantages within the context of bladder cancer. Urine cytology is a standard diagnostic method in clinical practice because it is particularly sensitive for detecting high-grade tumors and carcinoma in situ[233,234]. Although it is easier to obtain and less expensive than solid tissue biopsies, somatic genome analysis in cytology remains challenging due to the variable (and sometimes low) amount of collected tumor cells. We hypothesized that immunocytochemistry (ICC) could serve as a surrogate marker for the presence of inactivating *ARID1A* alterations. In the current study, we

explored the usefulness of ICC in the detection of ARID1A expression in urine cytology specimens and its correlation with *ARID1A* mutational status in tissue biopsies.

Materials and methods

Patients and Specimens: The current study was approved by the Ethical Committee Nordwest und Zentralschweiz in Basel, Switzerland (EKNZ 2014-313). All histological samples were tumor biopsies obtained during routine clinical treatment at the University Hospital Basel (Basel, Switzerland), the Cantonal Hospital Baselland (Liestal, Switzerland), and the St. Clara Hospital (Basel, Switzerland). Formalin-fixed and paraffin-embedded (FFPE) tissue specimens and cytology specimens were processed according to routine diagnostic procedures.

To establish protocols for ARID1A immunohistochemistry (IHC) and ICC, histological and cytological tumor materials from 18 UCs with known *ARID1A* mutational status from an ongoing genomic profiling study were used, including 3 UCs with *ARID1A* mutations and 15 UCs without a mutation. A tissue microarray (TMA) was used to estimate the prevalence of ARID1A loss of expression by IHC. The TMA contained 164 tissue samples from 150 patients with NMIBC and 100 tissue samples from 81 patients with muscle-invasive bladder cancer. These samples had been resected between 2006 and 2013. Finally, we constructed a patient cohort using archived cytological specimens and matched tissue from 62 patients with high-grade NMIBC. The characteristics of these patients, all of whom had received intravesical BCG instillations, are shown in Table 1. Patients with cancer recurrence or progression within 2 years after the administration of BCG were considered as BCG non-responders. All histological specimens from these 62 patients were staged and graded by an experienced uropathologist and cytopathologist (L.B) according to the current World Health Organization classification of bladder tumors[235]. Cytological specimens were classified according to the Paris System for Reporting Urinary Cytology[223]. They consisted of cytospin preparations and smears and had been processed according to routine procedures using Delaunay solution (1000 mL of acetone and absolute alcohol each, and 20 drops of 1 mol/L trichloroacetic acid) or Sprayfix (Avantor Performance Materials J.T. Baker Chemicals, Center Valley, Pennsylvania) as a fixative, stained according to the Papanicolaou method, and coverslipped. The archival period was ≤5 years.

IHC and ICC: Serial sections measuring 4 µm were obtained for IHC staining of ARID1A. This staining was performed using the D2A8U rabbit monoclonal antibody (Cell Signaling Technology, Allschwil, Switzerland). IHC on histological specimens was performed using standard protocols on the Ventana BenchMark ULTRA automated immunostainer (Roche Diagnostics, Indianapolis, Indiana) at an antibody dilution of 1:100.

ICC for ARID1A was performed on the Papanicolaou-stained cytological specimens. After uncovering the glass slides in xylene, ICC was performed using the Bond-III automated immunostainer (Leica Biosystems, Wetzlar, Germany), which is the standard platform for ICC of cytological specimens at the Institute of Pathology at the University Hospital Basel[236,237]. The slides were pretreated in Epitope Retrieval solution 1 for 5 minutes at 80 °C and then incubated with the D2A8U antibody for ARID1A (dilution 1:400) for 30 minutes at room temperature. Antibody binding was detected using the Bond Polymer Refine Detection Kit, with 3-amino- 9-ethylcarbazol as a chromogen (Leica Biosystems). All immunostained slides were evaluated by one of us (L.B.) who was blinded with regard to *ARID1A* mutation status and the clinical data. Only nuclear staining was considered irrespective of staining intensity. Benign cells, regularly expressing ARID1A, on the same slide served as an internal positive staining control (Figure 9). To increase the stringency for statistical analysis, specimens were considered as negative for ARID1A by IHC and/or ICC when at least 50% of the tumor cells demonstrated loss of immunostaining.

Genomic Analysis: DNA was extracted from freshly cut 10-µm sections of tissue obtained from transurethral resection of the bladder tumor from 4 ARID1A-negative IHC samples using the Invitrogen RecoverAll Total Nucleic Acid Isolation Kit (Thermo Fisher Scientific, Waltham, Massachusetts) for FFPE. Libraries were prepared using the AmpliSeq Library Kit Plus (Thermo Fisher Scientific) according to the manufacturer's instructions. Panel next-generation sequencing (NGS) testing was performed using the targeted Oncomine Comprehensive Assay v3M (Thermo Fisher Scientific) containing 135 cancer-associated genes, including all exonic regions of *ARID1A*. For the tissue specimens of the above-mentioned genomic profiling study, FFPEderived DNA was subjected to library preparation as previously described[238]. Libraries were hybridized to a published panel of 50 bladder cancer–associated genes and sequenced using an Illumina MiSeq system (Illumina, San Diego, California), and data were analyzed with an established bioinformatics pipeline[166].

Statistical Analysis: Differences between the values were considered to be statistically significant at $P < .05$. Analyses were performed using the Fisher exact test for 2×2 tables in the MedCalc statistical software package (MedCalc; Ostend, Belgium). The mean, median, and standard deviations were calculated using Microsoft Excel (Microsoft Corporation, Redmond, Washington).

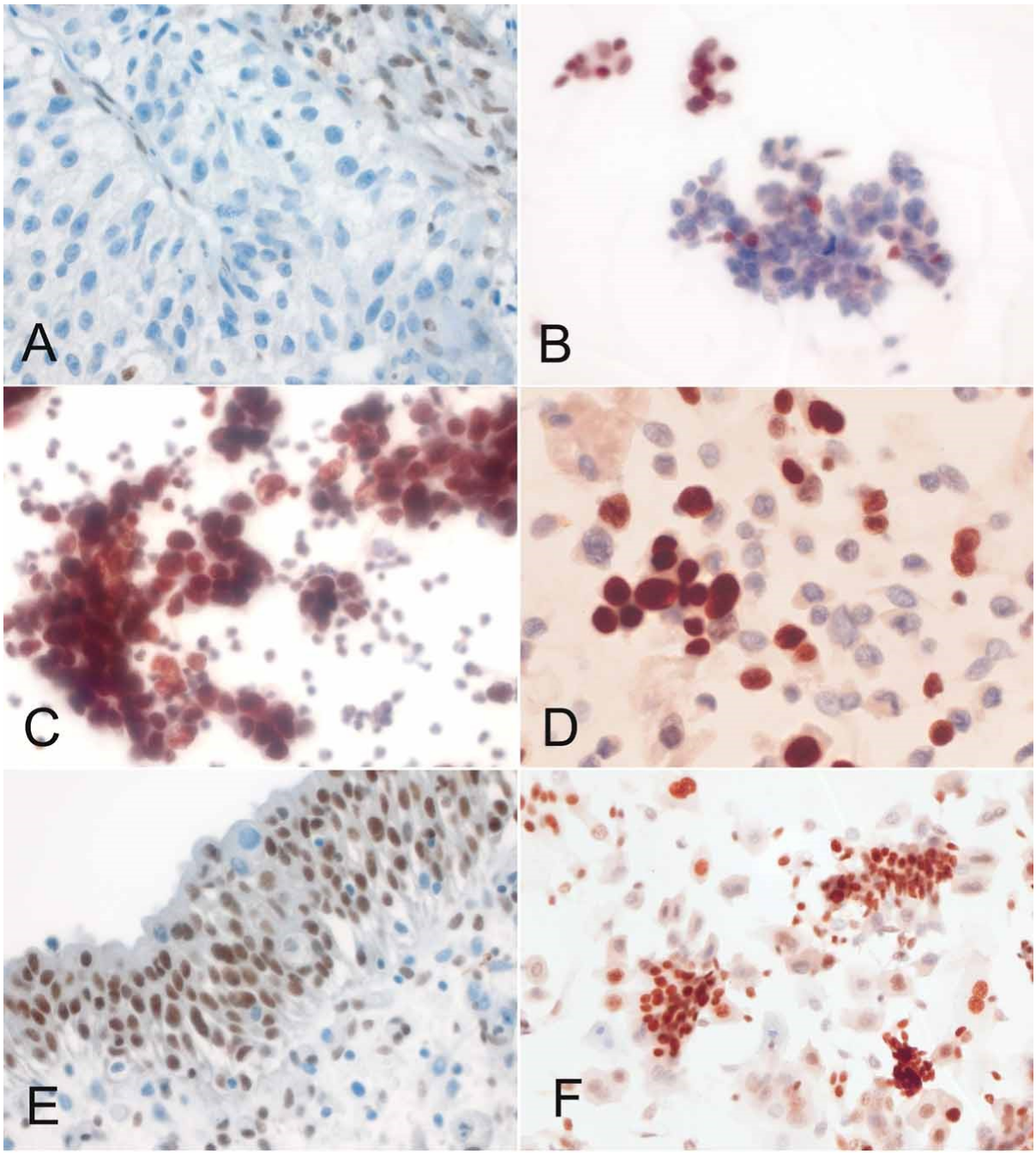

Figure 9. Immunohistochemistry (IHC) and immunocytochemistry (ICC) for nuclear ARID1A expression in histological and cytological specimens. (A and B) High-grade urothelial carcinoma (HGUC) with AT-rich interactive domain 1 (ARID1A) mutation and loss of ARID1A expression. (A) Benign stromal cells and (B) benign urothelial cells served as internal positive staining controls. (C) Cytology of HGUC with intact ARID1A expression. (D) Cytology of HGUC with heterogeneous loss of ARID1A expression. (E) Histology of benign ARID1A-positive urothelium with rare ARID1A-negative umbrella cells. (F) Benign bladder washing cytology specimen with ARID1A-positive cells and ARID1A-negative umbrella cells (all images: original magnification ×630).

Results

IHC and ICC Analyses of ARID1A Expression: Tumor cell positivity and negativity could be differentiated clearly (Figure 9). Generally, positive nuclear ARID1A expression was diffuse and strong across all tumor cells. In cytology, 11 of 77 samples demonstrated heterogeneous expression of ARID1A as evidenced by a percentage of tumor cells exhibiting loss of ARID1A expression concurrent to a percentage that retained expression. Among these 11 cases, the percentage of ICC-negative cells ranged from 10% to 90% (mean, 40% ± 30%; median, 20%). In total, 9 of 77 samples were considered to have a loss of ARID1A expression. As mentioned above, a value of 50% was used as a cutoff value for negative or positive ARID1A expression status, respectively. In some positive samples, urothelial umbrella cells (multinucleated superficial cells of the bladder's transitional epithelium) were found to be negative for ARID1A. The prevalence of ARID1A loss of expression as determined on the TMA was 3.6% in NMIBC cases (6 of 164 cases) and 10% in muscle-invasive bladder cancers (10 of 100 cases) (P = .059).

ARID1A Protein Expression in Matched Cytology and Histology: From the initial study cohort, the TMA cohort, and the control cohort, we obtained 77 cytology samples and 322 histology samples. In some samples, either the histology or cytology specimen was missing. Dropouts included cases with low cellularity on cytology or with failed staining. Overall, matching histology and cytology specimens were obtained for 45 patients. Table 2 shows the comparison between ARID1A expression in IHC, ICC, and NGS across all study cohorts. When ARID1A protein was expressed in cytology, 34 of 37 matched histology samples (92%) were found to have corresponding positive IHC. It is interesting to note that the 3 cytology samples with divergently negative ARID1A IHC expression all were metachronous to the cytology specimens and differed with regard to the tumor grade compared with their corresponding cytology samples, raising the possibility of independent tumors or genomic evolution with altered *ARID1A* status during expression.

Loss of ARID1A expression in cytology was concordantly IHC negative in 6 of 8 matched histological tumors. In 2 of these matched cases, histology was ARID1A positive despite ARID1A-negative cytology. The specimens from these 2 patients had been collected synchronously.

In the current study cohort, the response rate to BCG therapy of patients found to have ARID1A loss of expression on cytology (75%; 4 patients) was similar to that of the patients with retained ARID1A expression (69%; 49 patients). Two patients were lost to follow-up, and 3 patients received additional cancer treatment other than BCG. No statistical analyses were applicable due to the low number of patients with loss of expression.

ARID1A Mutational Status: ARID1A expression on IHC and ICC was conserved for all 16 samples with wild-type *ARID1A*. NGS confirmed *ARID1A* mutations in all 6 samples demonstrating loss of *ARID1A* expression. One sample had conserved ARID1A expression despite an *ARID1A* mutation that was described as a pathogenic nonsense mutation (A82) (Table 3)[239]. The specific mutations are summarized in Table 3. The sensitivity and specificity were not calculated due to the low number of samples.

Discussion

The results of the current study demonstrated that ARID1A ICC on urine cytology provides consistent, well-interpretable results and can serve as a surrogate marker for inactivating *ARID1A* mutations in bladder cancer. ARID1A ICC has potential as a predictive marker for the personalized treatment of patients with high-grade UC[224,225,240]. However, it is unlikely to serve as a useful diagnostic marker with which to clarify atypical urinary cytology because ARID1A protein loss prevails in <20% of UCs. In addition, benign umbrella cells can be ARID1A negative and differentiating reactive cells from neoplastic urothelial cells often is challenging in immunostained cytological specimens. Therefore, loss of ARID1A ICC should be evaluated only in specimens with clearly recognizable cells of HGUC.

To the best of our knowledge, only a few studies to date have investigated the loss of ARID1A protein expression in histological UC specimens on IHC, but none has investigated urinary cytological specimens. Previous reports regarding the association between loss of ARID1A expression and cancer stage were conflicting. In a cohort consisting solely of cystectomy specimens, Faraj et al found a loss of ARID1A expression more often in earlier stages of disease and in less aggressive cancers[241]. In contrast, both Balbas-Martinez et al and Li et al reported a strong association between UC with weak or negative ARID1A expression and higher-grade and higher-stage disease, thereby indicating a potential association with aggressive disease[229,230]. In the current study, loss of ARID1A expression tended to be associated with higher-stage tumors, a finding that is consistent with ARID1A as an adverse prognostic marker.

The prevalence of loss of ARID1A expression in the TMA cohort in the current study was lower than previously reported for *ARID1A* mutations[224,242,243]. There are several possible explanations for this discrepancy, including differences in patient cohorts, the reporting of nonpathogenic mutations in previous studies, and intratumoral heterogeneity for *ARID1A* mutations. In the case of intratumoral heterogeneity, *ARID1A* mutations and the resulting loss of expression could be missed using single TMA spots compared with multiple spots per tumor or whole-tissue sections. In addition, a remaining allele in the case of a heterozygous *ARID1A* mutation most likely will suffice for recognizable nuclear protein expression if not silenced by

another mechanism such as promotor methylation or genetic deletion. To the best of our knowledge, the relative percentage of homozygous or heterozygous *ARID1A* inactivation by different mechanisms has only been studied in part to date. In a study by Wiegand et al, the majority of *ARID1A* mutations were heterozygous, and approximately 73% of *ARID1A*-mutated ovarian clear cell carcinomas were found to have a weak or complete loss of protein expression[244]. Wang et al reported similar results because approximately 25% of gastric cancers with *ARID1A* mutations in their study were found to have conserved protein expression[245]. In a study by Guan et al of uterine endometroid carcinoma, only approximately 50% of tumors with *ARID1A* mutations had a complete loss of ARID1A immunoreactivity (5 of 10 tumors)[246]. These results demonstrate that the prevalence of ARID1A loss of expression by IHC and/or ICC can, in fact, be lower than the prevalence of *ARID1A* mutations. Assuming that biallelic *ARID1A* inactivation by mutations and/or other mechanisms with complete loss of protein expression is functionally most relevant, IHC and/or ICC analysis might represent an advantage over genomic testing.

Decreased ARID1A protein expression also has been reported to be associated with heterozygous mutations leading to a haploinsufficiency phenomenon[231]. In the current study of UC cases, we did not find evidence of such haploinsufficiency resulting in preserved but weak protein expression. Positive ARID1A expression was almost always strong, with little variability of staining intensity observed beyond what one can expect due to unavoidable preanalytical variability including fixation. Nevertheless, further studies are needed to investigate the prevalence and functional importance of haploinsufficiency of *ARID1A* in UC.

There was no perfect correlation of ARID1A expression status between matched histology and cytology specimens by IHC and/or ICC noted in the current study. Overall, discordance was found in 5 of 45 matched pairs from the TMA cohort and the study cohort, including cases with ARID1A loss on IHC but retained ICC expression and vice versa. Spatial or temporal heterogeneity of *ARID1A* mutation and expression appears to be the most common explanation for such discrepancies, as was documented in some of the discordant cases in the current study. Heterogeneity of molecular markers is well known in UC and also paralleled by the notorious heterogeneity of histological appearance[116,127]. Such heterogeneity makes biomarker testing a challenge because focal alterations can be missed by cytological or histological sampling. Conversely, focal alterations or private mutations occurring late during clonal evolution might be biologically less relevant than early and ubiquitous alterations that affect all tumor cells. In principle, cytology appears to be particularly promising for capturing the full heterogeneity of a tumor because it potentially samples the whole bladder and hence the current tumor surface. In fact, recent data from Scott et al have suggested that NGS of sufficiently cellular urinary cytology specimens might more effectively capture the full genetic

heterogeneity of disease including ARID1A mutations compared with the same analysis performed on cystectomy specimens[247].

The current study was limited by its small cohort size and the low absolute number of *ARID1A*-mutated UC specimens, thereby precluding strong conclusions. However, the demonstrated feasibility of ARID1A ICC on cytological specimens creates an opportunity to gain additional insight into the role of *ARID1A* in future studies using urine cytology from HGUC. It is interesting to note that *ARID1A* mutations recently have gained particular attention as potential predictors of response to the immune checkpoint inhibitors that have become a growing therapeutic option for patients with high-grade, advanced UC[143]. According to preclinical models, inactivating *ARID1A* mutations are believed to be a positive predictor of response to immune checkpoint inhibitors via interference with DNA mismatch repair, leading to an increased mutational burden[225]. This is counterintuitive to the proposed negative predictive value of *ARDI1A* mutations within the context of intravesical BCG treatment as another type of immunotherapy[224]. The presumably complex role of ARID1A as a potential predictive marker for treatment with BCG and immune checkpoint inhibitors calls for more studies. Intriguingly, a recent study also suggested a higher vulnerability of ARID1A-deficient cancer cells to inhibition of the antioxidant glutathione and the glutamate-cysteine ligase synthetase catalytic subunit, which directs us toward a new therapeutic opportunity in the future[240].

Discussion

Depicting, monitoring, and understanding pathomechanisms of disease progression is crucial when facing all cancer entities, not only in urological cancers like PC and UC, especially in the era of personalized medicine[99].

Our understanding of disease progression is the evolutionary process of cancer cell populations acquiring beneficial features. This allows for clonal expansion of the fittest clone. The first expansion assumingly takes place long before any clinically detectable sign of the cancer is manifest. The pattern of this evolution is diverse. It may be punctuated, linear, neutral, or branched. Over time, it is very likely to see different patterns within the same cancer. Especially if selective pressure, in the form of therapy, is applied.

In our first manuscript, i.e., Donor-derived, metastatic urothelial cancer after kidney transplantation associated with a potentially oncogenic BK polyomavirus, we hypothesize that a single event leads to the onset of an aggressive, metastatic UC in the context of an immunosuppressed patient. A 17 bp deletion in the viral genome may have led to a reduced viral reproduction capability and concomitant host-cell lysis. The subsequent prolonged presence of LTag proteins harbors oncogenic potential by binding to pRb and p53, two of the most potent TSG we know. In the context of clonal evolution, the acquisition of this deletion would correspond to a punctual evolution. Investigating the different tumor sites, we could see an additional heterozygous loss on the X chromosome and a gain on chromosome 6, only present in the bladder manifestation. Their biological relevance remains unclear. It is counter-intuitive to assume that a lymph node metastasis next to the left iliacal vessels would derive directly from the kidney transplant in the right fossa iliaca. Therefore, one might assume the presence of different tumor branches located in the bladder.

Surprisingly, from an evolutionary perspective, the 17 bp deletion was detectable in the virus's episomal configuration. Therefore, it was, assumingly, already present before the integration of the viral genome into the host genome. As we could show in our functional cell-culture experiments, the viral life cycle was impaired when this deletion was present. This means, at the time the deletion occurred, it was most likely disadvantageous to the lifeform owning the affected genome. The fitness advantage gained by this event was solely beneficial to the subsequent cancer population. This highlights the importance of biological context when we evaluate genomic alterations.

The biological context of genomic alterations is not solely determined by the features of a single cancerous cell but also by its surrounding microenvironment. It is the interaction

between malignant and normal cells within a tumor. Besides mesenchymal cells and others, immune cells play a vital role in this microenvironment.

Four years after surgery, the patient we investigated showed no sign of recurrence. It is possible but unlikely that surgical treatment alone achieved this. Usually, patients with metastatic UC undergo adjuvant systemic treatment[141]. We hypothesize that the discontinuation of immunosuppression may have heavily impacted the microenvironment of so far undetected, but likely present, micro-metastases. This might have caused immune cells to attack the remaining tumor cells since the tumor derives from the kidney donor's cells, alien to the host's immune system.

Our second manuscript, i.e., heterogeneity of DNA ploidy in the context of clonal evolution in prostate cancer, focusses on spatial heterogeneity within one tumor location. Cases were selected based on morphological criteria. All patients in this study underwent radical prostatectomy, and the investigated tumors are therapy-naïve. Furthermore, all cancers are still at a localized, assumingly early stage of development. This is in line with our finding of co-existing diploid and aneuploid tumor clones that might be in the, assumingly early, state of clonal interference. Since we hypothesize that at least one of the aneuploid clones derived from a diploid population, it shows a branched evolutionary pattern.

Usually, tumor clones are detected by sophisticated and often expensive diagnostic tools, investigating tumor cells on a genomic or protein-expression level. In this study, we could show that using H&E-staining, the most basic staining in pathology, was sufficient to determine a cancer cell's ploidy and hereby identify different tumor clones.

Our investigation is just a snapshot of tumor evolution in a few hand-picked cases. However, our finding of cancer populations with different ploidy status is in line with PC's morphological heterogeneity, detected using non-nuclear features, i.e., Gleason-score. Altogether, this indicates that in the early stages of PC, few or none selective sweeps occur, and the selective pressure on cancer cells is low.

The third manuscript, i.e., immunocytochemistry for ARID1A as a potential biomarker in urine cytology of bladder cancer, has a different implication than the previous two. Rather than depicting the tumor's clonal evolution, it intends to evaluate a biomarker to predict a therapy's success. One could also say: to predict a cancer population's success under the selective pressure of therapy. The importance of useful biomarkers cannot be underestimated, especially in the context of PM.

We established a tool capable of predicting, to some extent, therapy response to BCG therapy in patients with high-grade UC. An important note is that we achieved this using urinary

cytology specimens, a sample obtained in a non-invasive way. However, the biological process behind a biomarker influences its quality. In this case, we still lack the biological knowledge of how BCG response is influenced by the ARID1A-protein.

In summary, we showed that depicting the genomic evolution behind a cancer manifestation, even on the level of single case studies, can provide a deeper understanding of disease progression and subsequent success or failure of therapy.

As a consequence of tumor evolution, ITH is a critical pathomechanism of disease progression. It provides an individual cancer entity with a pool of options for therapy-resistance. Surgery may reduce the size of this pool, and systemic treatment may further drain it. Still, there is a wide range of tasks ahead of us in this regard.

The application of therapeutic agents targeting specific mutations relies, first and foremost, on their detection. The implementation and use of NGS are expensive. One way to limit the costs of a sequencing run is by limiting the sequencing depth. By doing this, the resolution of mutation-detection is limited accordingly, causing an underestimation of ITH in a given sample[248]. While a decrease in price over time may overcome this, biopsy bias might still lead to an underestimation of ITH. Only looking at every cancer site on a single cell level can assess ITH's true extend, which is impossible. Nevertheless, the number of biopsies should be increased without putting an inappropriate additional burden on the patient, whenever possible. Another approach could be improving liquid biopsies. It harbors the potential to acquire a snapshot of tumor characteristics independent from tumor location, accomplishing this with little to no invasiveness.

Yet, the number of mutations found with today’s clinical routine approach of sequencing and sampling already outnumbers the number of available therapeutic options. This is mainly due to the lack of available agents. As targeted anti-cancer therapy is still in its infancy, this is not surprising. Due to the current high revenues on drugs approved for oncologic purposes, the number of available drugs will surely increase. Nevertheless, the pharmaceutical industry seems to develop new drugs on already established drug targets since it is a safer “bet” than investing in the development of drugs designed against new targets[249]. An example of this development is the high number of available drugs targeting the PD-1 immune-checkpoint.

The discrepancy between detected mutations and those that are actionable creates the problem of reporting to clinicians (and patients). Especially conflicting situations may arise if the biological relevance of a mutation is still unclear at the time of its detection. Several systems have been proposed grouping mutations into different tiers according to our current knowledge about them[250]. Yet, there is still a lack of guidelines and international harmonization regarding this topic.

The tasks mentioned above are mainly technical and caused by the way we approach anti-cancer medicine. In contrast to this, the main challenge we face lies within the disease itself. It is its complexity.

As mentioned before, a biomarker can only be as useful as our understanding of its role in the disease. If the mutation or the protein we use as a biomarker is only crucial in a partial aspect of the disease, we will only be able to use it as a surrogate for this aspect. Another example of the complexity of understanding genomic alterations in cancer is the varying biological impact of the 17bp deletion we reported in our first manuscript, changing from obstacle to benefit within a single patient.

One effort to gain more insights is the implementation of systems biology into cancer research[251]. It means that a wide range of data is included in computational modeling to understand changes on different levels. This might range from a cellular level, including the genome, transcriptome, and proteome of a cancer cell up to a population scale level. This machine-learning approach may become very useful in a foreseeable “big-data” future.

Furthermore, every cancer-related alteration's biological context varies so much that we face problems we usually only see in rare diseases research[104]. Hence, we can apply the tools used in this area of research. The most important of which is post-approval data acquisition.

Today in oncology, after an agent targeting a specific, actionable mutation is found, and it gained approval by regulatory institutions due to successful phase III studies, there is no system in place to routinely acquire further disease-specific data. The implementation of databases containing a patient’s actionable mutation and its biological context, alongside information of the course of the disease, may be the groundwork on which systems biology may be successful. This would increase the number of samples used for analyses, making the disease less “rare” for researchers, and allow for more comparison of tumor evolution, even across different cancer types[248]. Furthermore, this would open the door to further approaches in anti-cancer drug design.

Despite being a hallmark of cancer, recent insights into genomics revealed a threshold to genome instability and mutations above which they are no longer beneficial to a cancer cell or cell population. This “just-right” mutational dosage[252] may explain why aneuploidy sometimes drives disease progression and sometimes slows it down[192].

The concept of exploiting this “just-right” dosage in the clinical context is called synthetic lethality. A specific mutation, beneficiary to a cancer cell, may become a drawback if other intracellular pathways are blocked. As an example, a common oncogenic alteration is a truncating mutation of *BRCA1* or *BRCA2*. These are genes involved in a primary mechanism

of DNA damage repair (DDR), i.e., homologous recombinational repair (HRR). Their mutations are associated with various familial cancer[253]. If the primary DDR is impaired, a cell, normal or malignant, relies on secondary DDR-pathways like base excision repair (BER) (reviewed in[254]). PARP is a protein family involved in BER that can be inhibited by the drug Olaparib[255]. Therefore, in the presence of mutations in HRR associated genes, Olaparib becomes a potent agent[161] – the synthesis of altered pathways becomes lethal to a cell.

The concept of a “just-right” dosage implies that mutational changes also cause cellular stress[192]. Systems biology may provide the information needed for understanding what alterations cause which form of metabolic stress in a cell. This information may lead to therapeutic options to raise stress to a cell toxic level. One source of stress may be a cell’s interaction with its microenvironment. The association of response to immunotherapy and a high rate TMB may be an example of this[78].

The recent success of immune therapy highlights the importance of the tumor microenvironment. It appears more straightforward to modulate immune cell – cancer interactions, therefore controlling the microenvironment, rather than designing drugs to a seemingly endless diversity of genomic mutations. However, also in this therapeutic approach, we see therapy-resistant clones. Cells with altered post-translational protein synthesis seem to be less responsive[248], underlining cancer's diversity as a disease and the need for further work.

In the end, the human body and its cells result from billions of years of evolution[256]. Everything we acquired in this struggle and effort by countless generations is written into our genetic code. Ultimately, this code is the cancer cells' toolbox for developing pathomechanisms of disease progression. Our success in anti-cancer therapy depends on our understanding of cancer cell evolution and our control over it[2].

Either we understand the root, or we keep cutting branches. This simple complexity is the challenge we face.

References

1. Greaves M, Maley CC. Clonal evolution in cancer. *Nature*. 2012;481(7381):306-313. doi:10.1038/nature10762

2. Nowell PC. The clonal evolution of tumor cell populations. *Science*. 1976;194(4260):23-28. doi:10.1126/science.191.4224.241-a

3. Hanahan D, Weinberg RA. Hallmarks of Cancer: The Next Generation. *Cell*. 2011;144(5):646-674. doi:10.1016/J.CELL.2011.02.013

4. López S, Lim EL, Horswell S, et al. Interplay between whole-genome doubling and the accumulation of deleterious alterations in cancer evolution. *Nat Genet*. 2020;52(3):283-293. doi:10.1038/s41588-020-0584-7

5. Sakr WA, Haas GP, Cassin BF, Pontes JE, Crissman JD. The frequency of carcinoma and intraepithelial neoplasia of the prostate in young male patients. *J Urol*. 1993;150(2 Pt 1):379-385. doi:10.1016/s0022-5347(17)35487-3

6. Malaise EP, Chavaudra N, Tubiana M. The relationship between growth rate, labelling index and histological type of human solid tumours. *Eur J Cancer*. 1973;9(4):305-312. doi:10.1016/0014-2964(73)90099-6

7. Reid BJ, Li X, Galipeau PC, Vaughan TL. Barrett's oesophagus and oesophageal adenocarcinoma: time for a new synthesis. *Nat Rev Cancer*. 2010;10(2):87-101. doi:10.1038/nrc2773

8. Maley CC, Galipeau PC, Li X, Sanchez CA, Paulson TG, Reid BJ. Selectively Advantageous Mutations and Hitchhikers in Neoplasms: p16 Lesions Are Selected in Barrett's Esophagus. *Cancer Res*. 2004;55(1):12-15. doi:10.1158/0008-5472.can-03-3249

9. Tao Y, Ruan J, Yeh S-H, et al. Rapid growth of a hepatocellular carcinoma and the driving mutations revealed by cell-population genetic analysis of whole-genome data. *Proc Natl Acad Sci U S A*. 2011;108(29):12042-12047. doi:10.1073/pnas.1108715108

10. Alexandrov LB, Nik-Zainal S, Wedge DC, et al. Signatures of mutational processes in human cancer. *Nature*. 2013;500(7463):415-421. doi:10.1038/nature12477

11. Swanton C, Soria J-C, Bardelli A, et al. Consensus on precision medicine for metastatic cancers: a report from the MAP conference. *Ann Oncol*. 2016;27(8):1443-

1448. doi:10.1093/ANNONC/MDW192

12. Lavaud P, Andre F. Strategies to overcome trastuzumab resistance in HER2-overexpressing breast cancers: focus on new data from clinical trials. *BMC Med*. 2014;12. doi:10.1186/S12916-014-0132-3

13. Santarius T, Shipley J, Brewer D, Stratton MR, Cooper CS. A census of amplified and overexpressed human cancer genes. *Nat Rev Cancer*. 2010;10(1):59-64. doi:10.1038/nrc2771

14. Knudson AG, Jr. Mutation and Cancer: Statistical Study of Retinoblastoma. *Proc Natl Acad Sci U S A*. 1971;68(4):820. doi:10.1073/PNAS.68.4.820

15. Chen Z, Trotman LC, Shaffer D, et al. Crucial role of p53-dependent cellular senescence in suppression of Pten-deficient tumorigenesis. *Nature*. 2005;436(7051):725-730. doi:10.1038/nature03918

16. Carver BS, Tran J, Gopalan A, et al. Aberrant ERG expression cooperates with loss of PTEN to promote cancer progression in the prostate. *Nat Genet*. 2009;41(5):619. doi:10.1038/NG.370

17. Vogelstein B, Kinzler KW. Cancer genes and the pathways they control. *Nat Med*. 2004;10(8):789-799. doi:10.1038/nm1087

18. Serrano M, Lin AW, McCurrach ME, Beach D, Lowe SW. Oncogenic ras Provokes Premature Cell Senescence Associated with Accumulation of p53 and p16INK4a. *Cell*. 1997;88(5):593-602. doi:10.1016/S0092-8674(00)81902-9

19. Evan GI, Wyllie AH, Gilbert CS, et al. Induction of apoptosis in fibroblasts by c-myc protein. *Cell*. 1992;69(1):119-128. doi:10.1016/0092-8674(92)90123-T

20. Takano T, Ohe Y, Sakamoto H, et al. Epidermal growth factor receptor gene mutations and increased copy numbers predict gefitinib sensitivity in patients with recurrent non-small-cell lung cancer. *J Clin Oncol*. 2005;23(28):6829-6837. doi:10.1200/JCO.2005.01.0793

21. Alexandrov LB, Ju YS, Haase K, et al. Mutational signatures associated with tobacco smoking in human cancer. *Science*. 2016;354(6312):618-622. doi:10.1126/science.aag0299

22. Berger AH, Knudson AG, Pandolfi PP. A Continuum Model for Tumour Suppression. *Nature*. 476(7359):163. doi:10.1038/NATURE10275

23. Vogelstein B, Kinzler KW. The multistep nature of cancer. *Trends Genet*. 1993;9(4):138-141. doi:10.1016/0168-9525(93)90209-Z

24. Williams MJ, Sottoriva A, Graham TA. Measuring Clonal Evolution in Cancer with Genomics. *Annu Rev Genomics Hum Genet*. 2019;20(1):309-329. doi:10.1146/annurev-genom-083117-021712

25. Bozic I, Antal T, Ohtsuki H, et al. Accumulation of driver and passenger mutations during tumor progression. *Proc Natl Acad Sci U S A*. 2010;107(43):18545-18550. doi:10.1073/pnas.1010978107

26. de Visser JAGM, Rozen DE. Clonal interference and the periodic selection of new beneficial mutations in Escherichia coli. *Genetics*. 2006;172(4):2093-2100. doi:10.1534/genetics.105.052373

27. Maley CC, Galipeau PC, Finley JC, et al. Genetic clonal diversity predicts progression to esophageal adenocarcinoma. *Nat Genet*. 2006;38(4):468-473. doi:10.1038/ng1768

28. Turke AB, Zejnullahu K, Wu Y-L, et al. Pre-existence and clonal selection of MET amplification in EGFR mutant NSCLC. *Cancer Cell*. 2010;17(1):77. doi:10.1016/J.CCR.2009.11.022

29. Chen J, Sprouffske K, Huang Q, Maley CC. Solving the puzzle of metastasis: the evolution of cell migration in neoplasms. *PLoS One*. 2011;6(4):e17933. doi:10.1371/journal.pone.0017933

30. Donato C, Kunz L, Castro-Giner F, et al. Hypoxia Triggers the Intravasation of Clustered Circulating Tumor Cells. *Cell Rep*. 2020;32(10):108105. doi:10.1016/j.celrep.2020.108105

31. Gupta GP, Massagué J. Cancer Metastasis: Building a Framework. *Cell*. 2006;127(4):679-695. doi:10.1016/J.CELL.2006.11.001

32. Federer-Gsponer JR, Quintavalle C, Müller DC, et al. Delineation of human prostate cancer evolution identifies chromothripsis as a polyclonal event and FKBP4 as a potential driver of castration resistance. *J Pathol*. 2018;245(1):74-84. doi:10.1002/path.5052

33. Stephens PJ, Greenman CD, Fu B, et al. Massive genomic rearrangement acquired in a single catastrophic event during cancer development. *Cell*. 2011;144(1):27-40. doi:10.1016/j.cell.2010.11.055

34. Wu H-X, Wang Z-X, Zhao Q, et al. Tumor mutational and indel burden: a systematic pan-cancer evaluation as prognostic biomarkers. *Ann Transl Med*. 2019;7(22):640. doi:10.21037/ATM.2019.10.116

35. Gleason DF. Classification of prostatic carcinomas. *Cancer Chemother reports*. 1966;50(3):125-128. http://www.ncbi.nlm.nih.gov/pubmed/5948714. Accessed April 21, 2020.

36. Epstein JI, Egevad L, Amin MB, Delahunt B, Srigley JR, Humphrey PA. The 2014 International Society of Urological Pathology (ISUP) Consensus Conference on Gleason Grading of Prostatic Carcinoma. *Am J Surg Pathol*. 2015;40(2):244-252. doi:10.1097/PAS.0000000000000530

37. Holland AJ, Cleveland DW. Boveri revisited: chromosomal instability, aneuploidy and tumorigenesis. *Nat Rev Mol Cell Biol*. 2009;10(7):478-487. doi:10.1038/nrm2718

38. Knouse KA, Davoli T, Elledge SJ, Amon A. Aneuploidy in Cancer: Seq-ing Answers to Old Questions. *Annu Rev Cancer Biol*. 2017;1(1):335-354. doi:10.1146/annurev-cancerbio-042616-072231

39. Davoli T, Xu AW, Mengwasser KE, et al. Cumulative haploinsufficiency and triplosensitivity drive aneuploidy patterns and shape the cancer genome. *Cell*. 2013;155(4):948-962. doi:10.1016/j.cell.2013.10.011

40. Li X, Galipeau PC, Paulson TG, et al. Temporal and spatial evolution of somatic chromosomal alterations: a case-cohort study of Barrett's esophagus. *Cancer Prev Res (Phila)*. 2014;7(1):114-127. doi:10.1158/1940-6207.CAPR-13-0289

41. Taylor AM, Shih J, Ha G, et al. Genomic and Functional Approaches to Understanding Cancer Aneuploidy. *Cancer Cell*. 2018;33(4):676-689.e3. doi:10.1016/j.ccell.2018.03.007

42. Davoli T, Uno H, Wooten EC, Elledge SJ. Tumor aneuploidy correlates with markers of immune evasion and with reduced response to immunotherapy. *Science (80-)*. 2017;355(6322):eaaf8399. doi:10.1126/science.aaf8399

43. Reiter JG, Baretti M, Gerold JM, et al. An analysis of genetic heterogeneity in untreated cancers. *Nat Rev Cancer*. 2019;19(11):639-650. doi:10.1038/s41568-019-0185-x

44. Jones S, Chen W, Parmigiani G, et al. Comparative lesion sequencing provides insights into tumor evolution. *Proc Natl Acad Sci U S A*. 2008;105(11):4283.

doi:10.1073/PNAS.0712345105

45. Gerlinger M, Rowan AJ, Horswell S, et al. Intratumor heterogeneity and branched evolution revealed by multiregion sequencing. *N Engl J Med*. 2012;366(10):883-892. doi:10.1056/NEJMoa1113205

46. Stratton MR. Exploring the Genomes of Cancer Cells: Progress and Promise. *Science (80-)*. 2011;331(6024):1553-1558. https://www.sciencemag.org/lookup/doi/10.1126/science.1204040. Accessed April 21, 2020.

47. Navin N, Krasnitz A, Rodgers L, et al. Inferring tumor progression from genomic heterogeneity. *Genome Res*. 2010;20(1):68-80. doi:10.1101/gr.099622.109

48. Shah SP, Morin RD, Khattra J, et al. Mutational evolution in a lobular breast tumour profiled at single nucleotide resolution. *Nature*. 2009;461(7265):809-813. doi:10.1038/nature08489

49. Hunter KW, Amin R, Deasy S, Ha N-H, Wakefield L. Genetic insights into the morass of metastatic heterogeneity. *Nat Rev Cancer*. 2018;18(4):211-223. doi:10.1038/nrc.2017.126

50. Naxerova K, Jain RK. Using tumour phylogenetics to identify the roots of metastasis in humans. *Nat Rev Clin Oncol*. 2015;12(5):258-272. doi:10.1038/nrclinonc.2014.238

51. Hainsworth JD, Meric-Bernstam F, Swanton C, et al. Targeted Therapy for Advanced Solid Tumors on the Basis of Molecular Profiles: Results From MyPathway, an Open-Label, Phase IIa Multiple Basket Study. *J Clin Oncol*. 2018;36(6):536-542. doi:10.1200/JCO.2017.75.3780

52. Hamburg MA, Collins FS. The Path to Personalized Medicine. *N Engl J Med*. 2010;363(4):301-304. doi:10.1056/NEJMp1006304

53. Biankin A V., Piantadosi S, Hollingsworth SJ. Patient-centric trials for therapeutic development in precision oncology. *Nature*. 2015;526(7573):361-370. doi:10.1038/nature15819

54. Gray SW, Cronin A, Bair E, Lindeman N, Viswanath V, Janeway KA. Marketing of personalized cancer care on the web: an analysis of Internet websites. *J Natl Cancer Inst*. 2015;107(5). doi:10.1093/jnci/djv030

55. O'Brien SG, Guilhot F, Larson RA, et al. Imatinib Compared with Interferon and Low-

Dose Cytarabine for Newly Diagnosed Chronic-Phase Chronic Myeloid Leukemia. *N Engl J Med*. 2003;348(11):994-1004. doi:10.1056/NEJMoa022457

56. Slamon DJ, Leyland-Jones B, Shak S, et al. Use of chemotherapy plus a monoclonal antibody against HER2 for metastatic breast cancer that overexpresses HER2. *N Engl J Med*. 2001;344(11):783-792. doi:10.1056/NEJM200103153441101

57. Chapman PB, Hauschild A, Robert C, et al. Improved Survival with Vemurafenib in Melanoma with BRAF V600E Mutation. 2011;364(26). doi:10.1056/NEJMoa1103782

58. Bethesda MNCI. Cancer Moonshot. https://www.cancer.gov/research/key-initiatives/moonshot-cancer-initiative. Published 2016. Accessed April 18, 2020.

59. Sun J, Wei Q, Zhou Y, Wang J, Liu Q, Xu H. A systematic analysis of FDA-approved anticancer drugs. *BMC Syst Biol*. 2017;11(Suppl 5):87. doi:10.1186/s12918-017-0464-7

60. Pao W, Girard N. New driver mutations in non-small-cell lung cancer. *Lancet Oncol*. 2011;12(2):175-180. doi:10.1016/S1470-2045(10)70087-5

61. Cancer Genome Atlas Research Network TCGAR. Comprehensive genomic characterization of squamous cell lung cancers. *Nature*. 2012;489(7417):519-525. doi:10.1038/nature11404

62. Stransky N, Egloff AM, Tward AD, et al. The mutational landscape of head and neck squamous cell carcinoma. *Science*. 2011;333(6046):1157-1160. doi:10.1126/science.1208130

63. Cancer Genome Atlas Network TCGA. Comprehensive molecular characterization of human colon and rectal cancer. *Nature*. 2012;487(7407):330-337. doi:10.1038/nature11252

64. Garraway LA. Genomics-driven oncology: framework for an emerging paradigm. *J Clin Oncol*. 2013;31(15):1806-1814. doi:10.1200/JCO.2012.46.8934

65. Hyman DM, Puzanov I, Subbiah V, et al. Vemurafenib in multiple nonmelanoma cancers with BRAF V600 mutations. *N Engl J Med*. 2015;373(8):726. doi:10.1056/NEJMOA1502309

66. Diamond EL, Subbiah V, Lockhart AC, et al. Vemurafenib for *BRAF* V600–Mutant Erdheim-Chester Disease and Langerhans Cell Histiocytosis. *JAMA Oncol*. 2018;4(3):384. doi:10.1001/jamaoncol.2017.5029

67. Lemery S, Keegan P, Pazdur R. First FDA Approval Agnostic of Cancer Site — When a Biomarker Defines the Indication. *N Engl J Med*. 2017;377(15):1409-1412. doi:10.1056/NEJMp1709968

68. Drilon A, Laetsch TW, Kummar S, et al. Efficacy of Larotrectinib in TRK Fusion-Positive Cancers in Adults and Children. *N Engl J Med*. 2018;378(8):731-739. doi:10.1056/NEJMoa1714448

69. Wilson, J., M. G, Jungner G. Principles and practice of screening for disease. *Public Health Pap*. 1968;34. https://www.who.int/ionizing_radiation/medical_radiation_exposure/munich-WHO-1968-Screening-Disease.pdf. Accessed April 6, 2020.

70. Jackson SE, Chester JD. Personalised cancer medicine. *Int J Cancer*. 2015;137(2):262-266. doi:10.1002/ijc.28940

71. Chia S, Low J-L, Zhang X, et al. Phenotype-driven precision oncology as a guide for clinical decisions one patient at a time. *Nat Commun*. 2017;8(1):435. doi:10.1038/S41467-017-00451-5

72. Pauli C, Hopkins BD, Prandi D, et al. Personalized *In Vitro* and *In Vivo* Cancer Models to Guide Precision Medicine. *Cancer Discov*. 2017;7(5):462-477. doi:10.1158/2159-8290.CD-16-1154

73. Lee SH, Hu W, Matulay JT, et al. Tumor Evolution and Drug Response in Patient-Derived Organoid Models of Bladder Cancer. *Cell*. 2018;173(2):515-528.e17. doi:10.1016/j.cell.2018.03.017

74. Said R, Guibert N, Oxnard GR, Tsimberidou AM. Circulating tumor DNA analysis in the era of precision oncology. *Oncotarget*. 2020;11(2):188. doi:10.18632/ONCOTARGET.27418

75. Hironaka-Mitsuhashi A, Sanchez Calle A, Ochiya T, Takayama S, Suto A. Towards Circulating-Tumor DNA-Based Precision Medicine. *J Clin Med*. 2019;8(9). doi:10.3390/jcm8091365

76. Thierry AR, Mouliere F, El Messaoudi S, et al. Clinical validation of the detection of KRAS and BRAF mutations from circulating tumor DNA. *Nat Med*. 2014;20(4):430-435. doi:10.1038/nm.3511

77. Oxnard GR, Thress KS, Alden RS, et al. Association Between Plasma Genotyping and Outcomes of Treatment With Osimertinib (AZD9291) in Advanced Non-Small-Cell

Lung Cancer. *J Clin Oncol*. 2016;34(28):3375-3382. doi:10.1200/JCO.2016.66.7162

78. Gandara DR, Paul SM, Kowanetz M, et al. Blood-based tumor mutational burden as a predictor of clinical benefit in non-small-cell lung cancer patients treated with atezolizumab. *Nat Med*. 2018;24(9):1441-1448. doi:10.1038/s41591-018-0134-3

79. Khagi Y, Goodman AM, Daniels GA, et al. Hyper-Mutated Circulating Tumor DNA: Correlation with Response to Checkpoint Inhibitor-Based Immunotherapy. *Clin Cancer Res*. 2017;23(19):5729. doi:10.1158/1078-0432.CCR-17-1439

80. Murtaza M, Dawson S-J, Pogrebniak K, et al. Multifocal clonal evolution characterized using circulating tumour DNA in a case of metastatic breast cancer. *Nat Commun*. 2015;6:8760. doi:10.1038/ncomms9760

81. Crowley E, Di Nicolantonio F, Loupakis F, Bardelli A. Liquid biopsy: monitoring cancer-genetics in the blood. *Nat Rev Clin Oncol*. 2013;10(8):472-484. doi:10.1038/nrclinonc.2013.110

82. Diaz LA, Bardelli A, Bardelli A. Liquid biopsies: genotyping circulating tumor DNA. *J Clin Oncol*. 2014;32(6):579-586. doi:10.1200/JCO.2012.45.2011

83. Yao W, Mei C, Nan X, Hui L. Evaluation and comparison of in vitro degradation kinetics of DNA in serum, urine and saliva: A qualitative study. *Gene*. 2016;590(1):142-148. doi:10.1016/J.GENE.2016.06.033

84. Wan JCM, Massie C, Garcia-Corbacho J, et al. Liquid biopsies come of age: towards implementation of circulating tumour DNA. *Nat Rev Cancer*. 2017;17(4):223-238. doi:10.1038/nrc.2017.7

85. Schreiber RD, Old LJ, Smyth MJ. Cancer Immunoediting: Integrating Immunity's Roles in Cancer Suppression and Promotion. *Science (80-)*. 2011;331(6024):1565-1570. doi:10.1126/science.1203486

86. Chen DS, Mellman I. Oncology Meets Immunology: The Cancer-Immunity Cycle. *Immunity*. 2013;39(1):1-10. doi:10.1016/J.IMMUNI.2013.07.012

87. Hodi FS, O'Day SJ, McDermott DF, et al. Improved Survival with Ipilimumab in Patients with Metastatic Melanoma. *N Engl J Med*. 2010;363(8):711-723. doi:10.1056/NEJMoa1003466

88. Borghaei H, Paz-Ares L, Horn L, et al. Nivolumab versus Docetaxel in Advanced Nonsquamous Non–Small-Cell Lung Cancer. *N Engl J Med*. 2015;373(17):1627-1639.

doi:10.1056/NEJMoa1507643

89. Robert C, Schachter J, Long G V., et al. Pembrolizumab versus Ipilimumab in Advanced Melanoma. *N Engl J Med*. 2015;372(26):2521-2532. doi:10.1056/NEJMoa1503093

90. Taube JM, Klein A, Brahmer JR, et al. Association of PD-1, PD-1 Ligands, and Other Features of the Tumor Immune Microenvironment with Response to Anti-PD-1 Therapy. *Clin Cancer Res*. 2014;20(19):5064-5074. doi:10.1158/1078-0432.CCR-13-3271

91. Rizvi NA, Hellmann MD, Snyder A, et al. Cancer immunology. Mutational landscape determines sensitivity to PD-1 blockade in non-small cell lung cancer. *Science*. 2015;348(6230):124-128. doi:10.1126/science.aaa1348

92. Snyder A, Makarov V, Merghoub T, et al. Genetic Basis for Clinical Response to CTLA-4 Blockade in Melanoma. *N Engl J Med*. 2014;371(23):2189-2199. doi:10.1056/NEJMoa1406498

93. Tran E, Turcotte S, Gros A, et al. Cancer Immunotherapy Based on Mutation-Specific CD4+ T Cells in a Patient with Epithelial Cancer. *Science (80-)*. 2014;344(6184):641-645. doi:10.1126/science.1251102

94. Miao D, Van Allen EM. Genomic determinants of cancer immunotherapy. *Curr Opin Immunol*. 2016;41:32-38. doi:10.1016/j.coi.2016.05.010

95. Bowen A, Casadevall A. From the Cover: Increasing disparities between resource inputs and outcomes, as measured by certain health deliverables, in biomedical research. *Proc Natl Acad Sci U S A*. 2015;112(36):11335. doi:10.1073/PNAS.1504955112

96. Scannell JW, Bosley J. When Quality Beats Quantity: Decision Theory, Drug Discovery, and the Reproducibility Crisis. *PLoS One*. 2016;11(2):e0147215. doi:10.1371/journal.pone.0147215

97. Swanton C. Intratumor heterogeneity: evolution through space and time. *Cancer Res*. 2012;72(19):4875-4882. doi:10.1158/0008-5472.CAN-12-2217

98. Bhang HC, Ruddy DA, Krishnamurthy Radhakrishna V, et al. Studying clonal dynamics in response to cancer therapy using high-complexity barcoding. *Nat Med*. 2015;21(5):440-448. doi:10.1038/nm.3841

99. Tannock IF, Hickman JA. Limits to Personalized Cancer Medicine. *N Engl J Med*. 2016;375(13):1289-1294. doi:10.1056/NEJMsb1607705

100. Antonarakis ES, Lu C, Wang H, et al. AR-V7 and Resistance to Enzalutamide and Abiraterone in Prostate Cancer. *N Engl J Med*. 2014;371(11):1028-1038. doi:10.1056/NEJMoa1315815

101. Johnson GL, Stuhlmiller TJ, Angus SP, Zawistowski JS, Graves LM. Molecular Pathways: Adaptive Kinome Reprogramming in Response to Targeted Inhibition of the BRAF-MEK-ERK Pathway in Cancer. *Clin Cancer Res*. 2014;20(10):2516. doi:10.1158/1078-0432.CCR-13-1081

102. Delbridge ARD, Grabow S, Strasser A, Vaux DL. Thirty years of BCL-2: translating cell death discoveries into novel cancer therapies. *Nat Rev Cancer*. 2016;16(2):99-109. doi:10.1038/nrc.2015.17

103. Haffner MC, Mosbruger T, Esopi DM, et al. Tracking the clonal origin of lethal prostate cancer. *J Clin Invest*. 2013;123(11):4918-4922. doi:10.1172/JCI70354

104. Moscow JA, Fojo T, Schilsky RL. The evidence framework for precision cancer medicine. *Nat Rev Clin Oncol*. 2018;15(3):183-192. doi:10.1038/nrclinonc.2017.186

105. Chamie K, Litwin MS, Bassett JC, et al. Recurrence of high-risk bladder cancer: a population-based analysis. *Cancer*. 2013;119(17):3219-3227. doi:10.1002/cncr.28147

106. Kawanishi H, Takahashi T, Ito M, et al. Genetic analysis of multifocal superficial urothelial cancers by array-based comparative genomic hybridisation. *Br J Cancer*. 2007;97(2):260-266. doi:10.1038/sj.bjc.6603850

107. van Tilborg AAG, de Vries A, de Bont M, Groenfeld LE, van der Kwast TH, Zwarthoff EC. Molecular evolution of multiple recurrent cancers of the bladder. *Hum Mol Genet*. 2000;9(20):2973-2980. doi:10.1093/hmg/9.20.2973

108. Höglund M. On the origin of syn- and metachronous urothelial carcinomas. *Eur Urol*. 2007;51(5):1185-1193; discussion 1193. doi:10.1016/j.eururo.2006.11.025

109. Slaughter DP, Southwick HW, Smejkal W. Field cancerization in oral stratified squamous epithelium; clinical implications of multicentric origin. *Cancer*. 1953;6(5):963-968. doi:10.1002/1097-0142(195309)6:5<963::aid-cncr2820060515>3.0.co;2-q

110. Koss LG. Mapping of the urinary bladder: its impact on the concepts of bladder

cancer. *Hum Pathol*. 1979;10(5):533-548. doi:10.1016/S0046-8177(79)80097-0

111. Cianciulli AM, Leonardo C, Guadagni F, et al. Genetic instability in superficial bladder cancer and adjacent mucosa: An interphase cytogenetic study. *Hum Pathol*. 2003;34(3):214-221. doi:10.1053/hupa.2003.30

112. Stoehr R, Knuechel R, Boecker J, et al. Histologic-Genetic Mapping by Allele-Specific PCR Reveals Intraurothelial Spread of p53 Mutant Tumor Clones. *Lab Investig*. 2002;82(11):1553-1561. doi:10.1097/01.LAB.0000035022.29742.85

113. Majewski T, Yao H, Bondaruk J, et al. Whole-Organ Genomic Characterization of Mucosal Field Effects Initiating Bladder Carcinogenesis. *Cell Rep*. 2019;26(8):2241-2256.e4. doi:10.1016/j.celrep.2019.01.095

114. Tsai YC, Simoneau AR, Spruck CH, et al. Mosaicism in human epithelium: macroscopic monoclonal patches cover the urothelium. *J Urol*. 1995;153(5):1697-1700. doi:10.1016/S0022-5347(01)67507-4

115. Warrick JI, Sjödahl G, Kaag M, et al. Intratumoral Heterogeneity of Bladder Cancer by Molecular Subtypes and Histologic Variants. *Eur Urol*. 2019;75(1):18-22. https://www.sciencedirect.com/science/article/pii/S0302283818306535?via%3Dihub. Accessed April 26, 2020.

116. Cheng L, Neumann RM, Nehra A, Spotts BE, Weaver AL, Bostwick DG. Cancer heterogeneity and its biologic implications in the grading of urothelial carcinoma. *Cancer*. 2000;88(7):1663-1670. doi:10.1002/(sici)1097-0142(20000401)88:7<1663::aid-cncr21>3.0.co;2-8

117. Robertson AG, Kim J, Al-Ahmadie H, et al. Comprehensive Molecular Characterization of Muscle-Invasive Bladder Cancer. *Cell*. 2017;171(3):540-556.e25. doi:10.1016/j.cell.2017.09.007

118. Pouessel D, Neuzillet Y, Mertens LS, et al. Tumor heterogeneity of fibroblast growth factor receptor 3 (FGFR3) mutations in invasive bladder cancer: implications for perioperative anti-FGFR3 treatment. *Ann Oncol*. 2016;27(7):1311-1316. doi:10.1093/ANNONC/MDW170

119. Lamy P, Nordentoft I, Birkenkamp-Demtröder K, et al. Paired Exome Analysis Reveals Clonal Evolution and Potential Therapeutic Targets in Urothelial Carcinoma. *Cancer Res*. 2016;76(19):5894-5906. doi:10.1158/0008-5472.CAN-16-0436

120. Nordentoft I, Lamy P, Birkenkamp-Demtröder K, et al. Mutational Context and Diverse

Clonal Development in Early and Late Bladder Cancer. *Cell Rep*. 2014;7(5):1649-1663. doi:10.1016/J.CELREP.2014.04.038

121. Faltas BM, Prandi D, Tagawa ST, et al. Clonal evolution of chemotherapy-resistant urothelial carcinoma. *Nat Genet*. 2016;48(12):1490-1499. doi:10.1038/ng.3692

122. Liu D, Abbosh P, Keliher D, et al. Mutational patterns in chemotherapy resistant muscle-invasive bladder cancer. *Nat Commun*. 2017;8(1):2193. doi:10.1038/s41467-017-02320-7

123. Seiler R, Ashab HAD, Erho N, et al. Impact of Molecular Subtypes in Muscle-invasive Bladder Cancer on Predicting Response and Survival after Neoadjuvant Chemotherapy. *Eur Urol*. 2017;72(4):544-554. doi:10.1016/J.EURURO.2017.03.030

124. Plimack ER, Dunbrack RL, Brennan TA, et al. Defects in DNA Repair Genes Predict Response to Neoadjuvant Cisplatin-based Chemotherapy in Muscle-invasive Bladder Cancer. *Eur Urol*. 2015;68(6):959-967. doi:10.1016/j.eururo.2015.07.009

125. Mariathasan S, Turley SJ, Nickles D, et al. TGF-β attenuates tumour response to PD-L1 blockade by contributing to exclusion of T cells. *Nature*. 2018;554(7693):544. doi:10.1038/NATURE25501

126. Powles T, Eder JP, Fine GD, et al. MPDL3280A (anti-PD-L1) treatment leads to clinical activity in metastatic bladder cancer. *Nature*. 2014;515(7528):558-562. doi:10.1038/nature13904

127. da Costa JB, Gibb EA, Nykopp TK, Mannas M, Wyatt AW, Black PC. Molecular tumor heterogeneity in muscle invasive bladder cancer: Biomarkers, subtypes, and implications for therapy. *Urol Oncol Semin Orig Investig*. December 2018. doi:10.1016/J.UROLONC.2018.11.015

128. Iyer G, Hanrahan AJ, Milowsky MI, et al. Genome Sequencing Identifies a Basis for Everolimus Sensitivity. *Science (80-)*. 2012;338(6104):221-221. doi:10.1126/SCIENCE.1226344

129. Petrylak DP, Wit R de, Chi KN, et al. Ramucirumab plus docetaxel versus placebo plus docetaxel in patients with locally advanced or metastatic urothelial carcinoma after platinum-based therapy (RANGE): a randomised, double-blind, phase 3 trial. *Lancet*. 2017;390(10109):2266-2277. doi:10.1016/S0140-6736(17)32365-6

130. Loriot Y, Necchi A, Park SH, et al. Erdafitinib (ERDA; JNJ-42756493), a pan-fibroblast growth factor receptor (FGFR) inhibitor, in patients (pts) with metastatic or

unresectable urothelial carcinoma (mUC) and *FGFR* alterations (FGFRa): Phase 2 continuous versus intermittent dosing. *J Clin Oncol*. 2018;36(6_suppl):411-411. doi:10.1200/JCO.2018.36.6_suppl.411

131. McGregor BA, Chung J, Bergerot PG, et al. Correlation of circulating tumor DNA (ctDNA) assessment with tissue-based comprehensive genomic profiling (CGP) in metastatic urothelial cancer (mUC). *J Clin Oncol*. 2018;36(6_suppl):453-453. doi:10.1200/JCO.2018.36.6_suppl.453

132. Agarwal N, Pal SK, Hahn AW, et al. Characterization of metastatic urothelial carcinoma via comprehensive genomic profiling of circulating tumor DNA. *Cancer*. 2018;124(10):2115-2124. doi:10.1002/cncr.31314

133. Sonpavde G, Nagy RJ, Apolo AB, et al. Circulating cell-free DNA profiling of patients with advanced urothelial carcinoma. *J Clin Oncol*. 2016;34(2_suppl):358-358. doi:10.1200/jco.2016.34.2_suppl.358

134. Christensen E, Birkenkamp-Demtröder K, Nordentoft I, et al. Liquid Biopsy Analysis of FGFR3 and PIK3CA Hotspot Mutations for Disease Surveillance in Bladder Cancer. *Eur Urol*. 2017;71(6):961-969. doi:10.1016/J.EURURO.2016.12.016

135. Vandekerkhove G, Todenhöfer T, Annala M, et al. Circulating Tumor DNA Reveals Clinically Actionable Somatic Genome of Metastatic Bladder Cancer. *Clin Cancer Res*. 2017;23(21):6487-6497. doi:10.1158/1078-0432.CCR-17-1140

136. Herr HW, Morales A. History of bacillus Calmette-Guerin and bladder cancer: an immunotherapy success story. 2008;179(1). https://www.sciencedirect.com/science/article/pii/S0022534707022884. Accessed April 15, 2020.

137. Morales A, Eidinger D, Bruce AW. Intracavitary Bacillus Calmette-Guerin in the treatment of superficial bladder tumors. *J Urol*. 1976;116(2):180-183. doi:10.1016/s0022-5347(17)58737-6

138. Babjuk M, Böhle A, Burger M, et al. EAU Guidelines on Non-Muscle-invasive Urothelial Carcinoma of the Bladder: Update 2016. *Eur Urol*. 2017;71(3):447-461. doi:10.1016/j.eururo.2016.05.041

139. Sylvester RJ, Brausi MA, Kirkels WJ, et al. Long-Term Efficacy Results of EORTC Genito-Urinary Group Randomized Phase 3 Study 30911 Comparing Intravesical Instillations of Epirubicin, Bacillus Calmette-Guérin, and Bacillus Calmette-Guérin plus

Isoniazid in Patients with Intermediate- and High-Risk . *Eur Urol*. 2010;57(5):766. doi:10.1016/J.EURURO.2009.12.024

140. Denzinger S, Fritsche H-M, Otto W, Blana A, Wieland W-F, Burger M. Early Versus Deferred Cystectomy for Initial High-Risk pT1G3 Urothelial Carcinoma of the Bladder: Do Risk Factors Define Feasibility of Bladder-Sparing Approach? *Eur Urol*. 2008;53(1):146-152. doi:10.1016/J.EURURO.2007.06.030

141. Alfred Witjes J, Lebret T, Compérat EM, et al. Updated 2016 EAU Guidelines on Muscle-invasive and Metastatic Bladder Cancer. *Eur Urol*. 2017;71(3):462-475. doi:10.1016/j.eururo.2016.06.020

142. Bellmunt J, Lalani A-KA, Jacobus S, et al. Everolimus and pazopanib (E/P) benefit genomically selected patients with metastatic urothelial carcinoma. *Br J Cancer*. 2018;119(6):707-712. doi:10.1038/s41416-018-0261-0

143. Kim HS, Seo HK. Immune checkpoint inhibitors for urothelial carcinoma. *Investig Clin Urol*. 2018;59(5):285-296. doi:10.4111/icu.2018.59.5.285

144. Heidenreich A, Bastian PJ, Bellmunt J, et al. EAU Guidelines on Prostate Cancer. Part 1: Screening, Diagnosis, and Local Treatment with Curative Intent—Update 2013. *Eur Urol*. 2014;65(1):124-137. doi:10.1016/J.EURURO.2013.09.046

145. Karavitakis M, Ahmed HU, Abel PD, Hazell S, Winkler MH. Tumor focality in prostate cancer: implications for focal therapy. *Nat Rev Clin Oncol 2011 81*. 2010;8(1):48-55. doi:10.1038/nrclinonc.2010.190

146. Cyll K, Ersvær E, Vlatkovic L, et al. Tumour heterogeneity poses a significant challenge to cancer biomarker research. *Br J Cancer*. 2017;117(3):367-375. doi:10.1038/bjc.2017.171

147. Andreoiu M, Cheng L. Multifocal prostate cancer: biologic, prognostic, and therapeutic implications. *Hum Pathol*. 2010;41(6):781-793. doi:10.1016/J.HUMPATH.2010.02.011

148. Gundem G, Van Loo P, Kremeyer B, et al. The evolutionary history of lethal metastatic prostate cancer. *Nature*. 2015;520(7547):353-357. doi:10.1038/nature14347

149. Arora R, Koch MO, Eble JN, Ulbright TM, Li L, Cheng L. Heterogeneity of Gleason grade in multifocal adenocarcinoma of the prostate. *Cancer*. 2004;100(11):2362-2366. doi:10.1002/cncr.20243

150. So MJ, Cheville JC, Katzmann JA, et al. Factors That Influence the Measurement of

Prostate Cancer DNA Ploidy and Proliferation in Paraffin Embedded Tissue Evaluated by Flow Cytometry. *Mod Pathol*. 2001;14(9):906-912. doi:10.1038/modpathol.3880410

151. Stopsack KH, Whittaker CA, Gerke TA, et al. Aneuploidy drives lethal progression in prostate cancer. *Proc Natl Acad Sci U S A*. 2019;116(23):11390. doi:10.1073/PNAS.1902645116

152. Priestley P, Baber J, Lolkema MP, et al. Pan-cancer whole-genome analyses of metastatic solid tumours. *Nature*. 2019;575(7781):210. doi:10.1038/s41586-019-1689-y

153. Epstein JI, Pizov G, Steinberg GD, et al. Correlation of Prostate Cancer Nuclear Deoxyribonucleic Acid, Size, Shape and Gleason Grade with Pathological Stage at Radical Prostatectomy. *J Urol*. 1992;148(1):87-91. doi:10.1016/S0022-5347(17)36518-7

154. Swanson GP, Chen W, Speights VOO. Failure of Ploidy and Proliferative Fraction to Predict Long-Term Outcome After Prostatectomy. *World J Oncol*. 2018;9(3):69-73. doi:10.14740/WJON1111W

155. Greene DR, Taylor SR, Wheeler TM, Scardino PT. DNA ploidy by image analysis of individual foci of prostate cancer: a preliminary report. *Cancer Res*. 1991;51(15):4084-4089. http://www.ncbi.nlm.nih.gov/pubmed/1855223. Accessed February 3, 2020.

156. Fraser M, Sabelnykova VY, Yamaguchi TN, et al. Genomic hallmarks of localized, non-indolent prostate cancer. *Nature*. 2017;541(7637):359-364. doi:10.1038/nature20788

157. Armenia J, Wankowicz SAM, Liu D, et al. The long tail of oncogenic drivers in prostate cancer. *Nat Genet*. 2018;50(5):645-651. doi:10.1038/s41588-018-0078-z

158. Boutros PC, Fraser M, Harding NJ, et al. Spatial genomic heterogeneity within localized, multifocal prostate cancer. *Nat Genet*. 2015;47(7):736-745. doi:10.1038/ng.3315

159. Fraser M, Berlin A, Bristow RG, van der Kwast T. Genomic, pathological, and clinical heterogeneity as drivers of personalized medicine in prostate cancer. *Urol Oncol Semin Orig Investig*. 2015;33(2):85-94. doi:10.1016/J.UROLONC.2013.10.020

160. Wyatt AW, Gleave ME. Targeting the adaptive molecular landscape of castration-resistant prostate cancer. *EMBO Mol Med*. 2015;7(7):878-894. doi:10.15252/emmm.201303701

161. Mateo J, Carreira S, Sandhu S, et al. DNA-Repair Defects and Olaparib in Metastatic Prostate Cancer. *N Engl J Med*. 2015;373(18):1697-1708. doi:10.1056/NEJMoa1506859

162. Azad AA, Volik S V., Wyatt AW, et al. Androgen Receptor Gene Aberrations in Circulating Cell-Free DNA: Biomarkers of Therapeutic Resistance in Castration-Resistant Prostate Cancer. *Clin Cancer Res*. 2015;21(10):2315-2324. doi:10.1158/1078-0432.CCR-14-2666

163. Romanel A, Tandefelt DG, Conteduca V, et al. Plasma AR and abiraterone-resistant prostate cancer. *Sci Transl Med*. 2015;7(312):312re10. doi:10.1126/SCITRANSLMED.AAC9511

164. Salvi S, Casadio V, Conteduca V, et al. Circulating AR copy number and outcome to enzalutamide in docetaxel-treated metastatic castration-resistant prostate cancer. *Oncotarget*. 2016;7(25):37839. doi:10.18632/ONCOTARGET.9341

165. Annala M, Struss WJ, Warner EW, et al. Treatment Outcomes and Tumor Loss of Heterozygosity in Germline DNA Repair–deficient Prostate Cancer. 2017;72(1):34-42. http://www.ncbi.nlm.nih.gov/pubmed/28259476. Accessed April 20, 2020.

166. Vandekerkhove G, Struss WJ, Annala M, et al. Circulating Tumor DNA Abundance and Potential Utility in De Novo Metastatic Prostate Cancer. *Eur Urol*. 2019;75(4):667-675. doi:10.1016/J.EURURO.2018.12.042

167. Müller DC, Rämö M, Naegele K, et al. Donor-derived, metastatic urothelial cancer after kidney transplantation associated with a potentially oncogenic BK polyomavirus. *J Pathol*. 2018;244(3):265-270. doi:10.1002/path.5012

168. Vajdic CM, van Leeuwen MT. Cancer incidence and risk factors after solid organ transplantation. *Int J Cancer*. 2009;125(8):1747-1754. doi:10.1002/ijc.24439

169. Hirsch HH, Babel N, Comoli P, et al. European perspective on human polyomavirus infection, replication and disease in solid organ transplantation. *Clin Microbiol Infect*. 2014;20 Suppl 7:74-88. doi:10.1111/1469-0691.12538

170. Weinreb DB, Desman GT, Amolat-Apiado MJM, Burstein DE, Godbold JH, Johnson EM. Polyoma virus infection is a prominent risk factor for bladder carcinoma in immunocompetent individuals. *Diagn Cytopathol*. 2006;34(3):201-203. doi:10.1002/dc.20429

171. Papadimitriou JC, Randhawa P, Rinaldo CH, Drachenberg CB, Alexiev B, Hirsch HH.

BK Polyomavirus Infection and Renourinary Tumorigenesis. *Am J Transplant*. 2016;16(2):398-406. doi:10.1111/ajt.13550

172. Harris KF, Christensen JB, Imperiale MJ. BK virus large T antigen: interactions with the retinoblastoma family of tumor suppressor proteins and effects on cellular growth control. *J Virol*. 1996;70(4):2378. https://www.ncbi.nlm.nih.gov/pmc/articles/PMC190080/. Accessed April 15, 2020.

173. Ruiz C, Lenkiewicz E, Evers L, et al. Advancing a clinically relevant perspective of the clonal nature of cancer. *Proc Natl Acad Sci U S A*. 2011;108(29):12054. doi:10.1073/PNAS.1104009108

174. Dumoulin A, Hirsch HH. Reevaluating and optimizing polyomavirus BK and JC real-time PCR assays to detect rare sequence polymorphisms. *J Clin Microbiol*. 2011;49(4):1382-1388. doi:10.1128/JCM.02008-10

175. Drachenberg CB, Hirsch HH, Papadimitriou JC, et al. Polyomavirus BK versus JC replication and nephropathy in renal transplant recipients: a prospective evaluation. *Transplantation*. 2007;84(3):323-330. doi:10.1097/01.tp.0000269706.59977.a5

176. Henriksen S, Tylden GD, Dumoulin A, Sharma BN, Hirsch HH, Rinaldo CH. The human fetal glial cell line SVG p12 contains infectious BK polyomavirus. *J Virol*. 2014;88(13):7556-7568. doi:10.1128/JVI.00696-14

177. Gosert R, Rinaldo CH, Funk GA, et al. Polyomavirus BK with rearranged noncoding control region emerge in vivo in renal transplant patients and increase viral replication and cytopathology. *J Exp Med*. 2008;205(4):841-852. doi:10.1084/jem.20072097

178. Bethge T, Hachemi HA, Manzetti J, Gosert R, Schaffner W, Hirsch HH. Sp1 sites in the noncoding control region of BK polyomavirus are key regulators of bidirectional viral early and late gene expression. *J Virol*. 2015;89(6):3396-3411. doi:10.1128/JVI.03625-14

179. Leboeuf C, Wilk S, Achermann R, et al. BK Polyomavirus-Specific 9mer CD8 T Cell Responses Correlate With Clearance of BK Viremia in Kidney Transplant Recipients: First Report From the Swiss Transplant Cohort Study. *Am J Transplant*. 2017;17(10):2591-2600. doi:10.1111/ajt.14282

180. Yan L, Salama ME, Lanciault C, Matsumura L, Troxell ML. Polyomavirus large T antigen is prevalent in urothelial carcinoma post-kidney transplant. *Hum Pathol*. 2016;48:122-131. doi:10.1016/j.humpath.2015.09.021

181. Lawrence MS, Stojanov P, Polak P, et al. Mutational heterogeneity in cancer and the search for new cancer-associated genes. *Nature*. 2013;499(7457):214-218. doi:10.1038/nature12213

182. Starrett GJ, Marcelus C, Cantalupo PG, et al. Merkel Cell Polyomavirus Exhibits Dominant Control of the Tumor Genome and Transcriptome in Virus-Associated Merkel Cell Carcinoma. *MBio*. 2017;8(1). doi:10.1128/mBio.02079-16

183. Ardelt PU, Rieken M, Ebbing J, et al. Urothelial Cancer in Renal Transplant Recipients: Incidence, Risk Factors, and Oncological Outcome. *Urology*. 2016;88:104-110. doi:10.1016/J.UROLOGY.2015.10.031

184. Dalianis T, Hirsch HH, T D, HH H. Human Polyomaviruses in Disease and Cancer. *Virology*. 2013;437(2):63-72. doi:10.1016/J.VIROL.2012.12.015

185. Kenan DJ, Mieczkowski PA, Burger-Calderon R, Singh HK, Nickeleit V. The oncogenic potential of BK-polyomavirus is linked to viral integration into the human genome. *J Pathol*. 2015;237(3):379-389. doi:10.1002/path.4584

186. Kenan DJ, Mieczkowski PA, Latulippe E, et al. BK Polyomavirus Genomic Integration and Large T Antigen Expression: Evolving Paradigms in Human Oncogenesis. *Am J Transplant*. 2017;17(6):1674-1680. doi:10.1111/ajt.14191

187. Holley T, Lenkiewicz E, Evers L, et al. Deep Clonal Profiling of Formalin Fixed Paraffin Embedded Clinical Samples. Emmert-Buck MR, ed. *PLoS One*. 2012;7(11):e50586. doi:10.1371/journal.pone.0050586

188. Davis MW. ApE – a plasmid editor. Available from: http:// biologylabs.utah.edu/jorgensen/wayned/ape/2016.

189. Merlo LMF, Wang LS, Pepper JW, Rabinovitch PS, Maley CC. Polyploidy, aneuploidy and the evolution of cancer. *Adv Exp Med Biol*. 2010;675:1-13. doi:10.1007/978-1-4419-6199-0_1

190. Torres EM, Williams BR, Amon A. Aneuploidy: Cells losing their balance. *Genetics*. 2008;179(2):737-746. doi:10.1534/genetics.108.090878

191. Otto SP, Whitton J. Polyploid incidence and evolution. *Annu Rev Genet*. 2000;34:401-437. doi:10.1146/annurev.genet.34.1.401

192. Ben-David U, Amon A. Context is everything: aneuploidy in cancer. *Nat Rev Genet*. 2020;21(1):44-62. doi:10.1038/s41576-019-0171-x

193. Braun M, Stomper J, Kirsten R, et al. Landscape of chromosome number changes in prostate cancer progression. *World J Urol*. 2013;31(6):1489-1495. doi:10.1007/s00345-013-1051-1

194. Berner A, Waere H, Nesland JM, Paus E, Danielsen HE, Fosså SD. DNA ploidy, serum prostate specific antigen, histological grade and immunohistochemistry as predictive parameters of lymph node metastases in T1-T3/M0 prostatic adenocarcinoma. *Br J Urol*. 1995;75(1):26-32. doi:10.1111/j.1464-410X.1995.tb07227.x

195. Sebo TJ, Cheville JC, Riehle DL, et al. Predicting prostate carcinoma volume and stage at radical prostatectomy by assessing needle biopsy specimens for percent surface area and cores positive for carcinoma, perineural invasion, Gleason score, DNA ploidy and proliferation, and preoperative ser. *Cancer*. 2001;91(11):2196-2204. doi:10.1002/1097-0142(20010601)91:11<2196::aid-cncr1249>3.0.co;2-#

196. Lorenzato M, Rey D, Durlach A, Bouttens D, Birembaut P, Staerman F. DNA image cytometry on biopsies can help the detection of localized gleason 3+3 prostate cancers. *J Urol*. 2004;172(4 I):1311-1313. doi:10.1097/01.ju.0000139375.52611.0e

197. Carmichael MJ, Veltri RW, Partin AW, Miller MC, Walsh PC, Epstein JI. Deoxyribonucleic acid ploidy analysis as a predictor of recurrence following radical prostatectomy for stage T2 disease. *J Urol*. 1995;153(3 Pt 2):1015-1019.

198. Forsslund G, Esposti P -L, Nilsson B, Zetterberg A. The prognostic significance of nuclear dna content in prostatic carcinoma. *Cancer*. 1992;69(6):1432-1439. doi:10.1002/1097-0142(19920315)69:6<1432::AID-CNCR2820690621>3.0.CO;2-7

199. Wang N, Wilkin C, Böcking A, Tribukait B. Evaluation of tumor heterogeneity of prostate carcinoma by flow-and image DNA cytometry and histopathological grading. *Anal Cell Pathol*. 2000;20(1):49-62. doi:10.1155/2000/489303

200. Pretorius ME, Wæhre H, Abeler VM, et al. Large scale genomic instability as an additive prognostic marker in early prostate cancer. *Cell Oncol*. 2009;31(4):251-259. doi:10.3233/CLO-2009-0463

201. Lennartz M, Minner S, Brasch S, et al. The combination of DNA ploidy status and PTEN/6q15 deletions provides strong and independent prognostic information in prostate cancer. *Clin Cancer Res*. 2016;22(11):2802-2811. doi:10.1158/1078-0432.CCR-15-0635

202. Warzynski MJ, Soechtig CE, Maatman TJ, et al. Dna heterogeneity determined by flow cytometry in prostatic adenocarcinoma—necessitating multiple site analysis. *Prostate*. 1995;27(6):329-335. doi:10.1002/pros.2990270606

203. Häggarth L, Auer G, Busch C, Norberg M, Häggman M, Egevad L. The significance of tumor heterogeneity for prediction of DNA ploidy of prostate cancer. *Scand J Urol Nephrol*. 2005;39(5):387-392. doi:10.1080/00365590500239883

204. Magnen C Le, Bubendorf L, Rentsch CA, et al. Characterization and clinical relevance of ALDH bright populations in prostate cancer. *Clin Cancer Res*. 2013;19(19):5361-5371. doi:10.1158/1078-0432.CCR-12-2857

205. Heselmeyer K, Schröck E, Du Manoir S, et al. Gain of chromosome 3q defines the transition from severe dysplasia to invasive carcinoma of the uterine cervix. *Proc Natl Acad Sci U S A*. 1996;93(1):479-484. doi:10.1073/pnas.93.1.479

206. Galipeau PC, Cowan DS, Sanchez CA, et al. 17p (p53) allelic losses, 4N (G2/tetraploid) populations, and progression to aneuploidy in Barrett's esophagus. *Proc Natl Acad Sci U S A*. 1996;93(14):7081-7084. doi:10.1073/pnas.93.14.7081

207. Kops GJPL, Weaver BAA, Cleveland DW. On the road to cancer: Aneuploidy and the mitotic checkpoint. *Nat Rev Cancer*. 2005;5(10):773-785. doi:10.1038/nrc1714

208. O'Malley FP, Grignon DJ, Keeney M, Kerkvliet N, McLean C. DNA Heterogeneity in prostatic adenocarcinoma. A DNA flow cytometric mapping study with whole organ sections of prostate. *Cancer*. 1993;71(9):2797-2802. doi:10.1002/1097-0142(19930501)71:9<2797::AID-CNCR2820710918>3.0.CO;2-D

209. Helpap B. Future Directions in Research of Prostate Carcinoma. *Pathol Res Pract*. 1993;189(5):497-509. doi:10.1016/S0344-0338(11)80356-0

210. Helpap B, Bubendorf L, Kristiansen G. Prostatakarzinom: Teil 2: Rückblick über die verschiedenen Tumorgradingverfahren der Jahre 1966–2015 und Zukunftsperspektiven des neuen Gradings der International Society of Urological Pathology (ISUP). *Pathologe*. 2016;37(1):11-16. doi:10.1007/s00292-015-0124-x

211. Helpap B, Köllermann J. Combined histoarchitectural and cytological biopsy grading improves grading accuracy in low-grade prostate cancer. *Int J Urol*. 2012;19(2):126-133. doi:10.1111/j.1442-2042.2011.02902.x

212. Helpap B, Ringli D, Tonhauser J, et al. The Significance of Accurate Determination of Gleason Score for Therapeutic Options and Prognosis of Prostate Cancer. *Pathol*

Oncol Res. 2016;22(2):349-356. doi:10.1007/s12253-015-0013-x

213. Andor N, Graham TA, Jansen M, et al. Pan-cancer analysis of the extent and consequences of intratumor heterogeneity. *Nat Med*. 2016;22(1):105-113. doi:10.1038/nm.3984

214. Cooper CS, Eeles R, Wedge DC, et al. Analysis of the genetic phylogeny of multifocal prostate cancer identifies multiple independent clonal expansions in neoplastic and morphologically normal prostate tissue. *Nat Genet*. 2015;47(4):367-372. doi:10.1038/ng.3221

215. Boyd LK, Mao X, Xue L, et al. High-resolution genome-wide copy-number analysis suggests a monoclonal origin of multifocal prostate cancer. *Genes Chromosom Cancer*. 2012;51(6):579-589. doi:10.1002/gcc.21944

216. Cheng L, Song SY, Pretlow TG, et al. Evidence of independent origin of multiple tumors from patients with prostate cancer. *J Natl Cancer Inst*. 1998;90(3):233-237. doi:10.1093/jnci/90.3.233

217. Kobayashi M, Ishida H, Shindo T, et al. Molecular analysis of multifocal prostate cancer by comparative genomic hybridization. *Prostate*. 2008;68(16):1715-1724. doi:10.1002/pros.20832

218. Lindberg J, Klevebring D, Liu W, et al. Exome sequencing of prostate cancer supports the hypothesis of independent tumour origins. *Eur Urol*. 2013;63(2):347-353. doi:10.1016/j.eururo.2012.03.050

219. Federer-Gsponer JR, Müller DC, Zellweger T, et al. Patterns of stemness-associated markers in the development of castration-resistant prostate cancer. *Prostate*. 2020;80(13):1108-1117. doi:10.1002/pros.24039

220. Li T, Su Y, Mei Y, et al. ALDH1A1 is a marker for malignant prostate stem cells and predictor of prostate cancer patients outcome. *Lab Investig*. 2010;90(2):234-244. doi:10.1038/labinvest.2009.127

221. Dugas SG, Müller DC, Le Magnen C, et al. Immunocytochemistry for ARID1A as a potential biomarker in urine cytology of bladder cancer. *Cancer Cytopathol*. August 2019:cncy.22167. doi:10.1002/cncy.22167

222. Malviya K, Fernandes G, Naik L, Kothari K, Agnihotri M. Utility of the Paris System in Reporting Urine Cytology. *Acta Cytol*. 2017;61(2):145-152. doi:10.1159/000464270

223. Barkan GA, Wojcik EM, Nayar R, et al. The Paris System for Reporting Urinary Cytology: The Quest to Develop a Standardized Terminology. *Acta Cytol*. 2016;60(3):185-197. doi:10.1159/000446270

224. Pietzak EJ, Bagrodia A, Cha EK, et al. Next-generation Sequencing of Nonmuscle Invasive Bladder Cancer Reveals Potential Biomarkers and Rational Therapeutic Targets. *Eur Urol*. 2017;72(6):952-959. doi:10.1016/j.eururo.2017.05.032

225. Shen J, Ju Z, Zhao W, et al. ARID1A deficiency promotes mutability and potentiates therapeutic antitumor immunity unleashed by immune checkpoint blockade. *Nat Med*. 2018;24(5):556-562. doi:10.1038/s41591-018-0012-z

226. Wang X, Nagl NG, Wilsker D, et al. Two related ARID family proteins are alternative subunits of human SWI/SNF complexes. *Biochem J*. 2004;383(Pt 2):319-325. doi:10.1042/BJ20040524

227. Wu R-C, Wang T-L, Shih I-M. The emerging roles of ARID1A in tumor suppression. *Cancer Biol Ther*. 2014;15(6):655-664. doi:10.4161/cbt.28411

228. cBioPortal. ARID1A mutation alteration frequency in bladder cancer.

229. Balbás-Martínez C, Rodríguez-Pinilla M, Casanova A, et al. ARID1A alterations are associated with FGFR3-wild type, poor-prognosis, urothelial bladder tumors. Vlahou A, ed. *PLoS One*. 2013;8(5):e62483. doi:10.1371/journal.pone.0062483

230. Li J, Lu S, Lombardo K, Monahan R, Amin A. ARID1A alteration in aggressive urothelial carcinoma and variants of urothelial carcinoma. *Hum Pathol*. 2016;55:17-23. doi:10.1016/j.humpath.2016.04.006

231. Wu JN, Roberts CWM. ARID1A mutations in cancer: another epigenetic tumor suppressor? *Cancer Discov*. 2013;3(1):35-43. doi:10.1158/2159-8290.CD-12-0361

232. Mathur R. ARID1A loss in cancer: Towards a mechanistic understanding. *Pharmacol Ther*. 2018;190:15-23. doi:10.1016/J.PHARMTHERA.2018.05.001

233. Babjuk M, Böhle A, Burger M, et al. EAU Guidelines on Non–Muscle-invasive Urothelial Carcinoma of the Bladder: Update 2016. *Eur Urol*. 2017;71(3):447-461. doi:10.1016/J.EURURO.2016.05.041

234. Yafi FA, Brimo F, Steinberg J, Aprikian AG, Tanguay S, Kassouf W. Prospective analysis of sensitivity and specificity of urinary cytology and other urinary biomarkers for bladder cancer. *Urol Oncol Semin Orig Investig*. 2015;33(2):66.e25-66.e31.

doi:10.1016/J.UROLONC.2014.06.008

235. Moch H, Cubilla AL, Humphrey PA, Reuter VE, Ulbright TM. The 2016 WHO Classification of Tumours of the Urinary System and Male Genital Organs-Part A: Renal, Penile, and Testicular Tumours. *Eur Urol*. 2016;70(1):93-105. doi:10.1016/j.eururo.2016.02.029

236. Vlajnic T, Savic S, Barascud A, et al. Detection of ROS1-positive non-small cell lung cancer on cytological specimens using immunocytochemistry. *Cancer Cytopathol*. 2018;126(6):421-429. doi:10.1002/cncy.21983

237. Savic S, Bode B, Diebold J, et al. Detection of ALK-Positive Non–Small-Cell Lung Cancers on Cytological Specimens: High Accuracy of Immunocytochemistry with the 5A4 Clone. *J Thorac Oncol*. 2013;8(8):1004-1011. doi:10.1097/JTO.0B013E3182936CA9

238. Beltran H, Wyatt AW, Chedgy EC, et al. Impact of therapy on genomics and transcriptomics in high-risk prostate cancer treated with neoadjuvant docetaxel and androgen deprivation therap. *Clin Cancer Res*. 2017;23(22):6802-6811. doi:10.1158/1078-0432.CCR-17-1034

239. Maru Y, Tanaka N, Ohira M, Itami M, Hippo Y, Nagase H. Identification of novel mutations in Japanese ovarian clear cell carcinoma patients using optimized targeted NGS for clinical diagnosis. *Gynecol Oncol*. 2017;144(2):377-383. doi:10.1016/J.YGYNO.2016.11.045

240. Ogiwara H, Takahashi K, Sasaki M, et al. Targeting the Vulnerability of Glutathione Metabolism in ARID1A-Deficient Cancers. *Cancer Cell*. 2019;35(2):177-190.e8. doi:10.1016/J.CCELL.2018.12.009

241. Faraj SF, Chaux A, Gonzalez-Roibon N, et al. ARID1A immunohistochemistry improves outcome prediction in invasive urothelial carcinoma of urinary bladder. *Hum Pathol*. 2014;45(11):2233-2239. doi:10.1016/J.HUMPATH.2014.07.003

242. Weinstein JN, Akbani R, Broom BM, et al. Comprehensive molecular characterization of urothelial bladder carcinoma. *Nature*. 2014;507(7492):315-322. doi:10.1038/nature12965

243. Ross JS, Wang K, Al-Rohil RN, et al. Advanced urothelial carcinoma: next-generation sequencing reveals diverse genomic alterations and targets of therapy. *Mod Pathol*. 2014;27(2):271-280. doi:10.1038/modpathol.2013.135

244. Wiegand KC, Shah SP, Al-Agha OM, et al. ARID1A mutations in endometriosis-associated ovarian carcinomas. *N Engl J Med*. 2010;363(16):1532-1543. doi:10.1056/NEJMoa1008433

245. Wang K, Kan J, Yuen ST, et al. Exome sequencing identifies frequent mutation of ARID1A in molecular subtypes of gastric cancer. *Nat Genet*. 2011;43(12):1219-1223. doi:10.1038/ng.982

246. Guan B, Mao T-L, Panuganti PK, et al. Mutation and loss of expression of ARID1A in uterine low-grade endometrioid carcinoma. *Am J Surg Pathol*. 2011;35(5):625-632. doi:10.1097/PAS.0b013e318212782a

247. Scott SN, Ostrovnaya I, Lin CM, et al. Next-generation sequencing of urine specimens: A novel platform for genomic analysis in patients with non–muscle-invasive urothelial carcinoma treated with bacille Calmette-Guérin. *Cancer Cytopathol*. 2017;125(6):416-426. doi:10.1002/cncy.21847

248. Turajlic S, Sottoriva A, Graham T, Swanton C. Resolving genetic heterogeneity in cancer. *Nat Rev Genet*. 2019;20(7):404-416. doi:10.1038/s41576-019-0114-6

249. Fojo T, Mailankody S, Lo A. Unintended consequences of expensive cancer therapeutics—the pursuit of marginal indications and a me-too mentality that stifles innovation and creativity: the John Conley Lecture. *JAMA Otolaryngol Head Neck Surg*. 2014;140(12):1225-1236. doi:10.1001/jamaoto.2014.1570

250. Mateo J, Chakravarty D, Dienstmann R, et al. A framework to rank genomic alterations as targets for cancer precision medicine: The ESMO Scale for Clinical Actionability of molecular Targets (ESCAT). *Ann Oncol*. 2018;29(9):1895-1902. doi:10.1093/annonc/mdy263

251. Faratian D, Bown JL, Smith VA, Langdon SP, Harrison DJ. Cancer systems biology. *Methods Mol Biol*. 2010;662:245-263. doi:10.1007/978-1-60761-800-3_12

252. Swanton C, McGranahan N, Starrett GJ, Harris RS. APOBEC Enzymes: Mutagenic Fuel for Cancer Evolution and Heterogeneity. *Cancer Discov*. 2015;5(7):704-712. doi:10.1158/2159-8290.CD-15-0344

253. Sopik V, Phelan C, Cybulski C, Narod SA. BRCA1 and BRCA2 mutations and the risk for colorectal cancer. *Clin Genet*. 2015;87(5):411-418. doi:10.1111/cge.12497

254. Lord CJ, Ashworth A. PARP inhibitors: Synthetic lethality in the clinic. *Science (80-)*. 2017;355(6330):1152-1158. doi:10.1126/science.aam7344

255. Nickoloff JA, Jones D, Lee SH, Williamson EA, Hromas R. Drugging the Cancers Addicted to DNA Repair. *J Natl Cancer Inst*. 2017;109(11). doi:10.1093/jnci/djx059

256. Nutman AP, Bennett VC, Friend CRL, Van Kranendonk MJ, Chivas AR. Rapid emergence of life shown by discovery of 3,700-million-year-old microbial structures. *Nature*. 2016;537(7621):535-538. doi:10.1038/nature19355